TECHNISCHE UNIVERSITÄT MÜNCHEN

Lehrstuhl für Siedlungswasserwirtschaft

Evaluation of adsorbents for road runoff treatment

Yang Li

Acknowledgments

I have thought several times about how to write my acknowledgments. At that moment, I still feel difficult to describe my gratitude exactly. There are so many people I want to thank and to share my work with. My advisor, my colleagues, my students, my friends, and my families, without your support and company, I could never move so far.

Give my great thank to my advisor, Prof. Dr. habil. Brigitte Helmreich. Because of her, all the things could happen. She showed me the lab work at the beginning and taught me how to work as a scientist. When I met problems, I went to her with the collapsed world, she always smiled and told me 'hey, not that bad.' 'Let us see what we can do.' It is because of her support and encouragement, I could have courage and confidence to face and solve the problems and move on. Thanks for discussion, for advice, for teaching, for sharing, for consideration… for all of her help.

I also want to send my gratitude to Prof. Harald Horn, who offered me the opportunity to study as a PhD student in the institute. Thanks and appreciations for his patience and belief, I could keep growing and become better.

Special thanks to Ms. Myriam Reif, Mr. Wolfgang Schröder, Mr. Hubert Moosrainer, Ms. Susanne Thiemann, and Nicole Zollbrecht, for their great assistance in experiment and their patience for my asking. I am extremely grateful to my students, Jiachao Li and Yue Li, for their help in experiments and friendship in life. Thanks are also sent to Ms Susanne Wießler and Marianne Lochner for their kind helps in the institute. Lots of acknowledges to my friends and colleagues in the institute, in particular, David Martinez, Danial Taherzadeh, Christina Klarmann, Tobias Rocktäschel, Mateo Urena, Evelyn Walters, Bastian Herzog, Riccardo Matruglio, Ahmed Labena, Mohamad Rajab and my roommate, Claus Lindenblatt. Thanks for their friendship and company, life become more colorful and charming.

I appreciate the study at the institute of Water Quality Control, Technische Universität München, not only for the knowledge obtained, but also for the people here. From these people above, I learned so much. The time spent with them would be a treasure in my memory. Munich is a beautiful city, and in Munich, there is a wonderful institute.

At last, I want to send the most heartfelt thanks to my families, my dear mother and husband. Their unconditional love, support and understanding are the source of my whole power.

Garching, 10.2012

Yang Li

Zusammenfassung

Mit zunehmender Urbanisierung nimmt der Anteil an versiegelten Flächen in städtischen Gebieten und damit auch die stoffliche Belastung von Regenwasserabflüssen zu. Handlungsanweisungen (Best management practices, BMPs) finden weitgehende Anwendung, um mögliche negative Auswirkungen dieser Abflüsse zu minimieren. Alleine durch Sedimentationsvorgänge, wie meist in BMPs gefordert, können jedoch nicht alle Schadstoffe aus den Regenwasserabflüssen entfernt werden. Im Abfluss von Straßenflächen befinden sich sowohl Schwermetalle wie auch organische Verbindungen sowohl in gelöster als auch in partikulär gebundener Form. Insbesondere gelöste Stoffe werden nicht durch eine Sedimentationsstufe zurückgehalten. Sie können sich dann in Böden oder Gewässern anreichern und eine massive Belastung für die Umwelt darstellen. Deshalb werden für die entsprechenden Handlungsanweisungen im Bereich der Versickerungs-BMPs (Infiltration) geeignete Adsorptionsmittel für die Entfernung von gelösten und feinpartikulären Schadstoffen benötigt.

Ziel dieser Arbeit war es, verschiedene Filtermaterialien hinsichtlich ihrer Reinigungsleistung für Straßenabflüsse zu untersuchen, um ein geeignetes Material für BMPs zu finden. Aufgrund ihrer guten Adsorptionsleistungen von Schwermetallen wurden die folgenden vier traditionellen Adsorptionsmittel gewählt: Aktivkohle (F300), Braunkohlekoks (HOK), halborganophiler Bentonit (Tixosorb) und Eisenschwamm (DRI). Zusätzlich wurden die Bioadsorbenten Rot-Algen (Palmaria Palmata)und Biertreber auf ihre Kapazität hin, Schwermetalle zu adsorbieren, getestet.

Die Bioadsorbenten Rot-Algen und Treber zeigten zufriedenstellende Adsorptionkapazitäten bezüglich gelösten Kupfers (Cu^{2+}) in Höhe von 12,7 mg/g beziehungsweise 9,01 mg/g. Dennoch werden diese Materialen auf Grund ihrer geringen mechanischen Belastbarkeitwohl nur in seltenen Fällen Anwendung in der Praxis finden. Bei den traditionellen Materialien zeigten F300 und HOK höhere Adsorptionskapazitäten für Naphthalin (NAP) und Methyl-tert-butyl ether (MTBE) als die anderen getesteten Adsorptionsmittel. Für MTBE konnten Adsorptionskapazitäten von 222 mg/g für F300 beziehungsweise 35 mg/g für HOK nachgewiesen werden. Die geringere Porengröße von Tixosorb als auch die Oxidations-Reduktions-Reaktion von DRI brachten keine Vorteile in der Entfernung von MTBE und Nap. Die Adsorption von Nap an HOK und F300 zeigte eine lineare Abhängigkeit. Verglichen

mit MTBE konnten auch höhere Adsorptionskapazitäten festgestellt werden.Der pH-Wert hatte keinen Einfluss auf die Adsorption von MTBE und NAP an F300 und HOK.

Die Adsorption von MTBE wurde durch die Anwesenheit von Streusalz oder natürlichem organischem Material (NOM) sowie anderen Adsorbaten nicht beeinflusst. Die Adsorptionskapazität von Nap ging hingegen bei der Verfügbarkeit von NOM oder anderen Adsorbaten (MTBE, Zn^{2+})zurück. Dennoch blieben die Reinigungsleistungen für Nap in Experimenten sehr hoch (96.9 – 100%).

In Säulenversuchen konnte eine Reihung hinsichtlich der Reinigungsleistung für die Materialien HOK mit Nap> Zn^{2+}> MTBE beziehungsweise für F300 mit Nap> MTBE >Zn^{2+} festgestellt werden. Die Anwesenheit von MTBE verringerte die Entfernung von Zn^{2+} deutlich. Die Beigabe von HOK in eine Säule mit F300 konnte die Adsorption von Zn^{2+} verbessern. Des Weiteren wurde beobachtet, dass es für die Reinigungsleistung keinen Unterschied macht, ob die Materialien geschichtet oder gemischt in die Säule eingebracht werden.

Fazit ist, dass F300 als Filtermaterial für Schwermetalle und organische Schadstoffe herangezogen werden kann. Die Zugabe von HOK zu F300 kann die Adsorptionskapazität für Schwermetalle zusätzlich erhöhen. So können spezifische Mischungsverhältnisse situationsangepasst sehr gute Reinigungsleistungen sowohl von organischen Stoffen wie auch Schwermetallen bei der Behandlung von Straßenabflüssen bringen.

Abstract

The development of urbanization causes the increase of impervious surfaces in urban area and aggravates the water contamination with the runoff originates from these surfaces. Best management practices (BMPs) are widely applied to reduce the impact of stormwater pollutant on the environment. However, the step of sedimentation, which is commonly contained in BMPs, is not enough to remove the dissolved pollutants, or fine particles from stormwater. In road runoff, both heavy metal and organic pollutant can be detected in dissolved phase or stay with fine particles. These parts of pollutant could escape from the sedimentation process and accumulate in soil or receiving water to cause further severe contamination in environment. Therefore, a suitable adsorbent material is needed in BMPs (infiltration system) for the removal of dissolved pollutants and fine particles before entering soil and groundwater.

The aim of this study was to evaluate and choose the suitable filter material for a BMP system applied for road runoff treatment. Four traditional adsorbents, activated carbon (F300), activated lignite (HOK), semi-organophilic bentonite (Tixosorb), and sponge iron (DRI), were chosen based on their performance in heavy metals removal. Besides, the bioadsorbents, red alga (Palmaria Palmata) and beer draff, were also chosen, but tested their adsorption capacity of heavy metal first.

In the experiments, bioadsorbents presented satisfied adsorption capacity of Cu^{2+}, 12.7 mg/g and 9.01 mg/g for red alga and beer draff, respectively. However, their poor mechanical strengths would limit their application in practice. In the four traditional materials, F300 and HOK displayed higher adsorption capacities of naphthalene (Nap) and methyl tert-butyl ether (MTBE) than other ones. The adsorption capacities of MTBE were 222 mg/g and 35 mg/g on F300 and HOK, respectively. The smaller pore size of Tixosorb and the oxidation-reduction reaction of DRI did not help in MTBE and Nap removal. Nap adsorption on HOK and F300 showed linear adsorption behavior. Compare to MTBE, the linear adsorption behavior of Nap showed higher adsorption capacities of Nap on both F300 and HOK. Moreover, in MTBE adsorption, F300 performed better than HOK. In the experiments of F300 and HOK, pH value has not presented any influence on either MTBE or Nap adsorption.

On MTBE adsorption, de-icing salt, natural organic matter (NOM) and other adsorbate did not show any influence. However, the presence of NOM and other adsorbate (MTBE or Zn^{2+}) showed their competition with Nap and caused the decrease in Nap adsorption capacity. Although Nap adsorption capacity was reduced with these influences, the removal efficiency of Nap was kept at high level (96.9-100%) in experiments.

In the column experiments, HOK and F300 removed pollutants following the orders as Nap > Zn^{2+} > MTBE and Nap > MTBE >Zn^{2+}, respectively. The presence of MTBE greatly decreased the removal of Zn^{2+}. The introduction of HOK into the column of F300 could improve the adsorption of Zn^{2+}. Furthermore, it was found the placement of adsorbents, mixture or two-layer, presented no difference for pollutants removal.

In all, F300 could be used as a filter material for heavy metal and organic pollutants removal. The introduction of HOK could enhance the adsorption capacity of heavy metal. With the consideration of the amount ratio of two materials for specific situation, a satisfied removal effect could be expected in the road runoff treatment.

Table of contents

1. Introduction

With the development of urbanization, the impervious surfaces (roads, roofs, etc.) have covered more and more urban areas. The increasing road surface significantly influences the urban environment (Kayhanian et al., 2006). The pollutants originated from traffic activities could accumulate on the road surface and enter the receiving waters with the stormwater runoff (Ngabe et al., 2000; Helmreich et al., 2010). Therefore, road runoff has been regarded as a major pollution source in urban area (Lee et al., 2004; Brown and Peake, 2006; Opher et al., 2009; Chen et al., 2012). The pollutants in road runoff include particles, heavy metals, polycyclic aromatic hydrocarbons (PAHs), mineral oil type hydrocarbons (MOTH), and volatile organic compounds (VOCs) (Hoffman et al., 1985; Baeckstroem et al., 2003; Chen et al., 2012).

The existences of pollutants in road runoff are different. Some of them are particle bound in runoff while the others are in dissolved phase. Correspondingly, the treatment methods are various with their existences. Particulate pollutants can be effectively removed from road runoff by sedimentation. The removal of dissolved pollutants and fine particles are relatively difficult, for which the infiltration through proper media is a possible treatment method (Faerm, 2003).

Best management practices (BMPs) are widely applied to reduce the impact of stormwater pollutant on the environment. The popular used structural measures of BMPs are detention/retention ponds, wetlands, infiltration and local disposal systems. Almost all of these structural BMPs contain a step of sedimentation to remove the particles and particulate pollutants. However, the removal of dissolved pollutants and fine particles are seldom considered. Infiltration systems performed better in the removal of fine particles and dissolved pollutants, but it may cause further contamination to top soil and ground water with improper media. Therefore, constructing a filter system with proper material offering adsorption process to remove the fine particles and dissolved pollutants is a promising option for road runoff treatment.

Based on the previous researches on adsorbent materials, six different materials were chosen and tested in this study for further use in an infiltration system for road runoff treatment.

2. State of the art

The impervious surface acts as a great contributor in the contamination of stormwater (Hoffman et al., 1985; Ball, 2002). In a residential area, the impervious area could cover 40-50% of the total surface while the portion of road surface could be 10-15%, taking up 30% of the impervious area (Ball, 2002). Moreover, road surface has been found to have higher contamination in its runoff than other urban sites. In the research of Marsalek et al. (1999), 20% of road runoff samples showed severe toxic effect whereas the corresponding percentage of urban stormwater runoff samples was only 1%. Therefore, there are comprehensive researches on the composition, sources, and contamination of the pollutants in road runoff (Legret and Pagotto, 1999; Brown and Peake, 2006; Huang et al., 2007; Gan et al., 2008; Davis and Birch, 2010).

2.1 Pollutants in road runoff

Road runoff is a source of various pollutants. Both organic and inorganic substances could be found in road runoff. These pollutants have different sources and characteristics.

2.1.1 Heavy metals

The typical heavy metals in road runoff, which are frequently considered in literatures, are lead (Pb), copper (Cu), zinc (Zn), and cadmium (Cd) (Legret and Pagotto, 1999; Faerm, 2002; Brown and Peake, 2006; Davis and Birch, 2010; Helmreich et al., 2010). The particular concern caused by these heavy metals is not only because of their potential toxicity but also of their accumulative character. Even if the concentrations of these heavy metals in road runoff are lower than the discharge criteria, they could amplify with accumulation in sediments or organisms, posing a serious threat to livings being and to the ecology (Hoffman et al., 1985; McCready et al., 2004; Brown and peake, 2006).

The vehicle running on the road is the main source for heavy metals in road runoff. Moreover, the surface of roads, atmospheric deposition, and the rainfall itself also contribute to the contamination of heavy metals in road runoff (Davis et al., 2001; Wik et al., 2008; Davis and Birth, 2010). **Table 1** shows the various sources of heavy metals in road runoff. It is reported that brake wear is the primary source of Cu, tire wear is the main contributor for Zn, and the Pb mainly originates from atmospheric deposition (Davis et al., 2001). Due to the prohibition of leaded petrol since 1990s,

there is a sharp decrease of Pb concentration in road runoff (**Table 2**). Therefore, atmospheric deposition contributes more to Pb pollution rather than fuel leaking (Athanasiadis, 2005).

Table 1 Typical heavy metals in road runoff and their sources

(Ball, 1998; Legret and Pagotto, 1999; Davis et al., 2001)

Heavy metals	Primary Sources
Pb	Atmospheric deposition; auto exhaust; tyre wear; lubricating oil and grease; bearing wear; brake abrasion
Zn	Tyre wear; brake abrasion; safety barriers with galvanized steel; motor oil; grease
Cu	Brake abrasion; metal plating; bearing and brush wear; moving engine parts; fungicides; insecticides; pesticides
Cd	Tyre wear; brake abrasion; insecticide application

Heavy metals could exist in road runoff in different forms. Some of them could attach to solids during the transport process while some of them could move in dissolved form. The total concentrations of Cu, Zn, Pb, and Cd is in the order that Zn (130-1760 µg/L) > Cu (8-200 µg/L) > Pb (5-118 µg/L) > Cd (0.056-4.4 µg/L) in road runoff (**Table 2**), among which the particulate fraction of these metals follows the order that Pb (82-100%) > Cd (36-66%) ≈Cu (44-67%) ≈ Zn (29-56%). Although the concentrations of heavy metals and their particulate fractions vary from locations and events, it is clear that Pb tends to bind onto the particle surface while Cd, Cu, and Zn are primarily in soluble form.

Additionally, it is reported the finer particles are more likely to be bound by heavy metals rather than the particles with larger size (Helmreich et al., 2010). In the study of Ball et al. (1998), the particles smaller than 43 µm, which was only 5.9% of the total solids, sorbed more than 50% of the metals. Similarly, Bradford (1977) found more than 60% of the trace metals were sorbed to the fine fraction of the street dust which only took 6% of the total solids mass. Westerlund and Viklander (2006) studied the relationship between particle size and heavy metal loading and found particle size of 4-6 µm was highly related with heavy metal concentration in road runoff.

4

Table 2 The total concentrations of heavy metals and their particulate fraction in road runoff

Metals	AADT[a]	Concentration (µg/L)	Particulate fraction (%)	Reference
Cu	30000	87	67%	Harrison et al., 1985
Cu	90000	136	65%	Marsalek et al., 1997
Cu	25000	24.2		Wu et al., 1998
Cu	12000	45	44%	Legret and Pagotto. 1999
Cu	15600	18.2	52%	Baeckstroem et al., 2003
Cu	9000	8.3	48%	Prestes et al., 2006
Cu	31000	90	-	Gan et al., 2008
Cu	57000	191	-	Helmreich et al., 2010
Cu[b]	84500	44-213	-	Davis and Birth, 2010
Cu[d]	**Ohio EPA**	**18**	-	Sansalone and Buchberger, 1997
Cu[e]	**BBodSchV**	**50**	-	BBodSchV, 1999
Zn	90000	337	56%	Marsalek et al., 1997
Zn	12000	356	38%	Legret and Pagotto. 1999
Zn	15600	130	29%	Baeckstroem et al., 2003
Zn	22170	1760	-	Gan et al., 2008
Zn	57000	847	-	Helmreich et al., 2010
Zn[b]	84500	156-635	-	Davis and Birth, 2010
Zn[d]	**Ohio EPA**	**120**	-	Sansalone and Buchberger, 1997
Zn[e]	**BBodSchV**	**500**	-	BBodSchV, 1999
Pb[c]	30000	353	94%	Harrison et al., 1985
Pb	90000	72	100%	Marsalek et al., 1997
Pb	25000	21	-	Wu et al., 1998
Pb	12000	58	93%	Legret and Pagotto. 1999
Pb	15600	5.64	92%	Baeckstroem et al., 2003
Pb	9000	15	82%	Prestes et al., 2006
Pb	22170	118	-	Gan et al., 2008
Pb	57000	56	-	Helmreich et al., 2010
Pb[b]	84500	9-88	-	Davis and Birth, 2010
Pb[d]	**Ohio EPA**	**82**	-	Sansalone and Buchberger, 1997
Pb[e]	**BBodSchV**	**25**	-	BBodSchV, 1999
Cd	30000	4.4	41%	Harrison et al., 1985
Cd	25000	2.5	-	Wu et al., 1998
Cd	12000	1	53%	Legret and Pagotto, 1999
Cd	15600	0.056	36%	Baeckstroem et al., 2003
Cd	9000	0.32	66%	Prestes et al., 2006
Cd	22170	1.6	-	Gan et al., 2008
Cd	57000	<0.5	-	Helmreich et al., 2010
Cd[d]	**Ohio EPA**	**5.6**	-	Sansalone and Buchberger, 1997
Cd[e]	**BBodSchV**	**5**	-	BBodSchV, 1999

[a] Annual average daily traffic (AADT); [b] Concentration range in the reference instead of average value; [c] Pb concentration before the ban of lead petrol; [d] Ohio EPA discharge criterion to surface water in Ohio; [e] BBodSchV Germany discharge criterion to ground water

As shown in **Table 2**, most concentrations of Cu and Zn are higher than the discharge criteria of Ohio EPA (Environment Protection Agency) and BBodSchV

(Bundes-Bodenschutz- und Altlastenverordnung in Germany). Therefore, a treatment of road runoff is necessary before its discharge into receiving water. BBodSchV is an ordinance for soil and ground water production. It sets the criteria of pollutants discharging to soil and ground water (by infiltration), and there is a discussion recently to reduce the criteria of BBodSchV for the minimum pollutants discharge. It is foreseeable that better treatment of road runoff would be required in near future.

2.1.2 Organic pollutants

In addition to heavy metals, organic compounds, PAHs, VOCs and MOTH, contribute greatly to road runoff pollution. Their existences in aquatic system pose severe threats to human health and the whole environment.

2.1.2.1 Polycyclic Aromatic Hydrocarbons (PAHs)

PAHs are a series of organic compounds composed of two or more aromatic rings. The PAHs in road runoff originate mainly from uncompleted combustion of fuels or leakage of crankcase oils and lubricating oils. As hydrophobic compounds, PAHs have relatively high values of log K_{OW} (partitioning coefficient between octanol and water). They thus prefer to remain (be adsorbed) on the surfaces of particles in road runoff, leaving only a small fraction dissolved in the water phase. Compared to other PAHs, naphthalene (Nap) has the lowest values of log K_{OW} (3.37) and log K_{OC} (organic carbon partition coefficient, 3.11) (Mackay et al., 1992). It therefore can be said that Nap is the most difficult PAH to remove by adsorption. Although the water solubility of Nap (30 mg/L, 25°C) is much lower than the polar compound methyl tert-butyl ether (MTBE), which can be also found in road runoff, it is higher than any other PAHs (Mackay et al., 1992).

The accesses for PAHs entering road runoff are atmosphere deposition (with dust and precipitation), and particles washed from road surface (Bruen et al., 2006). In a study of road runoff in Beijing, the mean concentration of total 16 PAHs are 0.548 and 3.872 µg/L in dissolved and particle phases, respectively (Zhang et al., 2008). In another city, Amman Jordan, Jiries et al., (2003) found the average concentration of total 16 PAHs varied at 0.196-0.389 µg/L in road runoff. The average concentration of Nap is 0.063-0.116 µg/L, which is much higher than other PAH (Jiries et al., 2003).

In the aquatic system, the toxicity of PAHs has been observed on the fresh water organisms. PAHs were identified as the major toxicants in the sediment which was

6

contaminated by road runoff (Maltby et al. 1995). Some PAHs compounds have been defined as priority hazardous substance by European Environmental Agency (EEA) (Directive 2000/60/EC) for their mutagenicity and carcinogicity.

2.1.2.2 Methyl tert-butyl ether (MTBE)

As a compound of VOCs in road runoff, MTBE is well known as the petrol additive. It was widely used as a common additive in petrol since 1970s to enhance the octane number and oxygen level. In 1990, the use of MTBE exploded because of the implementation of reformulated gasoline (RFG) and oxy-fuel programs of 'Clean Air Act'. With the addition of MTBE in petrol, high octane aromatics could be removed to avoid the ozone formation; and the emission of carbon monoxide and other toxicants, such as benzene and 1,3-butadiene, could be decreased to meet the new standards (Borden et al., 2002). In 1997, about 70% of all the petrol in US contains MTBE (Eweis et al., 1998). In Europe, EU Directive No. 85/536 of 5 December 1985 allowed the addition of MTBE as oxygenate additive in petrol up to 15% by volume (Bruen et al., 2006). Although there are some other options for oxygenates, like di-isopropyl ether (DIPE), tert-amyl ether (TAME), and tert-butyl alcohol (TBA), MTBE become a better selection because of its easy availability, low cost, favorable transfer, blending characteristics, and high octane rating (Borden et al., 2002).

With the widespread application, MTBE is frequently detected in stormwater, surface water and ground water (Achten and Puettmann, 2000; Borden et al., 2002; Schmidt, 2003). Although the exclusive study of MTBE in road runoff is limited, its existence was detected in urban storm runoff at a concentration range of 0.2-8.7 µg/g (USGS, 1996). Borden et al. (2002) found an even higher MTBE concentration of 13.5 µg/L in storm runoff, while the concentration of < 20-40 µg/L is the recommended standard for drinking water (US EPA, 1997).

Although the concentrations of MTBE in environment are lower than the threshold values, specific concern was caused for MTBE because of its potential toxicity and its physical and chemical characteristics. The high solubility of MTBE in water (51.6 g/L at 25°C), low values of log K_{OW} (1.06) (Mackay et al., 1992), and log K_{OC} (1.0-1.1) (Nichols and Drogos, 2000) reveal the polar character of MTBE and its strong mobility in the water environment. Once contact with water, it enters water system rapidly and transfers with runoff rather than adsorb to sediment. Contamination problems would be caused by MTBE to receiving water systems when fuel spills and

leaks occur (Malca and Freire, 2006). Besides, MTBE could cause unpleasant taste and odor in contaminated water, even at low concentration of 5-15 µg/L (Bruen et al., 2006). Moreover, it has been found that MTBE induces tumors in rats and therefore, is regarded as a suspected human carcinogen (NSTC, 1997).

Due to the potential water contamination of MTBE, ethyl tert-butyl ether (ETBE), as a substituent of MTBE, is also often used as petrol oxygenate, especially in Europe (France, Italy, and Spain) (Inal et al., 2009). ETBE can be converted from bio-ethanol and therefore is cleaner to environment than MTBE (Malca and Freire, 2006).

2.1.2.3 Mineral oil type hydrocarbon (MOTH)

Mineral oil is a byproduct of petroleum and the basis of lubricant oil. The lubricant leaking is the main access for MOTH entering road runoff. Unlike the other petroleum hydrocarbons containing longer chain of alkanes (C9-C17) or some PAHs with shorter chain of alkanes (C5-C12), MOTHs have the moderate length of alkane chain between them. As it is difficult and costly to determine the amount of individual compound of MOTHs, their concentrations are normally controlled with a general parameter of the total amount.

The concentration of MOTH varies among different researches. In a study of highway runoff, the concentration of MOTH was found varying in a wide range of 2.05-7.02 mg/L (Stotz, 1987). In another study of runoff from a residential street, the median concentration of MOTH was 0.16 mg/L (Dierkes et al., 2005). MOTH prefers transport in particulate phase, especially with fine particles (Faram et al., 2007). Hoffmann et al. (1982) believed the majority of MOTH was removed in the sedimentation process with particles. Other MOTH, which is not bound with particles, can be separated from road runoff by its different density. Besides the possible toxicity that some volatile compound of MOTH (e.g. n-hexane) might cause to human health, the existence of MOTH would also cause the taste problem in water with the threshold value of 10-100 µg/L.

2.2 Strategies for road runoff treatment

2.2.1 The existence pattern of the pollutants in road runoff

The pollutants in road runoff could be separated as particulate pollutants and dissolved pollutants by their existence patterns. The different existence patterns could cause great impact on their transportation in runoff and their further toxicities in

8

environment (Helmreich et al., 2010). Meanwhile, the treatment methods applied to remove these pollutants are also greatly related to their existence patterns. For example, the larger particles and the related particulate pollutants are expected to be removed in the sediment process while the finer particles and dissolved pollutants need other step in the treatment rather than sedimentation (Boving and Neary, 2007; Helmreich et al., 2010).

As discussed before (section 2.1.1), heavy metals could exist in both particulate and dissolved phases. The fine particles (< 50 µm), which account small fraction of the total solid mass, carry most of the heavy metals (Ball et al., 1998; Westerlund and Viklander, 2006; Helmreich et al., 2010). Among different heavy metals in road runoff, Pb is mainly in particulate phase compared to other heavy metals. Zn^{2+} and Cu^{2+} can be found in both particulate and dissolved phases (**Table 2**). However, their dissolved portions varie with pH value and are different from place to place (44-71% for Zn^{2+} and 33-56% for Cu^{2+}) (Legret and Pagotto, 1999; Baeckstroem et al., 2003). Compare to the particulate heavy metals, the dissolved heavy metals caused more concern for their higher mobility in environment. Moreover, the concentration of dissolved Zn^{2+} and Cu^{2+} even exceed the threshold values of EPA (**Table 2**).

Organic pollutants in road runoff are also found in both particulate and dissolved phases. For example, in the compounds of PAHs (section 2.1.2.1), the heavier molecular weight ones are intend to bind to the particles while the ones with lighter molecular weight are more soluble (Boving and Neary, 2007). Differently, MTBE is always found in dissolved phase due to its highly soluble characteristics.

With sedimentations, lots of measures of BMPs show their good performance in the removal of suspended solids and the related particulate pollutants. However, sediment is not sufficient to remove fine particles and dissolved pollutants from road runoff. Compared to other BMPs, the infiltration systems are expected to obtain better removal of dissolved pollutants because of its extra adsorption and infiltration functions.

2.2.2 Best management practices (BMPs)

BMPs are defined as the measures applied to reduce the impact of stormwater pollutants on the receiving waters and aquatic life (Bruen et al., 2006). Both structural and non-structural measures are included in BMPs. The structural measures of

BMPs comprise detention/retention ponds, wetlands, infiltration and local disposal systems (Lawrence et al., 2010). Additionally, the measures such as road cleaning, modification of land uses and management practices, the management of pollutant build-up, and the modification of use and disposal practices of pollutants are the non-structural BMPs (Lawrence et al., 2010). Although the non-structural BMPs seem to be performed easily in the actual application, it is noticed that the exclusive use of non-structural measures is deficient (Zeng et al., 2012). For instance, the road clean can only remove 30% pollutants and is difficult to apply for big areas (Zeng et al., 2012). Therefore, the structural BMPs are necessary and play an important role in stormwater treatment (Bruen et al., 2006; Zeng et al., 2012).

2.2.2.1 Structural BMPs for particulate pollutant removal

The removal of particles (suspended solids) has been widely considered in BMPs. It is because they could be easily removed by sedimentation and meanwhile the pollutants bond to these particles (particulate pollutants), which account a large fraction of pollutants in road runoff, could be removed simultaneously. Detention/retention ponds, wetlands, and infiltration systems are all effective for suspended solids removal (Shutes and Sriyaraj, 2001; Bruen et al., 2006).

Detention/retention pond is originally built to control flow peak of urban runoff. Meanwhile, the effect of pollutant control is found in these structures (Bruen et al., 2006). The difference between detention and retention ponds is that the detention pond is dry out of the wet weather while retention pond is permanently wet (Bruen et al., 2006). In a case study, the detention pond removes 71% of total suspended solids, 45% particulate organic carbon, 25% of phosphorus, and 26-55% for metal (Stanley, 1996). However, it is also found that the dissolved pollutants loads kept almost same with the loads in the runoff (Stanley 1996). Detention pond shows its limitation in the removal of dissolved pollutants.

Constructed wetlands are widely used for road runoff treatment. Suspended solids and heavy metals can be effectively removed in wetlands. In the research of Earles (1999), 90% of the total suspended solids, 65% of COD, 70% of the total phosphorus, and 50% of Zn were removed in the studied wetland.

Wong et al. (1999) compared the advantages and disadvantages of detention pond and constructed wetland. In both detention pond and wetland, the sedimentation

plays an important role in the pollutants removal. With the existence of macrophytes and epiphytic biofilm, the enhanced sedimentation and surface filtration in the constructed wetland could trap more fine particles and soluble pollutants than detention pond. However, the application of wetland is restricted to the landform (Wong et al., 1999).

Infiltration system includes the soakaways, infiltration trenches, and infiltration basins (Barraud et al., 1999; Hatt et al., 2007). It is effectual for both runoff control and pollutants removal. In the infiltration system, the stormwater infiltrated through soil not only reduce its pollutants loading, but also can be collected underground to recharge groundwater. With the mechanisms of infiltration, adsorption, and ion-exchange of the top soil, infiltration system could remove both particulate pollutant and dissolved pollutant (Hatt et al., 2007).

2.2.2.2 Structural BMPs for dissolved pollutants removal

Compare to the detention/retention ponds and constructed wetland, infiltration systems are more effective for the dissolved pollutants removal. However, the exclusive application of infiltration system shows further potential contamination to the surrounding soil and the ground water (Barraud et al., 1999; Pitt et al., 1999; Hatt et al., 2007). Barraud et al. (1999) found significant heavy metals and hydrocarbons contamination in the top soil. Pitt et al. (1999) reported that the infiltration of highly contaminated urban runoff may pollute groundwater and the adequate pretreatment was required. The similar suggestion is also given by Helmreich et al. (2010), who pointed out the treatment prior to infiltration was needed to avoid the direct contamination or the long-term impact on the infiltration site.

In order to eliminate the potential contamination to soil and ground water, it is necessary to construct filter systems for stormwater treatment, in which the filter material is offered to remove most of the dissolved pollutants before entering the infiltration system. The suitable material could provide adsorption process (e.g. ionic adhesion, ion exchange, and complexation) for dissolved pollutants (Faerm, 2003). Considering the adverse impact of de-icing salt in the ion-exchange process, high adsorption capacity is more expected than ionic exchange for filter material (Athanasiadis and Helmreich, 2005). The materials applied for adsorption of pollutants in road runoff are discussed in the following section.

2.3 Materials used for adsorption

Adsorption with suitable filter materials is expected to remove the dissolved heavy metals and organic substances from road runoff. The adsorbent with large surface area, vesicular structure, and abundant functional groups is believed to offer the strong affinity with target pollutant and high adsorption capacity. There are a large number of potential materials that can be used as adsorbents. However, not all of the adsorbents are suitable for the technical use in road runoff.

Activated carbon and activated lignite are potential materials for adsorption because of their high adsorption capacities, and easy availability. They are widely used to remove heavy metals (Pb^{2+}, Zn^{2+}, Hg^{2+}, Cd^{2+}, and Ni^{2+}) and organic pollutants (methane,1-hexanol, 1,3-dichloropropene) (Kadirvelu et al., 2001; Depci et al., 2012; Lithoxoos et al., 2012; Ridder et al., 2012; Song et al., 2012). The vesicular structure and abundant functional groups of activated carbon and activated lignite are believed as the main contributors for their high adsorption capacities (Soto et al., 2011; Song et al., 2012). Coal and the byproducts from agriculture and industry (fruit shells, coats and husks, cork, oil palms and so on) can be the sources for activated carbons (Soto et al., 2011; Foo and Hameed, 2012). The sufficient sources of activated carbon also expand its application in adsorption. Besides, the surface modification, improvement of carbonization, and the selection of activation methods (chemical, physical, or the combination) could somehow control or change the pore size distribution and the porosity of activated carbons thus increasing its efficiency in adsorption process (Cheng et al., 2005; Soto et al., 2011; Ridder et al., 2012).

Zeolites are also applied for the removal of heavy metals and organic pollutants. High-silica zeolites (with high SiO_2/Al_2O_3 ratio) with high expected adsorption uptake, such as ZSM-5, Mordenite, and zeolite Y, are popularly chosen for organic compounds removal (Anderson et al., 2000; Erdem-Şenatalar et al., 2004; Hung et al., 2005; Stefan, 2006). With ion exchange as the main mechanism, zeolites could also effectively adsorb the dissolved heavy metals from solution (Inglezakis et al., 2002; Athanasiadis and Helmreich, 2005). However, it is not suitable to be used in road runoff treatment for its ion exchange mechanism in adsorption. The adsorbed heavy metals would desorb from adsorbent in contact with de-icing salt in road runoff (Athanasiadis and Helmreich, 2005).

Resins are synthetic polymeric adsorbents, known by their selectivity, high efficiency and capacity in adsorptions (Soto et al., 2011). As ion-exchanger resin can effectively remove heavy metals from aqueous solution. However, similar to zeolite, the adsorbed heavy metals on resins can have the same risk to release and dissolve in solution again with the existence of de-icing salt in road runoff. Although there are some resins applied in organic compound removal, like Ambersorb 563, Optipore L493, Amberlite XAD4 and Amberlite XAD7 in the removal of organic substances as MTBE and tert-butyl alcohol (TBA) (Bi et al., 2005), the mechanism of ion-exchange in heavy metal adsorption makes resins not suitable to be used for road runoff treatment. Furthermore, the cost of resin is higher than other materials.

Clay minerals are also promising adsorption materials for their large specific surface area and sorption capacity (Cruz-Guzmán et al., 2006). Although natural clay mineral can be used for heavy metal adsorption, chemical modification is widely applied to increase its affinity with target substances, especially with hydrophobic compounds (Cruz-Guzmán et al., 2006; Soto et al., 2011;). The insert of alkylammonium-type cations could increase the hydrophobicity of clay mineral surface to attract organic molecules and add functional groups to increase heavy metals affinity. The modified clay minerals are widely used to remove heavy metals, such as Pb^{2+}, Cu^{2+}, Zn^{2+} and Hg^{2+}, and organic substances, such as benzene, tributyltin, and phenolic compounds (*p*-chlorophenol and *p*-nitrophenol) (Akçay M. and Akçay G., 2004; Oyanedel-Craver et al., 2007; Vreysen et al., 2008).

Oxides or hydroxides are also possible materials in adsorption. The complexing ligands in the oxides are considered for the uptake of heavy metals (Davis and Leckie, 1978; Smith, 1996; Liu et al., 2009) while the hydrophobicity and coordinative capacity of oxides are responsible for the organic pollutants removal (Choo and Kang, 2002). Recently, the application of zero-valent iron has caused increasing attention. It is found the zero-valent iron could remove heavy metals and organic pollutants with the oxidation-reduction reaction (Keum and Li, 2004; Bang et al., 2005). Moreover, their oxides or hydroxides could still work for further removal of pollutants.

Bioadsorbent is another group of adsorbents causing attention for adsorption. The sources of them are mostly the wastes from fermentation and agriculture, which are abundant and costless (Soto et al., 2011). Furthermore, vesicular structure and plenty of functional groups are found in lots of bioadsorbents leading to high

adsorption capacity of pollutants. Among various bioadsorbents, bacteria, yeast, algae, and fungi are popular ones causing great interest (Gupta and Ali, 2004; Volesky, 2007).

2.4 Theory of adsorption

Adsorption is a process that substance in solution accumulates on the surface of adsorbents. In the process, the dissolved substances (pollutants) are transferred from the liquid phase to the solid phase, and therefore removed from solution (Tchobanoglous et al., 2003). The adsorbate is the substance removed from solution and the adsorbent is the solid material on which adsorbate accumulates.

2.4.1 Sorption mechanisms

With different adsorbates and adsorbents, different mechanisms are involved in adsorption. Monolayer, multilayer, pore filling are the familiar mechanisms for adsorption (**Fig. 1**). Besides, in the adsorption of organic compounds, another phenomenon of partitioning might be observed, especially when the adsorbent contains high content of natural organic matter (NOM) (Stefan, 2006).
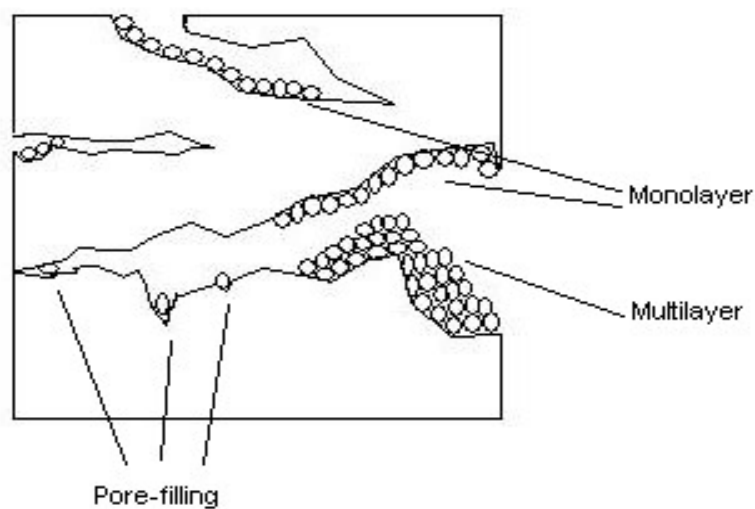
Fig. 1 The sketch of adsorption mechanisms

2.4.1.1 Monolayer, multilayer and pore filling

In adsorption processes, the adsorbates can be bound to the solid surface by chemical bonding, Van der Waals force, and electrostatic force to form monolayer or multilayer on the surface of adsorbent.

In monolayer adsorption, all the adsorbates are directly adsorbed on the adsorbent surface. As assumed in Langmuir isotherm model, which is the typical isotherm for monolayer adsorption, the adsorbent has a homogeneous surface, all adsorption sites are energetically equivalent, and there are no interactions between the adsorbed molecules (Langmuir, 1918).

Different from the monolayer assumptions of Langmuir, another popular isotherm, Freundlich isotherm model, supposes a heterogeneous surface of adsorbents with various adsorption sites (Freundlich, 1907). Brunauer-Emmett-Teller (BET) isotherm, which is widely applied for gas-solid system, is built up on multilayer adsorption (Soto et al., 2011). In the multilayer adsorption, adsorption behavior happens not only on the surface of adsorbent itself, the adsorbed molecules on adsorbent surface can be the new 'surface' to bind other free adsorbates (Stefan, 2006).

Pore filling is regarded as the suitable mechanism to describe the adsorption of organic compounds, for which the adsorption usually happens on meso- and micro-porous solids (Kleineidam et al., 2002). Based on the IUPAC classification, pores with widths not exceeding about 2 nm are micro-pores; pores with widths between 2 nm and 50 nm are meso-pores; and pores with widths exceeding about 50 nm are macropores (Sing et al., 1985). Polanyi-Dubinin-Manes (PDM) isotherm, derived from Dubinin-Astakhov (DA) equation, is usually used to depict the pore-filling mechanism (Davis et al. 2000; Kleineidam et al., 2002; Ran et al., 2004).

Dubinin-Radushkevich (D-R) isotherm model was applied for the experimental data of bioadsorbent to identify the physical or chemical processes in adsorption (Benhammou et al., 2005; Akar et al., 2009).

2.4.1.2 Partitioning

When adsorbent contains high amount of NOM, a partitioning behavior of organic adsorbate would be observed on the adsorbent. This partitioning behavior is described with a partitioning coefficient in a linear form for its linearity character of adsorption (Kleineidam et al., 2002; Ran et al., 2004; Bi et al., 2005).

The corresponding isotherms for these different adsorption mechanisms are discussed in the following sections.

2.4.2 Adsorption isotherms

Isotherm models are wildly used to analyze adsorption behaviors for different adsorbents and adsorbates by depicting the balance of adsorbate concentrations between solid (adsorbent surface) and aqueous phases. With different hypotheses, various isotherm models imply different mechanisms in adsorption process.

2.4.2.1 Linear isotherm

In linear isotherm model, the adsorbate concentration on solid surface is simply described proportionally to the concentration of aqueous phase with K (L/g) as the distribution coefficient.

$$q_e = K \cdot C_e \tag{1}$$

where q_e (mg/g or µg/g) is the adsorbed amount of adsorbate on adsorbent, C_e (mg/L or µg/L) are the initial and final concentrations of adsorbate in the aqueous phase.

The partitioning behavior is described in linear form, as Equation (2) (Kleineidam et al., 2002; Ran et al., 2004; Bi et al., 2005):

$$q_e = (K_{oc} \cdot f_{oc}) \cdot C_e \tag{2}$$

where $(K_{oc} \cdot f_{oc})$ is the partitioning coefficient with K_{oc} (L/kg), organic carbon normalized partitioning coefficient and f_{oc} (%), fraction of organic carbon of adsorbents.

2.4.2.2 Non-linear isotherm with two-fitting parameters

Freundlich and Langmuir isotherm models are the widely used two-fitting-parameter isotherms for non-linear adsorption analysis.

Freundlich isotherm model (Equation 3) and its linear form (Equation 4) (Freundlich, 1907):

$$q_e = K_f \cdot C_e^{1/n} \tag{3}$$

$$\log q_e = log K_f + 1/n \cdot log C_e \tag{4}$$

where K_f (mg/g) (L/mg)$^{1/n}$ and n ($n > 1$) are the coefficients of Freundlich model. K_f denotes the maximum adsorption capacity while n indicates the adsorption intensity or heterogeneity of adsorbents.

Langmuir isotherm model (Equation 5) and its linear form (Equation 6) (Langmuir, 1918):

$$q_e = q_m \cdot K_l C_e / (1 + K_l C_e) \tag{5}$$

$$C_e / q_e = 1/(K_l \cdot q_m) + C_e / q_m \tag{6}$$

where q_m (mg/g or µg/g) is the saturated amount of adsorbate on adsorbents. K_l (L/mg or L/µg) is Langmuir parameter, indicating the consumed energy in the adsorption process.

2.4.2.3 Non-linear isotherm with three-fitting parameters

Tóth and PDM models were taken as three-fitting-parameter isotherms in this study. With the introduced fitting parameter, Tóth isotherm (Zhao et al., 2011) improves Langmuir isotherm fitting with experimental data and develops the description of heterogeneous adsorption system by considering both low and high concentration boundaries (Foo and Hameed, 2010). PDM isotherm, which presents the pore-filling mechanism, is derived from DA equation (Kleineidam et al., 2002). DA equation based on Polanyi's potential theory was used for vapor system originally. Manes (1998) developed the application of DA equation to aqueous system as the PDM isotherm model. It is reported that PDM isotherm is very suitable for organic compound adsorption on micro-porous materials (Davis et al., 2000; Kleineidam et al., 2002; Ran et al., 2004).

Tóth isotherm (Equation 7) and **PDM isotherm** (Equation 8) (Zhao et al., 2011):

$$q_e = q_m \frac{K_t \cdot C_e}{(1 + (K_t \cdot C_e)^b)^{1/b}} \tag{7}$$

$$q_e = V_0 \cdot \rho_0 \cdot \exp\left(-\left(\frac{RT ln \frac{S}{C_e}}{E}\right)^a\right) \tag{8}$$

where 'q_m, K_t, b' and 'V_0, E, a' are the 'fitting parameters' in Tóth and PDM isotherms, respectively. K_t (L/g) is the Tóth adsorption coefficient; b (-) represent the heterogeneity of adsorbent surface. If $b=1$, Tóth isotherm is turned to Langmuir isotherm. The further the value of b is away from '1', the more heterogeneity the

adsorbent surface obtains (Terzyk et al., 2003). In PDM isotherm, V_0 (L/g) is the occupied micro-pore volume on adsorbent; ρ_0 (mg/L) denotes the density of adsorbate; R is the ideal gas constant, 8.3145 J/(mol·K); T (K) is the absolute temperature, 297 K in this study; S (mg/L) is the solubility of adsorbate ; E (kJ/mol) indicates the free energy of adsorption; a (-) is an empirical exponent which indicates the heterogeity of adsorbent surface. The maximum adsorption capacity q_m can be calculated by

$$q_m = V_0 \cdot \rho_0 \tag{9}$$

D-R isotherm (Equation 10-12) (Dubinin and Radushkevich, 1947):

$$\ln q_e = \ln q_m - K_D \varepsilon^2 \tag{10}$$

where K_D (mol^2/kJ^2) is the constant which is related to the calculated average sorption energy E, and ε (kJ·mol) is the Polanyi potential, which is described as:

$$\varepsilon = RT \cdot \ln(1+1/C_e) \tag{11}$$

where R is the gas constant, 8.3145 J/(mol·K); T (K) is the absolute temperature. q_e, q_m and C_e have the same meaning as before, but in different units, which are mol/g, mol/g and mol/L, respectively. The average sorption energy E is calculated as:

$$E = (2K_D)^{-0.5} \tag{12}$$

As an index of consumed energy in adsorption, E presents the free energy per mole of metal ions transferring from infinity in solution to the adsorbent surface (Onyango et al., 2004). If the magnitude of E is less than 8 kJ/mol, it suggests that the physical process dominates in adsorption; if the value of E is between 8 and 16 kJ/mol, the adsorption would have a chemical nature. Based on studies of other materials, this chemical nature was assumed to be the ion-exchange mechanism (Dubey and Gupta, 2005; Benhammou et al., 2005).

2.4.3 Adsorption kinetics

Adsorption kinetics is described as film diffusion, intra-particle diffusion or a combination of both. Film diffusion includes the movement of adsorbate from bulk solution to the external surface (shell and macro-pores) of the adsorbent, while intra-particle diffusion indicates the transfer of adsorbate into the inner pores (meso- and micro-pores) of adsorbent (Long et al., 2009).

Pseudo kinetics models (Lagergren et al., 1898; Ho et al., 1998, 1999; Kumar et al., 2006) are the most common models for adsorption kinetics. The non-linear and linear equations of pseudo kinetics model are as follows (Equation 13-16):

Pseudo first-order model (Lagergren et al., 1898):

$$dq_t/dt = K_1 \cdot (q_e - q_t) \tag{13}$$

$$\log(q_{e,exp} - q_t) = \log q_{e,cal} - K_1 \cdot t/2.303 \tag{14}$$

Pseudo second order model (Ho et al., 1998; 1999):

$$dq_t/dt = K_2 \cdot (q_e - q_t)^2 \tag{15}$$

$$t/q_t = 1/h + (1/q_{e,cal}) \cdot t; \quad h = K_2 \cdot q_{e,cal}^2 \tag{16}$$

where q_t (mg/g or µg/g) is the adsorbed amount of adsorbate at time t (min); $q_{e,exp}$ (mg/g or µg/g) and $q_{e,cal}$ (mg/g or µg/g) are the experimental and calculated adsorption amount at equilibrium; K_1 (1/min), K_2 (g/(mg·min) or g/(µg·min)) and h (mg/(g·min) or µg/(g·min)) are the kinetic constants in the pseudo kinetics models.

With an overall kinetics rate, they can conveniently describe the kinetics of adsorption (Azizian et al., 2004; Chang and Juang, 2004). However, they are not able to identify the adsorption mechanisms or rate-controlling step. Therefore, the intra-particle model (Weber and Morris, 1963) and Boyd model (Boyd et al., 1947; Gasser et al., 2006) were chosen to clarify the diffusion type and to find out the rate-controlling step in the adsorption process (Equation 17 and 18-20).

Intra-particle model (Weber and Morris, 1963):

$$q_t = K_i \cdot t^{1/2} \tag{17}$$

Boyd model (Boyd et al., 1947; Gasser et al., 2006):

$$q_t/q_e = 1 - (6/\pi^2)\exp(-B_t) \tag{18}$$

$$B_t = -0.4977 - \ln(1 - q_t/q_e) \tag{19}$$

$$B = \pi^2 \cdot D_i/r^2 \tag{20}$$

where the k_i (µg/(g·min$^{1/2}$)) is the intra-particle diffusion rate in Intra-particle model; B is the slope of B_t-t plot; D_i (cm^2/s) is the self-diffusion coefficient; r (cm) is the radius of the adsorbent granule, which is 1.75 mm in this study. If the diffusion coefficient (D_i) varies at 10^{-6}-10^{-8} cm^2/s, film diffusion is the rate limiting step while the value

between 10^{-11}-10^{-13} cm^2/s indicates the pore diffusion is the rate determining step (Michelson, 1975).

The comparison of the plots of these kinetics models are listed in **Table 3**.

Table 3 Models for adsorption kinetics

Kinetics Model	Linear Form	Plot
Pseudo first-order (Lagergren et al., 1898)	$log\ (q_e - q_t) = log\ q_{e,cal} - (K_1 / 2.303) \cdot t$	$log\ (q_e - q_t)$ VS t
Pseudo second-order (Ho et al., 1998; 1999)	$t / q_t = 1/h + (1/q_{e,cal}) \cdot t;$ $h = K_2 \cdot q_{e,cal}^2$	t / q_t VS t
Intra-particle (Weber and Morris, 1963)	$q_t = K_i \cdot t^{1/2}$	q_t VS $t^{1/2}$
Boyd (Boyd et al., 1947; Gasser et al., 2006)	$B_t = -0.4977 - ln\ (1 - q_t / q_e);$ $B = \pi^2 \cdot D_i / r^2$	B_t VS t

3. The aim of this study

In this study, different adsorbent materials were evaluated to choose a suitable one as a filter material in a BMP system applied to road runoff treatment to remove dissolved pollutants. The filter material is required not only to remove the heavy metals, but also to absorb the organic pollutants (PAHs and VOCs) in road runoff. Therefore, the potential adsorbent materials were chosen based on their performance in heavy metals removal.

Nap and MTBE were chosen as the representative compounds of PAHs and VOCs and set as the target organic pollutants in experiments due to their typical characteristics and common existence in road runoff.

Bioadsorbents, red alga (Palmaria Palmata) and beer draff, and other four traditional adsorbents, activated carbon (F300), activated lignite (HOK), semi-organophilic bentonite (Tixosorb), and sponge iron (DRI), were the adsorbents in experiments. The adsorption abilities of bioadsorbents for heavy metals were first tested. The other four materials were tested directly in experiments for Nap and MTBE removal since they had been widely applied as adsorbents for heavy metal removal (Smith, 1996; Kadirvelu et al., 2001; Oyanedel-Craver et al., 2007; Vreysen et al., 2008; Liu et al., 2009; Song et al., 2012).

Batch experiments and column experiments were carried out with single or multi-pollutants. Different isotherms (Freundlich, Langmuir, Tóth and Polanyi-Dubinin-Manes (PDM) models) and kinetics models (pseudo first/second-order models, intra-particle model and Boyd model) were applied to analyze the adsorption process. Additionally, the effects of pH value, de-icing salt, and natural organic matter (NOM) were determined.

By the experiments and analysis, the following goals are to be achieved: 1) the most effective adsorbent for road runoff treatment; 2) the control factor(s) for heavy metals, Nap, and MTBE adsorption; 3) the adsorption behaviors of the different adsorbents; 4) the best isotherm and kinetics model to fit the adsorption process; 5) the effect of pH, de-icing salt, and NOM on adsorption; 6) the removal efficiencies of the chosen adsorbents in column study.

4. Materials and methods

4.1 Adsorbents
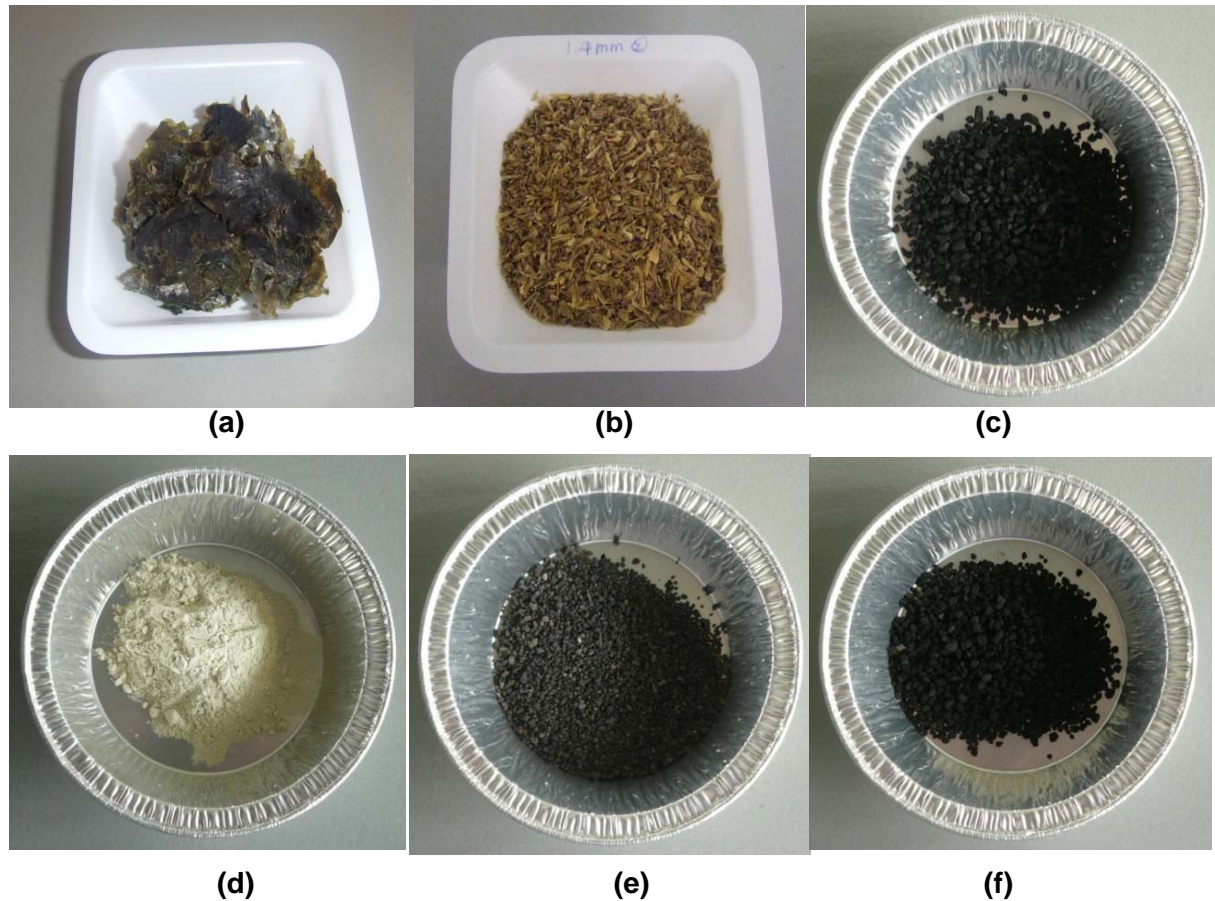
Fig. 2 Adsorbents (a) Red alga (*Palmaria palmata*), (b) Beer draff, (c) F300, (d) Tixosorb, (e) DRI, (f) HOK

There were six potential materials used in experiments as adsorbents. Two of them are bioadsorbents: red alga (*Palmaria palmata*), provided by Cfm Oskar Tropitzsch e.K., Germany, and beer draff, from Bavarian State Brewery Weihenstephan, Germany. The other four materials as adsorbents are granular activated carbon (F300, from Chemviron Carbon GmbH, Germany), granular activated lignite (HOK, from Rheinbraun Brennstoff GmbH, Germany), semi-organophilic bentonite (Tixosorb, from Sued-Chemie AG, Germany), and granular sponge iron (DRI, from Fentai Abrasive Material Company, China).

At the pretreatment step, red alga, beer draff, F300, and HOK were firstly rinsed several times with deionized water (Milli-Q) (18.2 MΩ·cm) until the filtrate was colorless. They were subsequently dried overnight at required temperatures (60±2°C for red alga and beer draff while 105±2°C for F300 and HOK). Then, red alga and

23

beer draff were ground into pieces. The size of red alga was under 450 μm while that of beer draff was kept at 450 μm-1.4 mm (to remove the big grain). F300 and HOK were sieved to obtain a granule size range of 1-2.5 mm. Afterwards, they were dried again (60±2°C for red alga and beer draff and 105±2°C for F300 and HOK) until a constant weight was achieved. Different from them, Tixosorb was used in its original powder form (<2 μm), while DRI was sieved to the size of 0.75-2 mm before drying (105±2 C). A desiccator was used to store all these dry materials until use.

4.2 Adsorbates

MTBE (≥99.9%, GC grade) and Nap (≥99.7%), both from Sigma-Aldrich Chemistry GmbH (Germany), were used as organic adsorbates while the stock solutions of copper nitrate ($CuNO_3$) and zinc nitrate ($ZnNO_3$) (Merck KGaA, Germany) containing 1,000 mg/L Cu^{2+} or Zn^{2+}, were used as heavy metal adsorbates in the following experiments. By diluting with the corresponding solvent, desired concentrations were obtained.

4.3 Solvents

All adsorption experiments were carried out in Milli-Q water. In the experiments with MTBE and Nap, a constant pH value of 7 was maintained by adding a phosphate buffer of potassium phosphate monobasic (KH_2PO_4, Sigma-Aldrich Chemie GmbH, Germany) 3.48 g/L and di-sodium hydrogen phosphate dehydrate ($Na_2HPO_4 \cdot 2H_2O$, Merck KGaA, Germany) 7.26 g/L. In the experiments with Cu^{2+} and Zn^{2+} and the experiments where the effect of pH was investigated, required pH values were controlled by adding nitric acid (HNO_3) and sodium hydroxide (NaOH).

4.4 Batch experiments

4.4.1 Experiments for heavy metals adsorption on bioadsorbents

Adsorption experiments were carried out in 50 mL polypropylene vessels. Batch experiments were conducted by varying the pH value (1, 2, 3, 4.5 and 6), contact time (5, 10, 20, 30, 50, 90, 120, 150 and 180 min), and adsorbate concentration (5, 10, 25, 50 and 100 mg/L). pH 6 was the maximum pH value in all experiments so as to avoid precipitation.
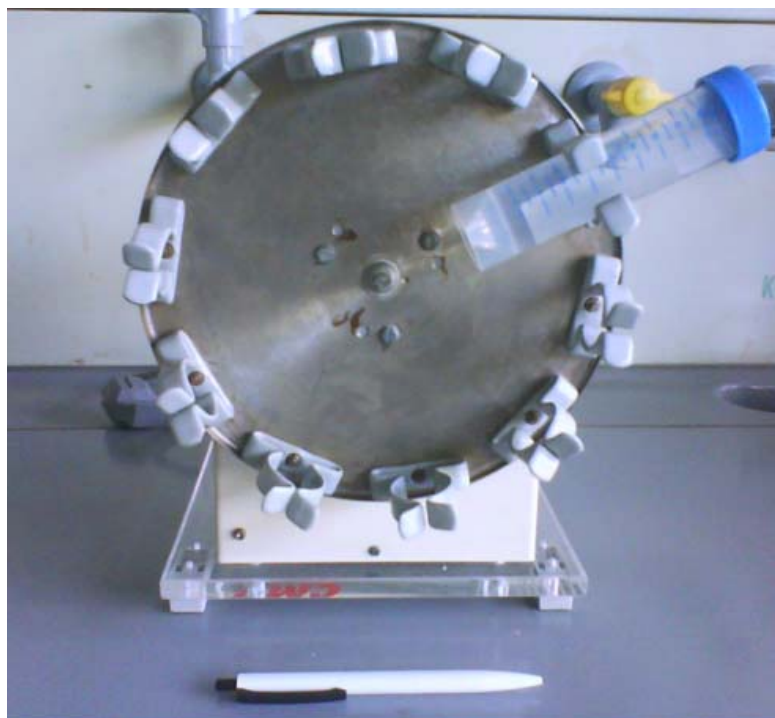
Fig. 3 Rotary shaker in the experiment for heavy metal adsorption

For equilibrium experiments, 0.1 g adsorbent was dispersed in a 50 mL aliquot of the metal ion solution at desired concentration in the vessel, which was then shaken on a rotary shaker at the speed of 40 rpm for 24 hours (**Fig. 3**). All experiments were carried out at room temperature (22±2°C) in duplicate.

Except during equilibrium experiments, the initial Cu^{2+} concentration and pH value were kept constant at 10 mg/L and pH 6 (unless otherwise stated).

In desorption experiments 0.1 g bioadsorbent was first treated for 12 h with a 10 mg/L copper solution, then filtered, and dried at 60±2°C overnight before use. The loaded sorbent was then agitated in 50 mL desorbing solution for 90 minutes at 40 rpm. For the desorbing solutions, HNO_3 and Sodium chloride (NaCl) were prepared in a wide range of concentrations (1 mmol/L, 10 mmol/L, and 100 mmol/L). To eliminate the disturbance of water, deionized water was used as blank. All experiments have been done twice.

4.4.2 Experiments for MTBE and Nap adsorption

4.4.2.1 Adsorption and kinetics experiments

Adsorption experiments were carried out over a wide range of concentrations, specifically 2.0 µg/L-15 g/L for MTBE and 1.0 µg/L-18 mg/L for Nap. Additionally, two pH values (pH 5 and pH 7) were chosen to identify their effects on adsorption.

In each experiment, 2 g adsorbent was added to a 100 mL aliquot of MTBE or Nap solution at the desired concentration. Mixing was performed by a rotary shaker at the speed of 20 rpm for 24 hours (**Fig. 4**). Afterwards, samples were filtrated with a glass microfiber filter (Whatman GF/C 1.2 µm filter) and stored at 4±1°C. All experiments were completed in duplicate at room temperature (24±2°C). Blank experiments were also conducted.

Fig. 4 Rotary shaker in the experiment for MTBE and Nap adsorption

Kinetics experiments were carried out following the similar process, but samples were taken at different reaction time, which were 3, 5, 10, 20, 30, 60, 120 and 180 min.

Glass bottles with different volumes and Teflon-lined screw caps were offered for all experiments. 100 mL bottles were used for reaction, while 24 mL and 2 mL vials were applied for the sampling of MTBE and extracted Nap, respectively. All experiments have been done twice.

4.4.2.2 Experiments to test the influence of de-icing salt

NaCl (≥99%, AppliChem GmbH, Darmstadt, Germany) acted as de-icing salt in experiments at two concentrations, 3 g/L and 5 g/L, to test its influence on MTBE and Nap adsorption, in which the initial concentrations of MTBE and Nap were both kept at 1 mg/L. All experiments have been done twice.

4.4.2.3 Experiments to test the influence of NOM

Humic acid (Carl Roth GmbH, Karlsruhe, Germany) was provided as NOM to test its influence on adsorption of MTBE and Nap in duplicate. The concentrations of NOM were controlled as total organic carbon (TOC) at 4 mg/L and 10 mg/L (after filtration with Whatman GF/C 1.2 µm filter). The initial concentrations of MTBE and Nap were over a wide range, which were 55 µg/L-2,000 mg/L for MTBE and 100 µg/L-28 mg/L for Nap.

4.4.2.4 Experiments with bi-adsorbate in adsorption

Co-adsorption experiments with bi-adsorbate were carried out to investigate the interaction and influence of the second adsorbate on MTBE and Nap adsorption. In experiments, Nap or Zn^{2+} was separately offered to MTBE adsorption as the second adsorbate, while MTBE or Zn^{2+} was provided to Nap adsorption separately as the second adsorbate. Experiments with high initial concentrations of MTBE and Nap (170-2,000 mg/L for MTBE and 4-28 mg/L for Nap) were conducted to avoid the competition between two adsorbates weakened as the presence of abundant available adsorption sites at low concentrations (Frimmel et al., 1999). Different from the variable initial concentrations of MTBE or Nap, the concentration of the second adsorbate was fixed. As the second adsorbate, MTBE, Nap and Zn^{2+} had an initial concentration of 1 mg/L, 1 mg/L and 1.5 mg/L, respectively. All experiments have been conducted in duplicate.

4.5 Column experiments

The rapid small-scale column tests (RSSCTs) were conducted at ambient temperature (23±2°C). Experimental apparatus were all constructed of glass and Teflon in order to minimize their influence on organics adsorption. The glass column has a diameter of 2 cm and a length of 23 cm (**Fig. 5**). A glass screen was provided at the bottom of the column to support the filter materials. Influent went through glass columns in up-flow mode (from bottom to top), since it had been proved more efficient than down-flow mode (from top to bottom) (Athanasiadis, 2005). The flow rate of influent was controlled at 3 mL/min by a peristaltic pump (Ismatec IPC-04, Ismatec SA, Zurich, Switzerland). The empty bed contact time (EBCT) was hereby kept at 20 min. **Table 4** lists other parameters for each RSSCT in detail. Prior to each run of RSSCTs, Milli-Q water was fed into the adsorber columns for approximately

one hour to soak the adsorbent material and remove the inside air bubbles, setting up the identical experimental conditions. After that, the influent was switched to the experimental solution with specific pollutant to start the RSSCTs. Samples of effluent were taken at required time and filtrated with a glass microfiber filter (Whatman GF/C 1.2 µm filter) before storing in fridge at 4±1°C. Glass bottles with Teflon-lined screw caps were applied for sampling.

Fig. 5 Columns in RSSCTs

Except the experiments with Zn^{2+}, the phosphate buffer (3.48 g/L KH_2PO_4) and 7.26 g/L $Na_2HPO_4 \cdot 2H_2O$) was used to obtain a constant pH value of 7 in influent. For the influent with Zn^{2+}, HNO_3 and NaOH were offered for pH control to prevent the formation of $Zn_3(PO_4)_2$ precipitation.

Breakthrough curves, in this study, were depicted as effluent concentration versus treated volume of water, to analyze the adsorption behavior of each RSSCT. The adsorbent usage rate (AUR), which indicates the amount of adsorbent needed per volume of contaminated water (with a unit of g/L), and adsorption capacity, which denotes the amount of adsorbed pollutant per amount of adsorbent (with a unit of mg/g), were used as criteria for adsorbent performance in RSSCTs. The low AUR value and high capacity value suggest good adsorbent performance in the efficient pollutant removal (Abu-Lail, 2010).

Table 4 The parameters of each RSSCT

Testing number	Pollutant(s)	Influent concentration (mg/L)	Adsorbent(s)	Adsorbent weight (g)
1	MTBE	16	F300	30
2	Nap	5	F300	30
3	Zn^{2+}	15	F300	30
4	MTBE	16	HOK	35
5	Nap	5	HOK	35
6	Zn^{2+}	15	HOK	35
7	MTBE/NOM	16/10[a]	F300	30
8	MTBE/Zn^{2+}	16/11	F300	30
9	MTBE/Zn^{2+}	16/11	F300/HOK (50 : 50 Mixture)	15/17.5
10	MTBE/Zn^{2+}	16/11	F300/HOK (50 : 50 Two-layer)	15/17.5

[a] the concentration of NOM is measured as TOC

4.6 Analytical procedure

4.6.1 Analyses for bioadsorbents in heavy metal removal

Cu^{2+}, Zn^{2+}, and Na^+ analyses were carried out by atomic absorption spectrometry (Varian Spectr AA-240Z with GTA 120) according to the standard methods 3111 and 3113 (Eaton et al., 2005).The samples were acidified prior to analysis to a pH below 2. The detection limits were 5 µg/L and 0.5 µg/L for Cu^{2+} and Zn^{2+}, respectively.

The study of Fourier transform infra-red spectroscopy (FTIR) was carried out by the FTIR Vertex 70 (Bruker Company, with ATR-CELL). Energy dispersive X-ray emission (EDX) analyses were done with an XL 30 FEG ESEM Instrument (Company Philips, with EDX detector). The adsorbent samples used in FTIR and EDX analysis were first treated in a 100 mg/L copper solution, agitating for 12 hours.

The process of potentiometric and conductometric titration includes protonation and titration. Protonation was achieved by dispersing 0.1 g of the adsorbents in 50 mL 0.01M HNO_3 for 2 hours. After filtration, washing and drying, the dried adsorbent was dispersed again in deionized water (2 g/L) for titration. While NaOH (0.05 mol/L) was added for titration, electrical conductivity and pH value were measured with a conductivity meter (WTW LF 191) and microprocessor pH-meter pH 526 (WTW), respectively.

4.6.2 Analyses for MTBE and Nap removal

MTBE concentrations were analyzed by gas chromatography (GC) and mass spectrometry (MS), using a GC/MS-System 2200 from Varian Inc., with the method of headspace-GC/MS. 10 mL of the MTBE sample were transferred into a 20 mL headspace vial containing 4 g of NaCl. The headspace vial was sealed with a septum cap and put into the headspace sampler, which was heated to 80°C and shaken for 20 minutes before analysis. The sampler subsequently took 1 mL of the gas-steam-mixture from the headspace and injected it into the GC (split injection at 150°C, ratio 1:2 to 1:30 depending on the MTBE concentration). The specification of the column was as follows: DB-1, length 30 m, inner diameter 0.25 mm, and film thickness 2 μm. The temperature program used was as follows: 80°C (1 min), heating up to 155°C with 12°C/min, and then with 40°C/min up to 220°C (9 min). Calibration was performed by the external standard method via a 5-point calibration curve. The detection limit was 0.1 μg/L and the accuracy was ± 10%.

Nap concentrations were measured by GC/MS (Varian, CP 3800 Saturn 2200) according to EPA 610 (1982). The detection limit was 0.1 μg/L and the accuracy was ± 10%.

The micro-pore volume, meso-pore volume, pore size distribution, and BET surface area of the adsorbents were characterized with the nitrogen adsorption and desorption principle at 77 K (Sorptomatic 1990, Porotec GmbH, Germany). The micro-pore and meso-pore volumes were calculated by the Horvath-Kawazoe (HK) theory (Horvath and Kawazoe, 1983) and Barrett-Joyner-Halenda (BJH) theory (Barrett et al., 1951), respectively. BET surface area was obtained based on the BET equation (Brunauer et al., 1938). Macro-pore volume and distribution were also measured by mercury intrusion porosimetry (Quantachrome Pore master 60, USA). In this study, the pore sizes for micro-, meso- and macro-pores are 5-20 Å, 20-300 Å, and >300 Å, respectively.

Elemental analysis of carbon (C), hydrogen (H), and nitrogen (N) of adsorbents was conducted by a Vario EL analyzer (Elementar, Germany) with the detection limit of 0.1 wt.%. TOC was measured by an analyzer of Elementar High TOC II analyzer (Elementar Analysensysteme GmbH, Germany) according to SM 5310 with the detection limit of 1 mg/L.

The degree to which adsorbates were adsorbed was determined via the following equation:

$$q_e = (C_0 - C_e) \cdot V / m_{adsorbent} \tag{21}$$

where C_0 (mg/L or µg/L) is the initial concentration of adsorbate in the aqueous phase, q_e, C_e have the same meaning as before, V (L) is the volume of solution, and $m_{adsorbent}$ (g) is the weight of adsorbent used in the experiments (2 g/100 mL in this study). The removal efficiency is calculated via Equation 22:

$$R\% = (1 - C_e/C_0) \cdot 100\% \tag{22}$$

5. Results and discussion

5.1 Biosorption of Cu^{2+} from aqueous solution by red alga (Palmaria palmata) and beer draff*

Biosorption, which is defined as adsorption onto the surface of microbial biomass through passive metal-bonding of a bioadsorbent (Davis et al., 2003; Voslesky, 2007), is regarded as an effective option for heavy metal removal, especially at low concentrations (Yan and Viraraghavan, 2003; Villaescusa et al., 2004; Voslesky, 2007).

Bioadsorbents are of great interest because they are abundantly available, costless, and effective in adsorption. Among various bioadsorbents, algae have a high capacity of metal-bonding, most likely due to the abundant existence of various functional groups as carboxyl, sulphonic, amino and hydroxyl groups (Holan et al., 1993; Voslesky, 2007; Murphy et al., 2007;). The main mechanisms of metal-bonding include ionic interactions and complex formation between metal cations and ligands on the bioadsorbent surface (Yun et al., 2001). However, quality and quantity of mechanisms in biosorption vary from types of adsorbent, reaction conditions, and types of adsorbed metal ions. In many biosorption processes more than one of these mechanisms take place simultaneously and it is difficult to distinguish between the single steps (Lacher and Smith, 2002).

In this section, the red alga (*Palmaria palmate*) and one kind of by-product from brewery (beer draff) were chosen to adsorb Cu^{2+} ions from aqueous solution. The effects of the pH, initial metal concentration and contact time on the adsorption behavior of these bio-sorbents were determined. Two kinetic models (pseudo first-order model and pseudo second-order model), three isotherm models (Langmuir, Freundlich and D-R models), and two spectroscopy (FTIR and EDX) were used to explain the possible mechanisms of the adsorption process. A sodium chloride solution and nitric acid were applied in desorption experiments. The former was used to clarify the influence of de-icing salt in the adsorption process and nitric acid was used to provide a method for recycling the materials after saturation with heavy metals.

5.1.1 Equilibrium experiments

5.1.1.1 Effect of pH

As shown in **Fig. 6**, the pH value was a crucial factor in Cu^{2+} adsorption. At low pH values (pH=1), almost no adsorption happened. The low adsorption capacity revealed an enhanced competition between hydrogen ions and copper ions. From pH 2 to pH 4.5, the adsorption capacity for both materials increased from 0.25 mg/g to 3.72 mg/g for red alga and 0.0 mg/g to 4.00 mg/g for beer draff and remained constant since pH 5. Therefore, pH 5-6 was the optimum range for Cu^{2+} adsorption on both materials, which was also in accordance with the pH value of polluted road runoff.
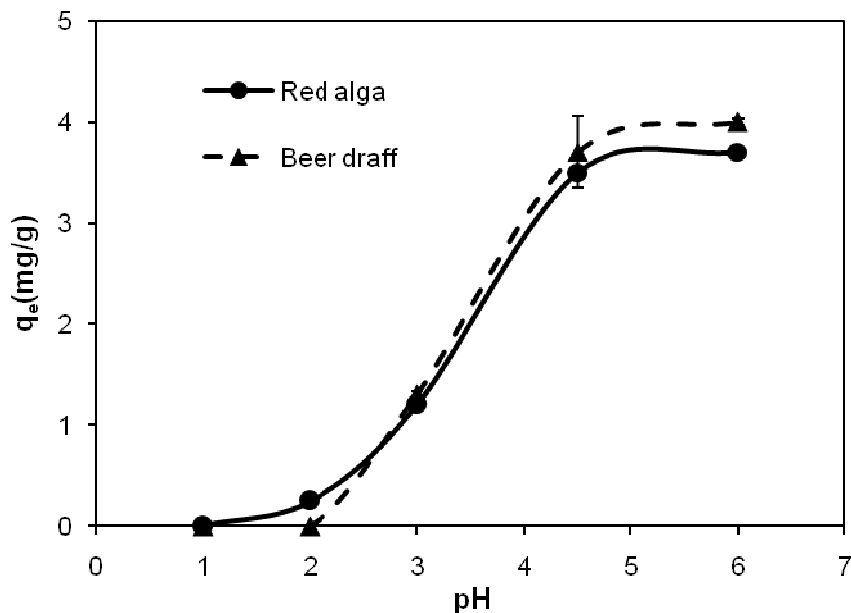
Fig. 6 Effect of pH on Cu^{2+} adsorption

5.1.1.2 Effect of initial concentration

The adsorption capacity of Cu^{2+} increased with the increase of the initial copper concentration (**Fig. 7**). However, the adsorption capacity increased distinctly at low initial concentrations (up to 20 mg/L), but relatively indistinctive from 20 to 100 mg/L. At initial concentrations of 5 mg/L and 10 mg/L, the amount of adsorbed Cu^{2+} was nearly the same for both materials (2.16 mg/g and 4.00 mg/g for beer draff; 2.21 mg/g and 3.72 mg/g for red alga). Nevertheless, the adsorption capacity of beer draff was lower than that of red alga at high initial concentrations (8.75 mg/g and 11.75 mg/g for beer draff and red alga respectively at 100 mg/L).

34
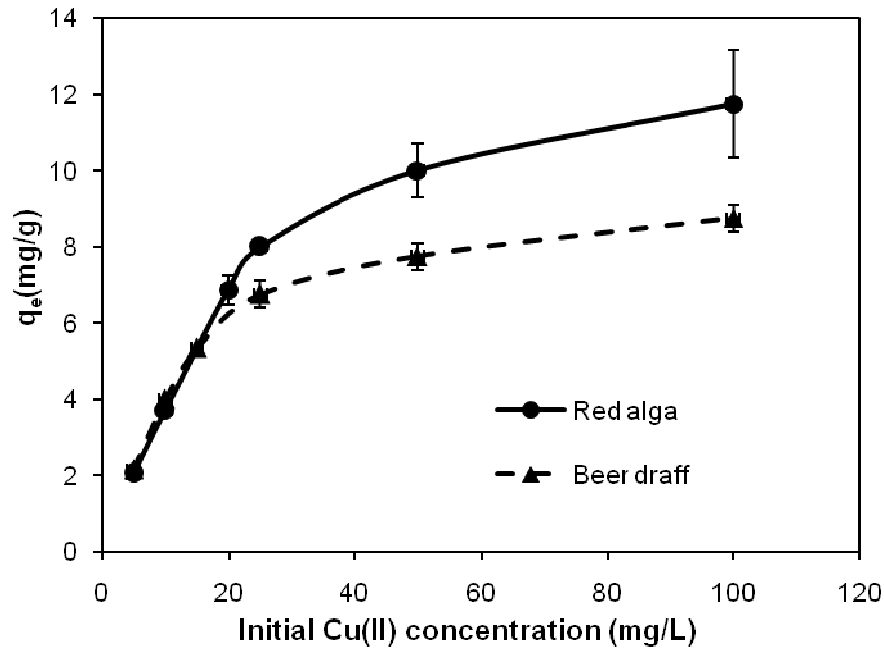
Fig. 7 Effect of initial concentration on Cu^{2+} adsorption (pH 6)

The significant increase of adsorption capacity with increasing initial adsorbate concentration was also observed on cork, yohimbe bark, and sawdust (Yu et al., 2001; Villaescusa et al., 2000, 2004; Ahmad et al., 2007). For cork, the adsorbed copper amount varied from 0.39 mg/g at initial copper concentration of 5 mg/L to 1.43mg/g at 20 mg/L, further to 2.64 mg/g at 100 mg/L. Yohimbe bark had similar adsorption behavior. The adsorbed copper amount increased from 0.90 mg/g to 2.84mg/g when the copper concentration increased from 10 mg/L to 30 mg/L and achieved 7.51 mg/g at a copper concentration of 100 mg/L.

Higher concentrations result in a greater driving force at the liquid solid interface, which in turn enhances the mass transfer (Ngah and Hanafiah, 2008). Less competition between the free bonding sites caused faster initial adsorption. When the unoccupied bonding sites decreased, copper adsorption became more difficult and slower until equilibrium was achieved.

5.1.1.3 Effect of contact time

The effect of contact time and initial copper concentration is presented in **Fig. 8**. Similar kinetic processes were presented at different concentrations. Fast adsorption occurred at the beginning and then slowed down until equilibrium was achieved. In the first 20 minutes, more than 50% of adsorption was achieved. However, the duration of the slow adsorption portion varied with concentrations and adsorbents;

the shortest was for red alga at 5 mg/L (in 5 min) and the longest was for beer draff at 100 mg/L (>180 min). Therefore, it was assumed that more than one mechanism (bonding site) took part in the adsorption process.
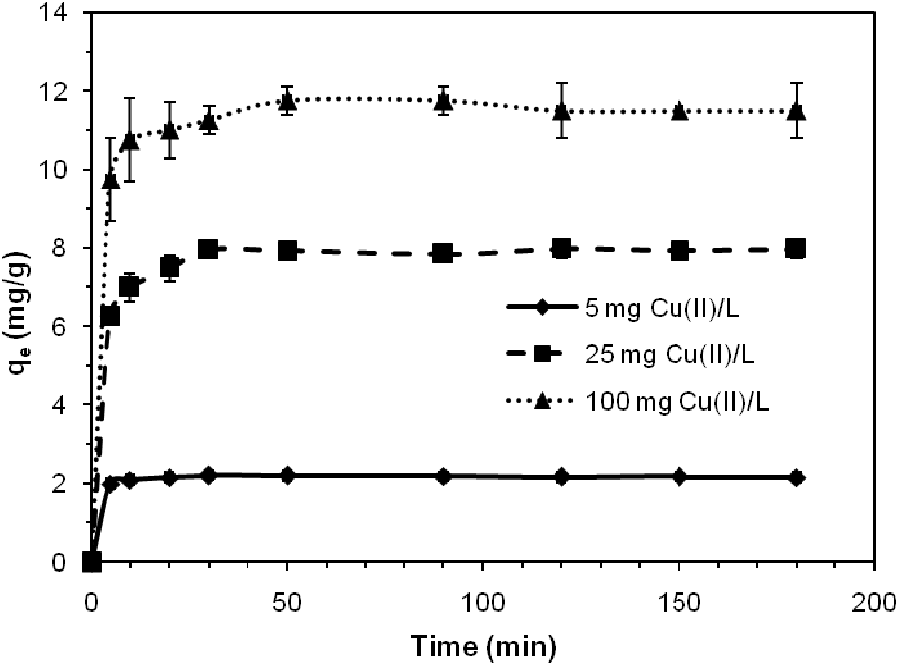
(a)
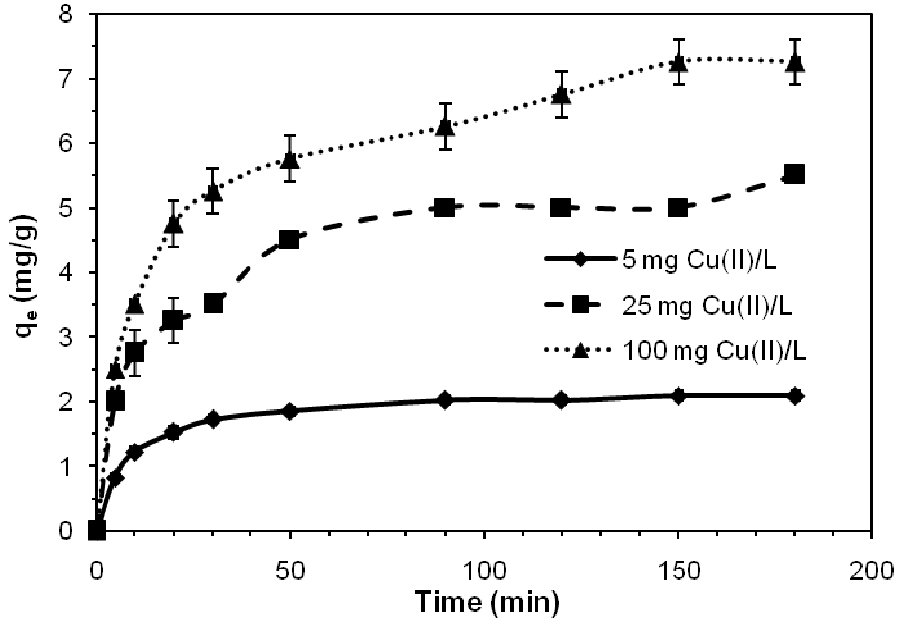
(b)

Fig. 8 Effect of initial Cu^{2+} concentration and contact time on adsorption capacity ((a) Red alga and (b) beer draff)

5.1.2 Kinetics models

Kinetic rate of Cu^{2+} adsorption were described by pseudo first-order and pseudo second-order models. Both of the two kinetic models are based on the kinetics of chemical reactions.

Both the values of R^2 and $q_{e,cal}$ are crucial to evaluate how well the data fit the kinetic model. If $q_{e,cal}$ is not equal to the equilibrium Cu^{2+} uptake, even if a high value of R^2 is achieved, the adsorption reaction is not likely to be first order (Vijayaraghavan et al., 2004). As shown in **Table 5**, correlation coefficients for red alga and beer draff were both higher than 0.830. Nevertheless the calculated adsorption capacities are much lower than experimental data ($q_{e,exp}$), indicating the insufficiency of the pseudo first-order model.

Correlation coefficients (**Table 5**) present good agreement at all conditions. Moreover, $q_{e,cal}$ was quite similar to $q_{e,exp}$. Therefore, the adsorption behavior of red alga and beer draff fit the pseudo second-order model more accurately rather than the pseudo first-order model. Kumar et al. (2006) and Vijayaraghavan et al. (2006) had the same conclusion in copper removal by green alga. The good fits further support the assumption of this model that adsorption is based on chemical sorption (Kumar et al., 2006).

Table 5 Constants in kinetic models for (a) red alga and (b) beer draff at different concentrations of Cu^{2+}

(a)

C_o (mg/L)	$q_{e,exp}$ (mg/g)	Pseudo first-order			Pseudo second-order			
		$q_{e,cal}$ (mg/g)	K_1 (1/min)	R^2	h (mg/(g·min))	K_2 (g/(mg·min))	$q_{e,cal}$ (mg/g)	R^2
5	2.21	0.30	0.09	0.978	4.12	0.84	2.22	1.000
25	8.00	2.42	0.08	0.977	5.68	0.09	8.00	1.000
100	11.75	2.31	0.06	0.830	14.71	0.11	11.5	0.999

(b)

C_o (mg/L)	$q_{e,exp}$ (mg/g)	Pseudo first-order			Pseudo second-order			
		$q_{e,cal}$ (mg/g)	K_1 (1/min)	R^2	h (mg/(g·min))	K_2 (g/(mg·min))	$q_{e,cal}$ (mg/g)	R^2
5	2.16	1.06	0.01	0.838	0.19	0.05	2.01	0.999
25	6.75	3.99	0.005	0.888	0.42	0.01	5.68	0.995
100	8.75	5.08	0.01	0.928	0.56	0.01	7.75	0.996

5.1.3 Adsorption isotherm models

Adsorption isotherm models are useful tools to describe the balance of adsorbate at constant pH and temperature. The isotherm model can be used for design and operation of adsorption units. Existing isotherm models describe different types of adsorption behavior.

Table 6 Coefficients in four isotherm models for red alga and beer draff

| Constants | Materials | | Constants | Materials | | Constants | Materials | |
	Red alga	Beer draff		Red alga	Beer draff		Red alga	Beer draff
Langmuir			**Freundlich**			**D-R**		
q_m (mg/g)	12.7	9.01	K_f (mg/g)(L/mg)$^{1/n}$	2.63	3.05	q_m (mg/g)	39.4	19.3
K_l (L/mg)	0.178	0.323	n	2.52	3.68	K_D (mol^2/kJ^2)	0.003	0.002
R^2	0.998	0.998	R^2	0.905	0.902	E (kJ/mol)	12.9	15.8
						R^2	0.943	0.941

As presented in **Table 6**, the Langmuir isotherm model fits the adsorption behavior well, indicating monolayer adsorption prevailed. The correlation coefficient R^2 is 0.998 for both red alga and beer draff. The values of q_m are 12.7 mg/g and 9.01 mg/g for red alga and beer draff, respectively (**Table 6**) and are similar to the experimental adsorption capacity, $q_{e,exp}$. Although K_l is a simple fitting parameter rather than a true adsorption constant, the high value of K_l can indicate a high affinity for adsorption (Davis et al., 2003). The higher value of K_l on beer draff might be related with the high amount of total acidic groups.

The good fitting of the Langmuir model can also be found in other studies (Villaescusa et al., 2000, 2004; Yu et al., 2001; Kumar et al., 2006). Compared with the q_m values of other materials, red alga and beer draff presented better adsorption capacities than cork (3.01 mg/g) and sawdust (1.79 mg/g). However, beer draff adsorbed less than yohimbe bark (9.54 mg/g) and grape stalks (10.2 mg/g), while red alga (*Palmaria 38almate*) performed worse than one of the green alga (*Ulva fasciata sp.*), which adsorbed maximum of 26.9 mg/g Cu^{2+}.

The correlation coefficients R^2 of the Freundlich model (**Table 6**) are 0.905 and 0.902 for red alga and beer draff, respectively. Compare to the Langmuir isotherm model, the Freundlich model did not fit the adsorption behavior on red alga and beer draff well.

As listed in **Table 6**, R^2 values are 0.943 and 0.941 for red alga and beer draff, respectively, indicating good match of the D-R model. The values of *E* are 12.9 kJ/mol and 15.8 kJ/mol for red alga and beer draff, lying in the range of 8-16 kJ/mol. This suggests copper adsorption on both materials is of a chemical nature. Therefore, chemical bonding was assumed to be the main chemical mechanism in this study, which will be further discussed in section 5.1.5.

5.1.4 Potentionmetric and conductomertric titration

In order to determine the bonding mechanism, the amount and pK_a values of various acidic groups on the adsorbents were calculated based on the inflection points in titration curves (Murphy et al., 2007).

Table 7 pK_a values and amount of acidic groups on adsorbent surface determined by titration

Adsorbent	pK_a values		Numbers of acidic groups (mmol/g biomass)		
			Total	Strong	Weak
Red alga (Palmaria palmata)	4.82	8.2	0.078	0.008	0.07
	5.36	8.47			
	6.57	8.56			
	7.06	8.62			
	7.78				
Beer draff	4.21	7.02	0.119	0.004	0.115
	4.28	7.62			
	4.36	8.22			
	4.53	8.48			
	4.64	8.57			
	4.93	8.67			
	5.2	8.71			
	5.76	8.88			
	6.18	8.92			
	6.65	8.97			

The pK_a values were calculated to distinguish various acidic groups. Based on other studies, carboxyl groups have been shown to play the first role in heavy metal bonding, while sulphonic and hydroxyl groups play the secondary role (Fourest and Volesky, 1997; Davis et al., 2003; Murphy et al., 2007; Ngah and Hanafiah, 2008). The pK_a value around 4.8 indicated the presence of carboxyl group. Other pK_a values in the range of 4-7 suggested the abundance of weak acidic groups. Due to the limited detection range of titration analysis, sulphonic and hydroxyl groups, which

have pK$_a$ values in the range of 1.0-2.5 and >10, respectively (Murphy et al., 2007), were not detected.

Beer draff has more acidic groups (0.119 mmol/g) than red alga (0.078 mmol/g), most of them being weak acid groups (0.115 mmol/g for beer draff and 0.070 mmol/g for red alga) (**Table 7**). The amount of acidic groups has been proved to be related with adsorption on seaweed (Murphy et al., 2007). The high correlation coefficients between the final pH value and adsorption capacity in this study also confirmed H$^+$ had taken part in copper adsorption. More acidic groups are typically related to a higher adsorption capacity. However, the bonding capacities and reaction rates varied for different acidic groups, presenting different adsorption phenomenon. Even the same functional groups can vary between adsorbent types and species (Murphy et al., 2007). The results in this study indicated the amount of acidic groups was not the exclusive factor to estimate the adsorption capacity of red alga (*Palmaria palmata*) and beer draff.

5.1.5 FTIR and EDX

The FTIR spectrum displays different adsorption peak values indicating various functional groups on the adsorbent surface (**Fig. 9**). The hydroxyl group (-OH) is represented by the peak around 3300 cm^{-1} (Murphy et al., 2007).The peaks at 1738 cm^{-1} and 1643 cm^{-1} present the carboxyl stretches in different compounds. 1738 cm^{-1} peak is a carboxyl stretch in ester, while the 1643 cm^{-1} presents the same stretch in amide (Ngah and Hanafiah, 2008). The S=O and C–S–O stretches of the sulphonic group, which are indicated by peaks around 850 and 1240 cm^{-1} (Fourest and Volesky, 1996), were also detected.

The comparison of the FTIR curves before and after adsorption indicates no significant difference on beer draff; only a slight variety exists at 3296 cm^{-1}, 1740 cm^{-1} and 1377 cm^{-1}, which are hydroxyl / amino, carboxyl groups and C–O stretch (Villaescusa et al., 2004; Ngah and Hanafiah, 2008). In addition, these three shifts happened in the first 4 hours of adsorption and shifted in 12 hours (**Fig. 9**), suggesting these functional groups and stretch conduced to a fast and flexible adsorption. Compared to the results of potentiometric and conductometric titration, the abundant weak acidic groups that exist in beer draff seem to have a large contribution to the affinity of Cu^{2+} in adsorption process. Therefore, the copper adsorption on beer draff was assumed to be a combination of several functional

40

groups. On the contrary, the FTIR curve of red alga presented significant fluctuations at wavenumbers of 3281 cm^{-1} (changed to 3296 cm^{-1}), 1333 cm^{-1} (changed to 1311 cm^{-1}), 1230 cm^{-1} (changed to 1219 cm^{-1}) and 841 cm^{-1} (replaced by 852 cm^{-1} and 839 cm^{-1}), which are hydroxyl, –NH stretch (amino), phenolic hydroxyl, and sulphonic group (Ngah and Hanafiah, 2008).The diversified performances of adsorption revealed that adsorption capacity varies among various functional groups and adsorbents.
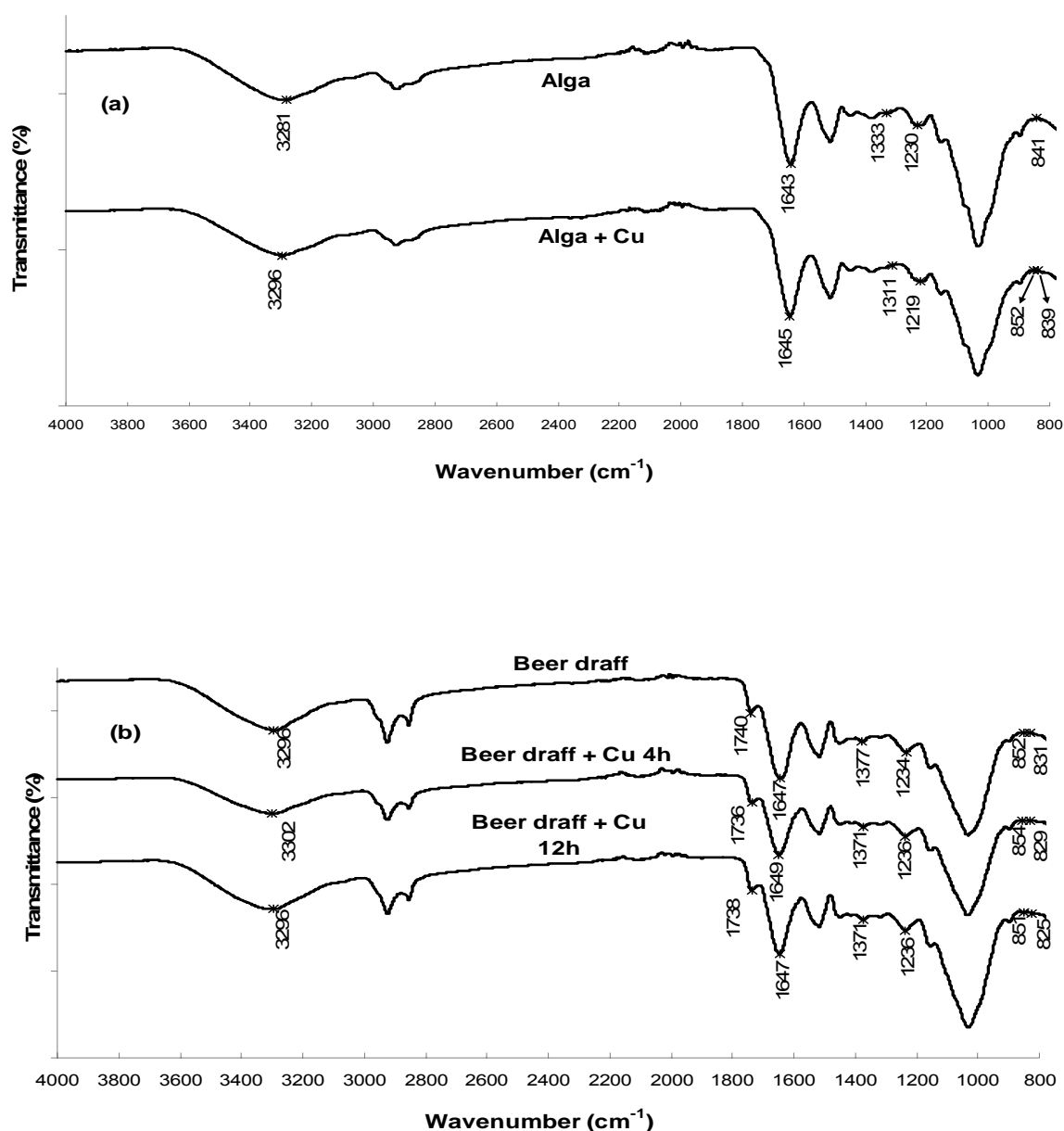
Fig. 9 FTIR of (a) red alga and (b) beer draff before and after Cu^{2+} adsorption

Energy dispersive X-ray emission (EDX) was used to investigate the characteristics of element abundance on the adsorbent. EDX spectrums of red alga before and after

adsorption are shown in **Fig. 10**. It can be seen that copper appeared after adsorption, from 0% to 3.24%. Furthermore, no other significant fluctuations of other elements were detected. Potassium (K) and Magnesium (Mg) slightly decreased and were ignored when taking account of measurement error. The EDX results of beer draff (**Fig. 11**) provide similar results, in which copper appeared significantly after adsorption and most elements had an even smaller decrease than that in red alga. Therefore, it is assumed that chemical bonding was the main mechanism in the adsorption process rather than ion-exchange.
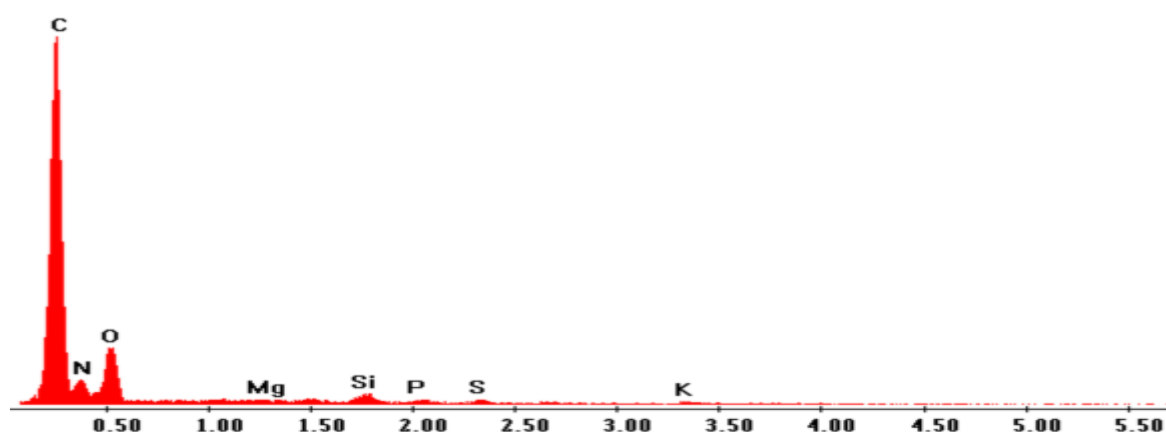
(a)
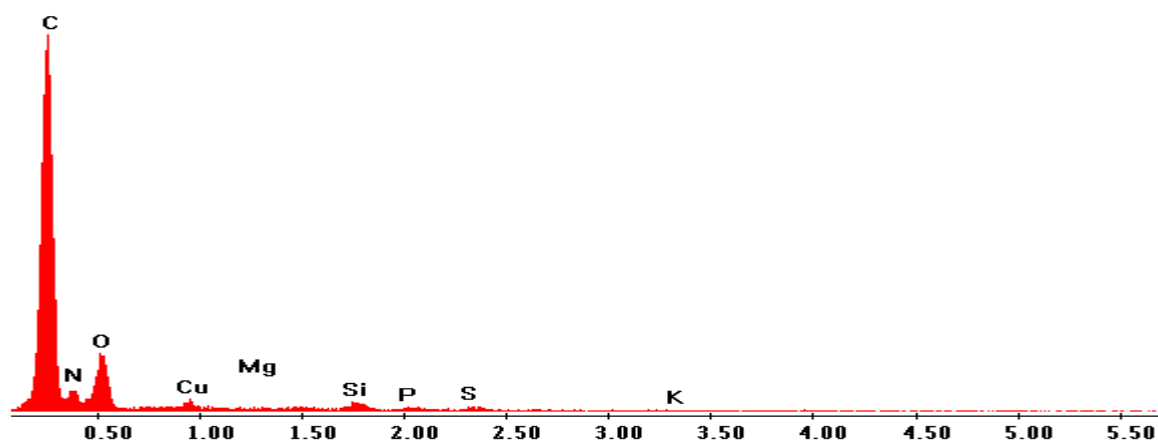
(b)

Fig. 10 EDX spectrum of red alga (a) before and (b) after Cu^{2+} adsorption
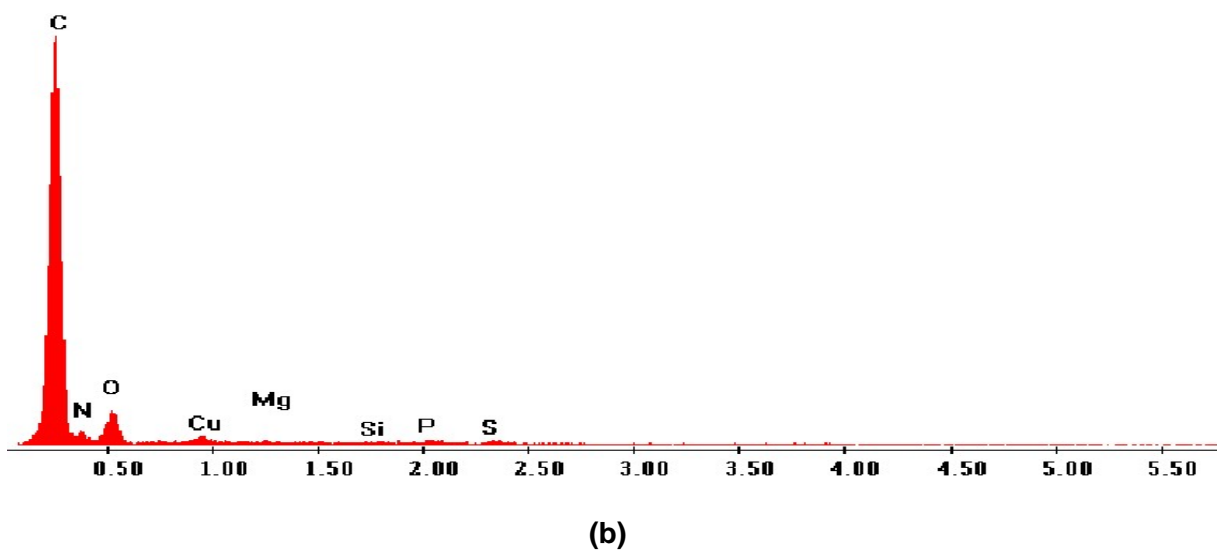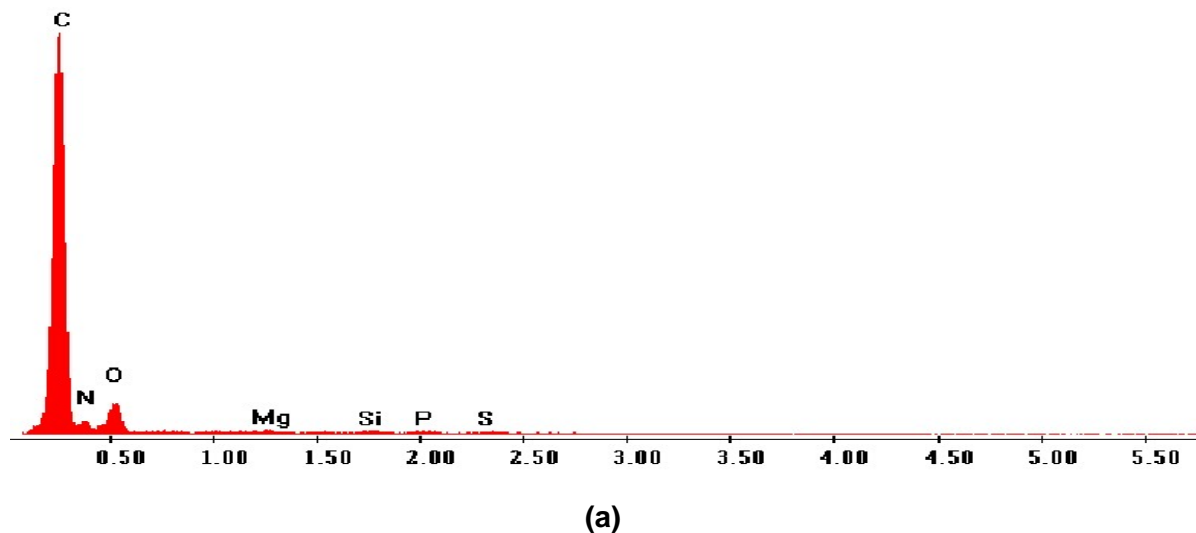
Fig. 11 EDX spectrum of beer draff (a) before and (b) after Cu^{2+} adsorption

5.1.7 Desorption experiments

Desorption experiments were carried out not only to evaluate if the materials can be regenerated after saturation with heavy metals, but also to clarify the stability of the adsorbed heavy metal on the surface of the materials in the presence of de-icing salt. The concentrations of sodium chloride used in desorption experiments were also in the range of normal de-icing salt concentrations in road runoff (Helmreich et al., 2010).

As shown in **Table 8**, HNO_3 solution performed very well in the desorption process. At the lowest concentration (1 mmol/L), more than 66% of adsorbed Cu^{2+} was removed by HNO_3 from both bioadsorbents. At a concentration of 10 mmol/L HNO_3 nearly 100% of adsorbed Cu^{2+} was set free.

On the contrary, the treatment of the Cu^{2+} loaded materials with sodium chloride (NaCl) solution, which was used as a de-icing salt, resulted in quite low desorption efficiency, especially for red alga. At the highest concentration of NaCl (100 mmol/L), only 7% of the adsorbed Cu^{2+} on red alga was desorbed. Meanwhile, beer draff attained 11% Cu^{2+} desorption at the same concentration. Therefore, red alga seems more suitable to be the adsorbent in road runoff treatment.

Table 8 Desorbed copper amount in HNO_3 and NaCl solution

Desorption reagent	Concentration (mmol/L)	Desorption (%)	
		Red alga	Beer draff
HNO_3	1	66.4	68.2
	10	96.3	100
	100	100	100
	Blank (deionized water)	<1	<1
NaCl	1	<1	3.1
	10	<1	4.1
	100	7.0	11.1
	Blank (deionized water)	<1	<1

From these results, HNO_3 at the concentration of 10 mmol/L was chosen to be the effective desorption reagent. Red alga performed better in holding adsorbed Cu^{2+} in the presence of de-icing salt. Furthermore, the performance of HNO_3 and NaCl in the desorption study also revealed ion-exchange was not the main mechanism in the adsorption of copper on red alga and beer draff.

5.1.8 Summary

According to the results, red alga and beer draff performed well in Cu^{2+} removal from aqueous solutions. The adsorption capacity of the materials for Cu^{2+} was strongly dependent on the pH value and initial Cu^{2+} concentration. The optimum pH range for adsorption was 5-6 for both materials. The relationship between final pH and adsorption capacity revealed hydrogen ions had taken part in the copper adsorption process.

The pseudo second-order model was in accordance with adsorption behavior on both materials, showing the chemical characteristic of the adsorption process. The Langmuir isotherm model fit well with the adsorption phenomenon, indicating that the maximum adsorption capacities were 12.7 mg/g and 9.01 mg/g for red alga and beer draff, respectively. The D-R model demonstrated the chemical nature of the

adsorption process. The negative values of $\triangle G^o$ revealed that the adsorption process on both materials was spontaneous.

Beer draff was found to have more weak acidic groups than red alga in the study of potentiometric and conductimetric titration. Considering the differences between the adsorption behavior of red alga and beer draff, the bonding capacities and reaction rates were assumed to be varied among different acidic groups. FTIR, EDX and desorption studies proved that chemical bonding was the main mechanism in adsorption rather than ion-exchange. The functional groups, such as amino, hydroxyl, carboxyl, phenolic hydroxyl group, sulphonic group and C–O, –NH stretch, might be involved in adsorption. Desorption experiments with NaCl indicated that the adsorption of Cu^{2+} to both materials mainly resulted from chemical bonding, not from ion exchange.

Although red alga and beer draff presented good adsorption capacities in experiments, they are not considered as the appropriate adsorbent materials for road runoff treatment. Firstly, their poor mechanical strengths limit their application in practice. In the experiment process, it was found that both red alga and beer draff were fragile. The fine particle would later cause severe blocking in filtration process and make the regular maintenance difficult. Moreover, as bioadsorbents, red alga and beer draff have been found to release some organic compounds in the adsorption and desorpion process with a chemical oxygen demand (COD) value as high as 250 mg/L. Therefore, the bioadsorbents were not tested in the following study for MTBE and Nap removal.

5.2 Evaluation of four adsorption materials for removal of MTBE and Nap

As discussed in section 2.3, activated carbon, activated lignite, clay mineral and oxides are widely used for adsorptions of heavy metals and some organic compounds. Moreover, they are more suitable to be applied in road runoff treatment than other adsorbents, such as zeolite and resin. Without the domination of ion exchange in adsorption process, the existence of de-icing salt would have less influence on activated carbon, activated lignite, clay mineral, and oxides. Correspondingly, the adsorbed pollutants, especially heavy metals would retain steadily on these adsorbents.

Considering their various morphologies and properties, F300, HOK, Tixosorb, and DRI were selected as adsorbents in this section. Their adsorption performance for MTBE and PAHs removal were evaluated to determine whether they are suitable filter materials for a BMP system for road runoff treatment. The BET surface area, micro-pore and meso-pore distributions, and element composition of these materials were measured. The effects of pH and initial concentration of adsorbate were also determined in experiments. Furthermore, their adsorption abilities of MTBE and Nap, which were calculated in Freundlich isotherm form (log-log form), were compared.

Due to the abundant researches of the heavy metal adsorption on these four kinds of materials (Smith, 1996; Kadirvelu et al., 2001; Oyanedel-Craver et al., 2007; Vreysen et al., 2008; Liu et al., 2009; Song et al., 2012), F300, HOK, Tixosorb, and DRI were directly evaluated by their adsorption performance for organic pollutants (MTBE and Nap) removal. The test for heavy metal adsorption on these four materials was not carried out in this section.

5.2.1 Physical property and adsorbents

The four adsorbents possess various morphologies and properties. HOK is an activated coke from lignite. F300 is an activated carbon from bituminous coal. Tixosorb is a semi-organophilic bentonite. Although natural bentonite has been used in heavy metal adsorption, Tixosorb replaced it in this study because of the strong hydration of natural bentonite and formation of hydrophilic surfaces, organic contaminants are unable to penetrate into it to be adsorbed (Park et al., 2011). Tixosorb is manufactured from crude Ca-bentonite by partly exchanging its interlayer cation (Ca^{2+}) with an organic cationic surfactant, dimethyl-diocta-decyl ammonium (DMDO) (Stockmeyer, 1995). In this way, the hydrophobicity of the bentonite surface increases while a portion of the interlayer cations still maintain their potential for heavy metal removal. Sponge iron, also called direct reduced iron (DRI), is an intermediate product from the reduction process of iron melting in steel industries. DRI is predominantly (90%) comprised of activated iron (zero-valent iron). This provides the necessary conditions for the oxidation-reduction reaction for heavy metal and organic pollutant removal (Keum and Li, 2004; Bang et al., 2005).

Physical properties such as pore volume, distribution, and surface composition, are essential to elucidate the behaviors of adsorbents in the adsorption process. **Table 9** summarizes the BET surface areas and pore volumes of these four adsorbents. F300

has the highest BET surface area of 1,084 m^2/g, followed by HOK with 308 m^2/g, Tixosorb with 6 m^2/g, and DRI with 1 m^2/g. Moreover, F300 also has the highest micro-pore volume (0.47 cm^3/g) and a median pore diameter of 6.38 Å. The median micro-pore diameter of HOK is similar in size at 6.70 Å to F300, while the micro-pore volume is lower at 0.15 cm^3/g. In the BET measurement, the pore volumes in Tixosorb and DRI were not obtained, indicating that they have very few or no pores in the range of 5-300 Å. Based on the mercury intrusion results, pore diameter of DRI concentrates at >200 nm.

Table 9 BET surface areas and pore volumes of adsorbents

Properties	Unit	Adsorbents			
		HOK	F300	Tixosorb	DRI
BET Surface area	m^2/g	308	1084	6	1
Micro-pore volume	cm^3/g	0.15	0.47	-	-
Median micro-pore diameter	Å	6.70	6.38	-	-
Meso-pore volume	cm^3/g	0.10	0.16	-	-
Median meso-pore diameter	Å	37.05	53.63	-	-

'-': out of measure range, not detected in measurement

In BET measurements, Tixosorb lost a great deal of water (in vapor form) during the outgassing step. It was deduced that Tixosorb contains micro-pores (< 5 Å), which only allows the entrance of water and excluded the penetration of nitrogen (used for porosity measurement).

A more detailed distribution of micro-pores for HOK and F300 is provided in **Fig. 12**. It can be seen that for each pore size, F300 has a higher pore volume than HOK. However, the sizes of pores that provide maximum volumes concentrated at the range of 5-8 Å for both HOK and F300. The kinetic diameters of MTBE and Nap are more or less similar at 6.2 Å and 6.55 Å, respectively (Li, et al., 2002; Ahmad, 2009).
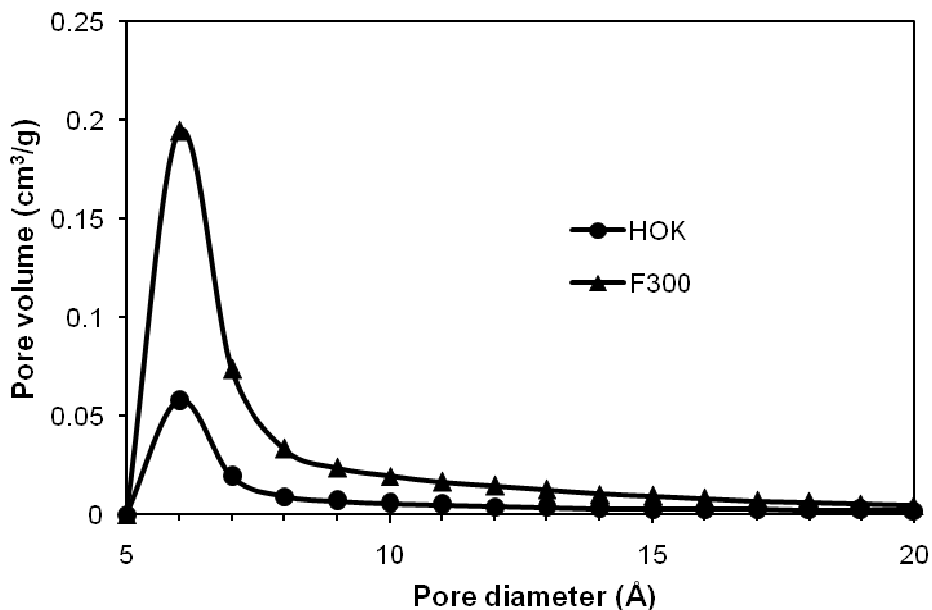
Fig. 12 Micro-pore distribution in HOK and F300

Elemental analysis of the four adsorbents is shown in **Table 10**. Each adsorbent is comprised of different amounts of C, H, and N. As the main element of HOK and F300, C makes up approximately 90% of the total mass. In the semi-organophilic bentonite, Tixosorb, the amount of C might reflect the loaded amount of organic cationic surfactant. In the case of DRI, Fe (90%) is the main element and C, H, N, and S are presented only small amounts.

Table 10 Elemental analysis of adsorbents

Element	Adsorbent			
	HOK	F300	Tixosorb	DRI
C	88.40%	87.88%	19.28%	0.30%
H	0.30%	0.30%	4.02%	<0.1%
N	0.30%	0.60%	0.71%	<0.1%
S	0.30%	0.70%	<0.1%	<0.1%

5.2.2 Influence of pH

To clarify the pH dependence of organic pollutant adsorption in aqueous solution, the adsorption of MTBE and Nap at different pH values (pH 5 and pH 7) was tested on HOK and F300. **Fig. 13** depicts MTBE adsorption at pH 5 and pH 7 on HOK. It can be seen that the adsorption of MTBE was independent of pH. The same

phenomenon was also found for the adsorption of Nap on HOK (**Fig. 14**). The adsorptions of MTBE and Nap on F300 under different pH values showed the same tendency (figures not presented).

This finding of pH-independent adsorptions of MTBE and Nap is quite different from that of heavy metal adsorption, which is strongly pH-dependent. This is due to the fact that both MTBE and Nap are non-ionic organic compounds (Park and Jaffe, 1993; Eckstein et al., 2002). They do not react with hydrogen, hydroxyl ions, or even the functional groups of adsorbents, which are the crucial factors influencing pH during heavy metal adsorption (Chen et al., 1997; Brown et al., 2000; Li et al., 2011).

In the following tests, a phosphate buffer was applied to obtain a constant pH value of 7 since the pH of road runoff has been shown to vary from 6.2 to 8.3 (Helmreich et al., 2010).
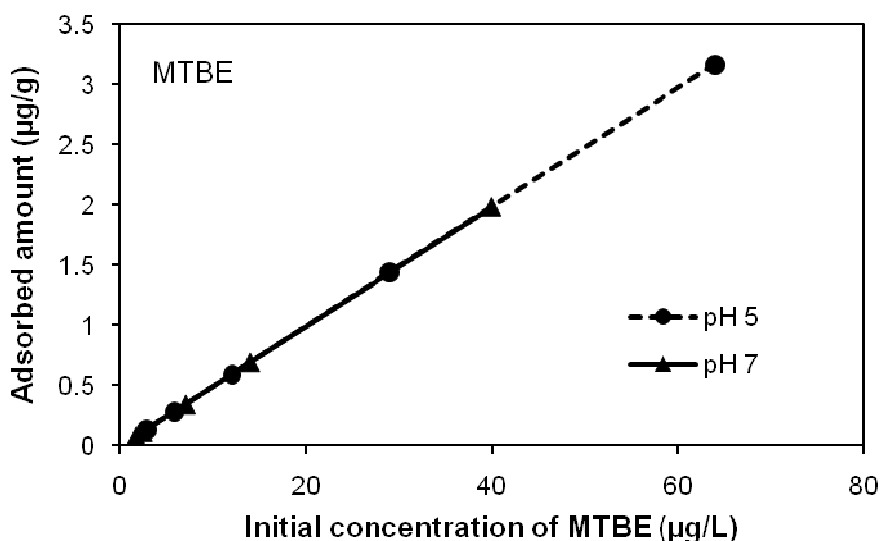
Fig. 13 Adsorption of MTBE on HOK at pH 5 and pH 7
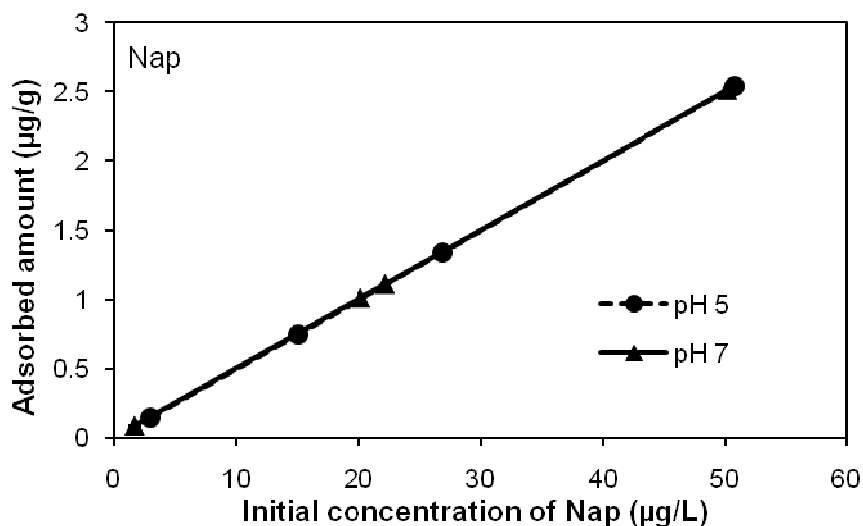
Fig. 14 Adsorption of Nap on HOK at pH 5 and pH 7

5.2.3 Adsorption of MTBE

The degree to which MTBE was adsorbed at various initial concentrations is summarized in **Fig. 15**. F300 and HOK displayed higher adsorption amounts compared to the other two tested materials. However, the disparity between F300 and HOK was still significant. At an initial concentration of 1,100 mg/L, F300 removed 50.5 mg/g (92%) of MTBE while HOK achieved only 21.5 mg/g (39%). Tixosorb and DRI presented poor adsorption capacities in MTBE removal. At the same initial concentration (1,100 mg/L), Tixosorb and DRI only removed 10.3 mg/g (19%) and 6.5 mg/g (12%) of MTBE, respectively.

It is well known that smaller pores can provide more adsorption sites and therefore higher adsorption potential (Li et al., 2002). HOK and F300 exhibited high adsorption capacities of MTBE and are also characterized as having high micro-pore volumes of 5-20 Å (**Fig. 12**). This illustrates the close relationship between MTBE adsorption and micro-pore volume. **Fig. 16** presents the adsorption capacity of MTBE in the log-log form of Freundlich isotherm (Equation 3 and 4) (Freundlich, 1907; Solisio, 2001) and its normalized values by micro-pore volumes of 7-11 Å on HOK and F300.
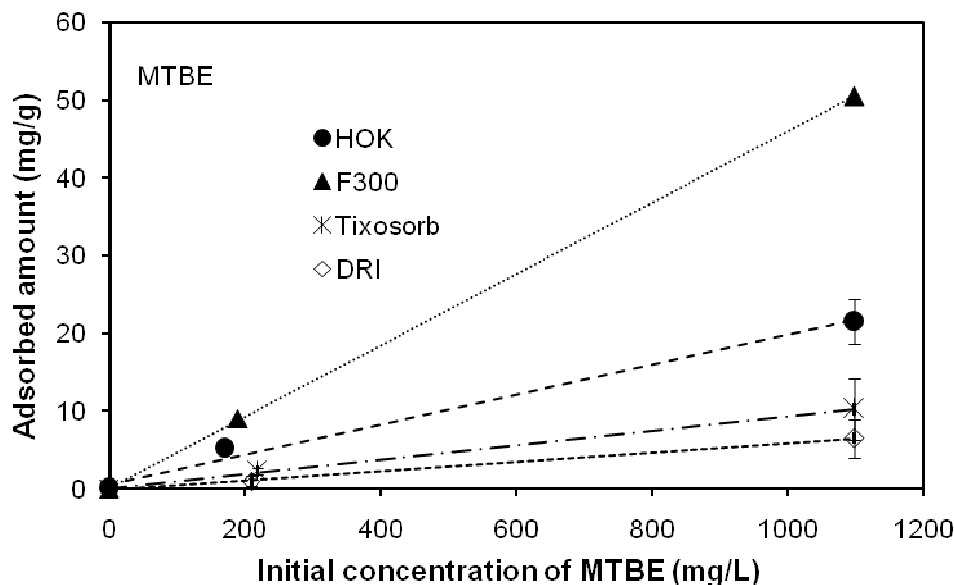
Fig. 15 Adsorption of MTBE on different adsorbents

As shown in **Fig. 16**, the normalized adsorption capacities of HOK and F300 by their micro-pore volumes of 7-11 Å are quite close. Pore sizes between 7-11 Å, which is 1.1-1.8 times the kinetic diameter of MTBE molecule, displayed a direct impact on MTBE adsorption. It therefore can be said the pore volumes of 7-11 Å, 0.045 cm^3/g for HOK and 0.167 cm^3/g for F300, had the greatest degree of MTBE adsorption. Rossner et al. (2009) studied the adsorptions of several emerging organic contaminants and found different contaminants were adsorbed to pores with different pore sizes. A high volume of pores with the required pore size for adsorbate brought higher adsorption capacity. To the system of multi-adsorbates, the heterogeneous pore sizes would be desirable for an effective adsorbent. For MTBE adsorption, Li et al. (2002) reported that similar crucial pore size with the range of 8-11 Å that is responsible for high MTBE adsorption capacity. The poor performance of Tixosorb and DRI also proved the importance of micro-pores size for MTBE adsorption. Smaller pores, which in the case of Tixosorb were less than 5 Å, excluded the entrance of MTBE, and the macro-pores of DRI (> 200 nm) could neither hold MTBE molecules on its surface.
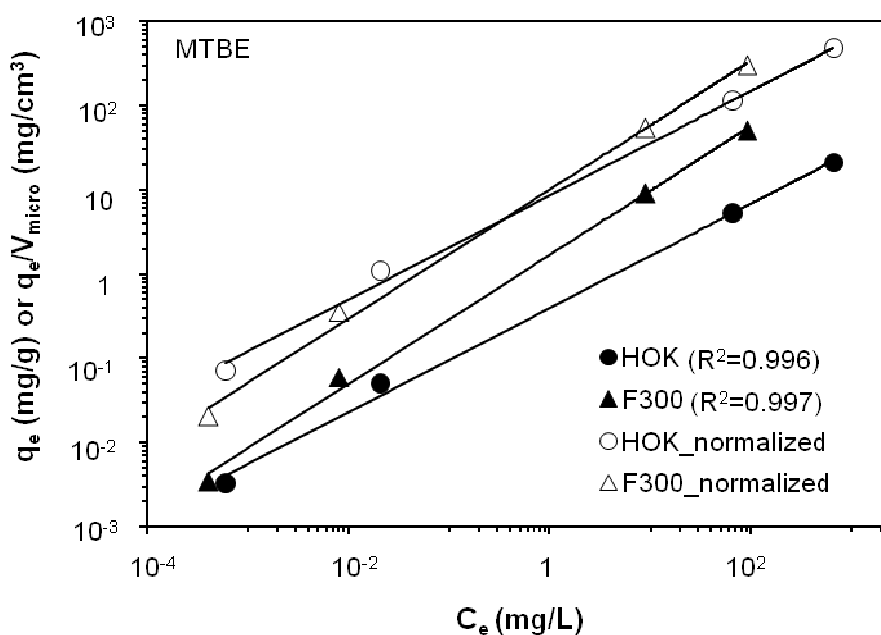
Fig. 16 MTBE adsorption on HOK and F300 (in log-log form) and the normalized adsorption capacity by micro-pore volume of pores at 7-11 Å

It was also noted that the removal efficiency of MTBE on HOK, F300, and DRI decreased with the increasing initial concentration. When the initial concentration rose from 64 µg/L to 1,100 mg/L, removal efficiency was reduced from 99% to 39% on HOK, from 99% to 92% on F300, and from 38% to 12% on DRI. This phenomenon most likely occurred due to the limited adsorption sites on the surfaces of the adsorbents. It can thus be stated that the number of proper adsorption sites controlled the adsorption capacities of these materials. Once the sites are saturated, the adsorption amount could not further elevate. However, the adsorption behavior of Tixosorb differed from those of the other materials. It was characterized by an increasing MTBE removal efficiency with increased initial concentration. As can be seen, the removal efficiency was 0% at 170 µg/L, increased to 16% at 1.1 mg/L, and finally stabilized around 20% at 220 mg/L of MTBE (19% at 1,100 mg/L). A linear removal of pollutants on organo clay was generally regarded as a partitioning behavior, where the pollutants were believed to be partitioned into the organic phase created by the surfactant (Lee and Kim, 2002; Cruz-Guzmán et al., 2004; Changchaivong and Khaodhiar, 2009; Park et al., 2011). The increased removal efficiency of Tixosorb in this study suggests the partitioning of MTBE is enhanced by high initial concentration. Therefore, Tixosorb is more suitable to be used in areas highly contaminated by MTBE.

5.2.4 Adsorption of Nap

Due to the limited solubility of Nap, initial concentrations during the experiments did not exceed 18 mg/L. At the studied concentrations, Nap was adsorbed linearly onto HOK, F300, and Tixosorb (**Fig. 17**), demonstrating their high adsorption capacities of Nap. On the other hand, equilibrium on DRI was achieved at around 4 mg/L, showing its limited adsorption capacity of Nap.

At an initial concentration of around 15±2 mg/L, the removal efficiency of Nap was nearly 100% on HOK and F300, followed by Tixosorb at 99%, while DRI only had a removal efficiency of only 8% at this concentration. Compared to the removal efficiency of MTBE, the higher values in Nap adsorption on adsorbents were attributed to the non-polar nature of Nap. The relatively low water solubility of Nap indicates its weak affinity with water. Contrary to MTBE, the adsorption of Nap does not require high amount of energy to break this interaction before adsorption. Therefore, the adsorption of Nap is energetically favored.

As with MTBE adsorption on Tixosorb, a linear adsorption of Nap with a lightly increased removal efficiency at high initial concentrations was also observed. When the initial concentration varied from 77 μg/L to 17 mg/L, the removal efficiency of Tixosorb increased from 91% to 99%, indicating its enhanced Nap adsorption at high concentration. Furthermore, higher removal efficiency was achieved for Nap adsorption (99%) than MTBE adsorption (20%). It was reported that the uptake due to partitioning was highly related to the solubility of the target organic compound. Compounds with low solubility were prone to partition more strongly to the organic medium made by the alkyl chains of the added surfactant (Oyanedel-Craver et al., 2007).
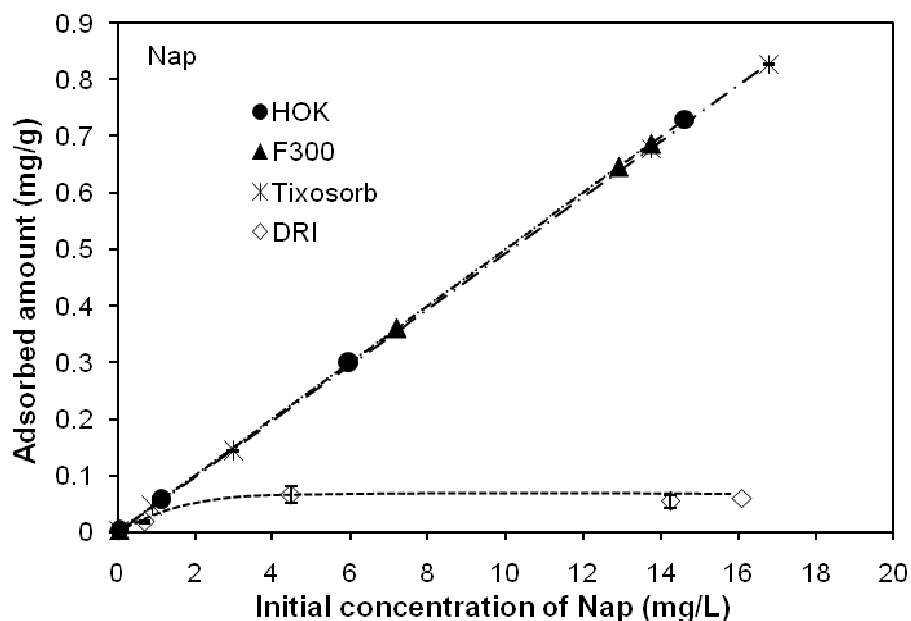
Fig. 17 Adsorption of Nap on different adsorbents

Fig. 18 illustrates Nap adsorption on HOK and F300 in log-log form. In contrast to MTBE, the micro-pore volume cannot explain all discrepancies in the amount that adsorbed onto HOK and F300. Although F300 has a higher pore volume than HOK at all pore sizes in the range of 5-20 Å, HOK demonstrated a higher adsorption capacity of Nap. Excluding the influence of micro-pore volume and the possible unstable equilibrium at low concentration, the surface chemistry character (hydrophobicity, aromaticity, etc.) of adsorbents must play an important role in Nap adsorption (Xu et al., 1997; Ania et al., 2007). Obviously, in aqueous solution these factors had a greater impact on Nap (non-polar, aromatic compound) adsorption compared to MTBE adsorption (Yang et al., 2006; Cabal et al., 2009). Therefore, when comparing the same series of adsorbents for Nap removal, the surface area and meso-pore volume were used as indicators for the adsorption capacity (Xu, et al., 1997; Yang et al., 2006). In contrast thereto, DRI with its low micro-pore volume and BET surface area, displayed poor adsorption performance.
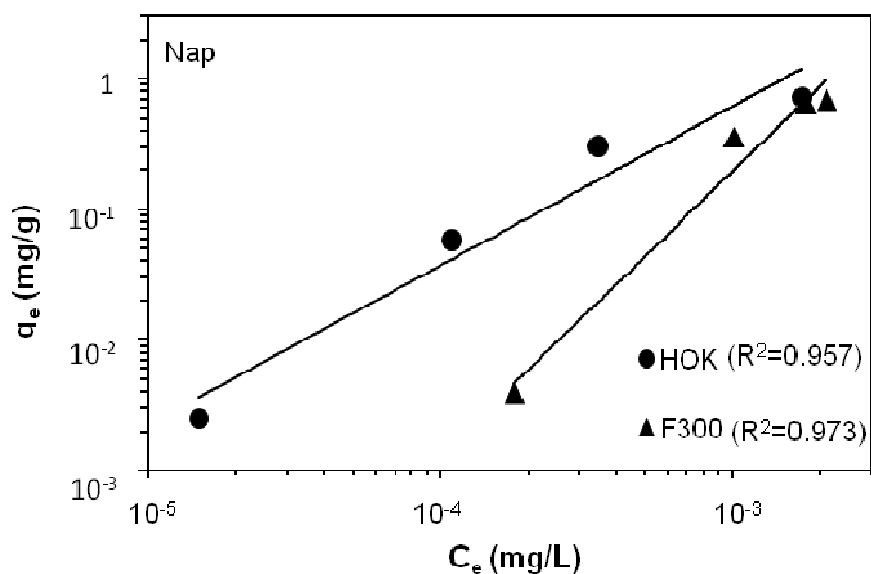
Fig. 18 Nap adsorption on HOK and F300 (in log-log form)

5.2.5 Adsorption comparison

As discussed in previous sections, the four adsorbents, HOK, F300, Tixosorb, and DRI, exhibited various adsorption behaviors for MTBE and Nap.

With their high volume of pores at 7-11 Å, HOK and F300 presented preferable performance in MTBE adsorption. The uptake of Nap demonstrates that the surface chemistry character is not less important than micro-pore volume.

Both for MTBE and Nap, Tixosorb illustrated enhanced adsorption behavior at high initial concentrations. However, better performance was found for Nap due to its non-polar character. With its increasing removal efficiency at a relatively high initial concentration, the semi-organophilic bentonite Tixosrob is quite suitable to be used for highly contaminated areas. Moreover, the effective removal of other target organic compounds can be achieved by inserting other surfactants (Park et al., 2011).

Sponge iron, DRI, exhibited limited adsorption capacity for both MTBE and Nap due to its low number of micro-pores and small surface area. Although the oxidation-reduction reaction of DRI worked well in removing nitro aromatic compounds (Keum and Li, 2004), it did not help in the cases of MTBE and Nap removal.

5.2.6 Summary

Based on various adsorption behaviors among different adsorbents and adsorbates, the following conclusions were drawn:

1) HOK and F300 were effective adsorbents for both MTBE and Nap removal. Tixosorb presented its suitability for MTBE and Nap removal in highly contaminated areas. However, DRI displayed very poor adsorption capacity for both MTBE and Nap.

2) pH had no effect on MTBE or Nap adsorption.

3) Micro-pore volume of pores at 7-11 Å was crucial for MTBE adsorption. Moreover, the surface chemistry character of adsorbents (hydrophobicity, aromaticity) played an important role in Nap adsorption. The oxidation-reduction reaction of DRI did not help in MTBE or Nap removal.

4) Tixosorb demonstrated enhanced adsorption for both MTBE and Nap removal at high initial concentrations. Due to the non-polar character of Nap, Tixosorb was more effective in removing Nap than MTBE.

5.3 Comparison of adsorption behaviors of MTBE and Nap on F300 and HOK

Because of the pretests with different adsorption materials, F300 and HOK were used for kinetics and isotherms studies. In this section, the adsorption behaviors of F300 and HOK in the removal of MTBE and Nap were studied and compared. Besides, the determination of maximum adsorption capacity and the adsorption kinetics are of great interest because the contact time of road runoff with adsorption filters are usually very short.

Compared to heavy metals, which is related to functional groups, pH value and surface potential of adsorbents (Demirbas, 2008), the adsorption of organic compounds seems more relevant with micro-pores, organic matter and surface area of adsorbents (Kleineidam et al., 2002; Seredych et al., 2005). The mechanism of organic compound adsorption and the role of adsorbents characteristics in the adsorption process are still ambiguous (Seredych et al., 2005; Ania et al., 2008).

Four kinetics models (pseudo first- / second-order models, intra-particle model and Boyd model) and four isotherm models (Freundlich, Langmuir, Tóth and Polanyi-Dubinin-Manes (PDM) models) were applied. Both adsorption capacities and adsorption mechanisms of MTBE and Nap were discussed on F300 and HOK.

5.3.1 Adsorption kinetics

5.3.1.1 Effect of reaction time on MTBE and Nap adsorption

The adsorption rates of MTBE and Nap were rapid for both materials, F300 and HOK. **Figure 19(a)** depicts that MTBE removal efficiency (R_e%) increased up to 95% on F300 at low initial concentration (54 µg/L) in the first 30 min while R_e% of Nap rises up to 99% (10µg/L on HOK and 1mg/L on F300) at the same period of time (**Fig. 19(b)**). Although there was still a slightly increase after 30 min for both organic pollutants, the majority of adsorption was completed in 30 min. A relatively slow adsorption was noted for MTBE at high concentrations (14 mg/L and 140 mg/L) onto HOK. The achieved removal efficiencies were only 70% for 14 mg/L and 52% for 140 mg/L. The slower adsorption of MTBE on HOK at high concentration compared to F300 suggested the lower MTBE adsorption capacity of HOK. Compared to MTBE (**Fig. 19(a))**, Nap adsorption was faster on both F300 and HOK (**Fig. 19(b))**. In the first 10 min, more than 90% of Nap was removed by both F300 and HOK. After 30 min, Nap removal rose up to 99%. The reason might be that Nap has a much higher log K_{OW} and log K_{OC} compared to MTBE and therefore, has a stronger tendency to be adsorbed to hydrophobic surfaces than MTBE.
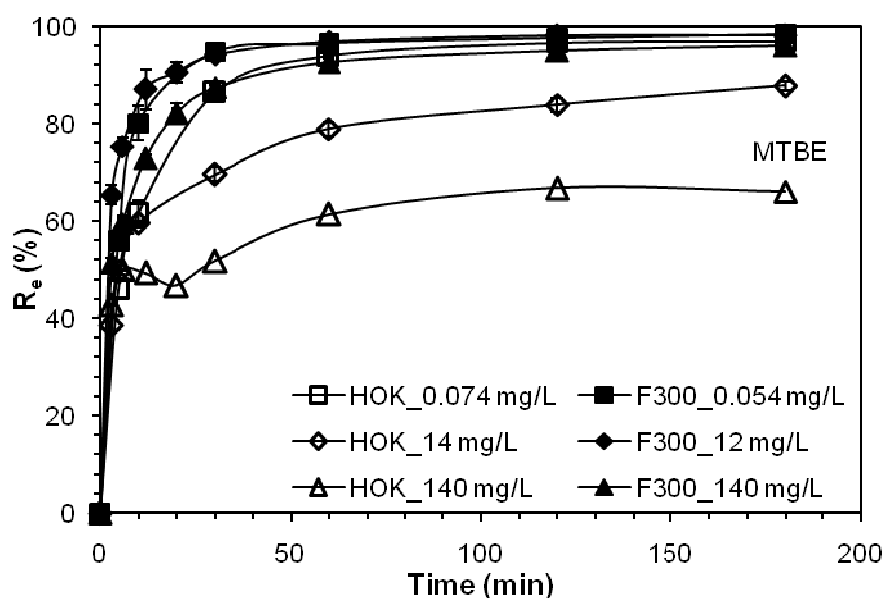
(a)
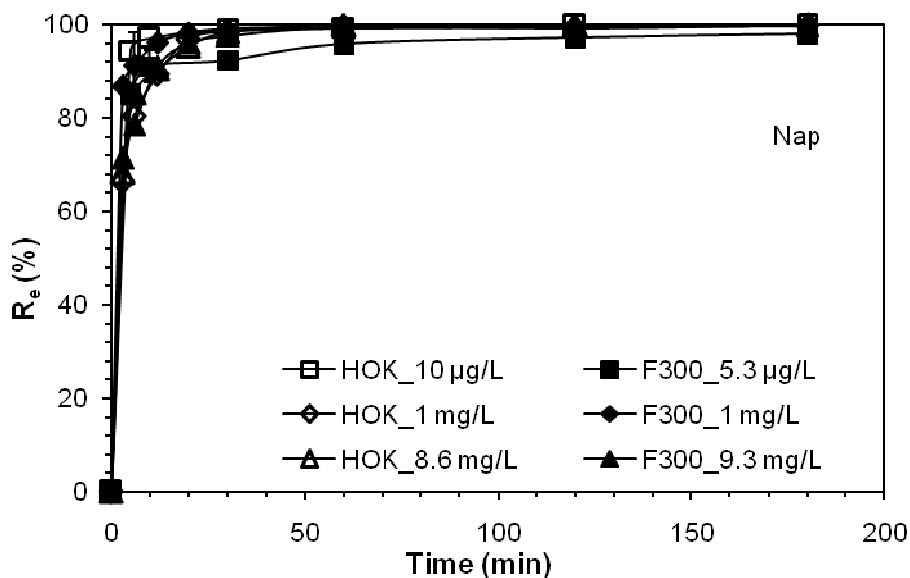
(b)

Fig. 19 Effect of reaction time on (a) MTBE and (b) Nap adsorption with different initial concentrations

5.3.1.2 Pseudo kinetics models

Compare to pseudo first-order kinetics model, pseudo second-order kinetics model presented better congruence with the experimental data for both MTBE and Nap adsorption. The correlation coefficients, R^2, of the pseudo second-order model were as high as 1 and the calculated adsorbed amounts, $q_{e,cal}$, were also close to the experimental data $q_{e,exp}$ (**Table 11**).On the other hand, the values of R^2 determined with the pseudo first-order kinetics model varied between 0.675-0.954 for MTBE and 0.404-0.824 for Nap. This indicates a weak correlation with the experimental data. Moreover, the values of $q_{e,cal}$ determined with pseudo first-order kinetics were not comparable with $q_{e,exp}$ (**Table 11**). The calculated values were 2-4 orders of magnitude lower than the experimental data.

It is noted the decreasing kinetics constant k_2 with the increasing initial concentrations indicates the gradually slowed adsorption behavior. That is because the adsorbent was gradually saturated and the adsorbate became more and more difficult to be adsorbed.

Table 11 Pseudo kinetics models for MTBE and Nap removal on F300 and HOK

$C_{0,exp}$	$q_{e,exp}$	Pseudo first-order			Pseudo second-order			
		$q_{e,cal}$	k_1	R^2	h	k_2	$q_{e,cal}$	R^2
F300_MTBE								
0.05	2.9	0.92	2.07E-02	0.748	1.48	1.77E-01	2.89	0.999
12	592	8.31	2.53E-02	0.791	500	5.00E-04	1000	0.999
140	6725	34.2	4.15E-02	0.954	2336	4.98E-05	6849	0.999
HOK_MTBE								
0.074	3.7	1.23	1.84E-02	0.792	0.94	6.98E-02	3.68	0.999
14	651	12.5	1.15E-02	0.873	143	1.43E-04	1000	0.998
140	5530	30.6	6.91E-03	0.675	1117	4.97E-05	4739	0.997
F300_Nap								
0.005	0.26	0.29	2.99E-02	0.749	0.28	4.09	0.26	0.999
1	55	2.37	3.92E-02	0.72	111	0.04	56	1
9.3	462	7.51	4.61E-02	0.824	500	0.002	500	0.999
HOK_Nap								
0.01	0.5	0.33	8.29E-02	0.737	2.81	11.1	0.5	1
1	52	2.62	3.68E-02	0.612	55.6	0.02	53	0.999
8.6	430	7.81	6.91E-03	0.404	500	0.002	500	0.999

$C_{o,exp}$ (mg/L); $q_{e,exp}$ (µg/g); $q_{e,cal}$ (µg/g); K_1 (1/min); h (µg/(g·min)); K_2 (g/(µg·min))

5.3.1.3 Intra-particle model

As shown in **Fig. 20(a)**, the plot of q_t versus $t^{1/2}$ for MTBE adsorption is characterized by three distinct trends, indicating the concomitance of film diffusion, meso-pore diffusion and micro-pore diffusion in MTBE adsorption (Long et al., 2009). A similar trend was also found for Nap adsorption except at low concentrations (5 µg/L on F300 and 10 µg/L on HOK), where only two curves were noted (**Fig. 20(b)**). The lack of micro-pore diffusion can be attributed to the chemical properties of Nap. Compared to MTBE, Nap is more hydrophobic due to its high values of log K_{OW} and log K_{OC}. Therefore it has a stronger affinity for hydrophobic adsorbents than MTBE. Thus, it is plausible that Nap was retained either on the external surface (shell and macro-pores) or meso-pores without any subsequent transfer to the micro-pores. However, the appearance of the third stage of micro-pore diffusion at other high concentrations of Nap indicated the contribution of micro-pores adsorption for Nap removal.
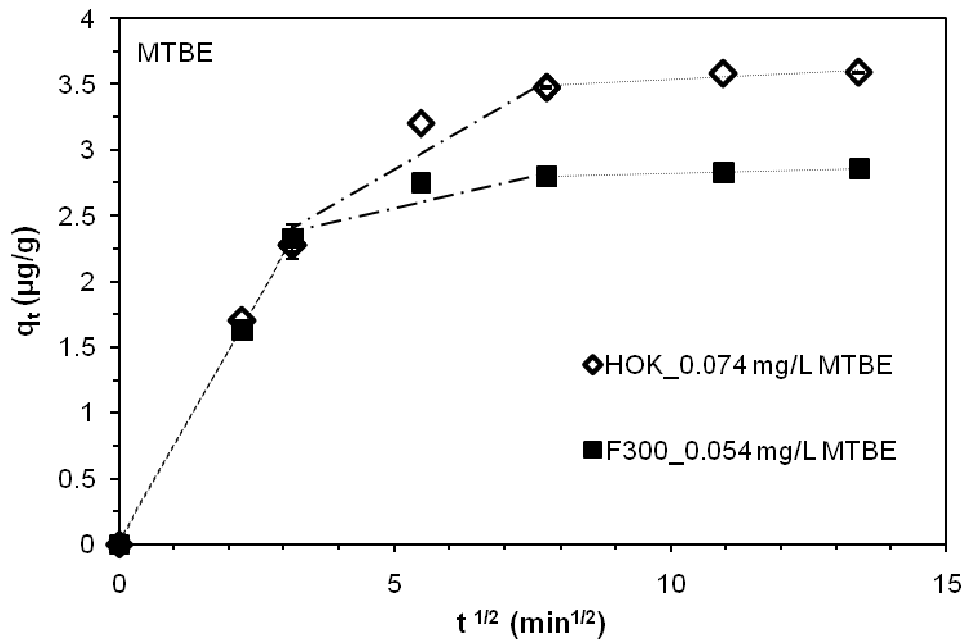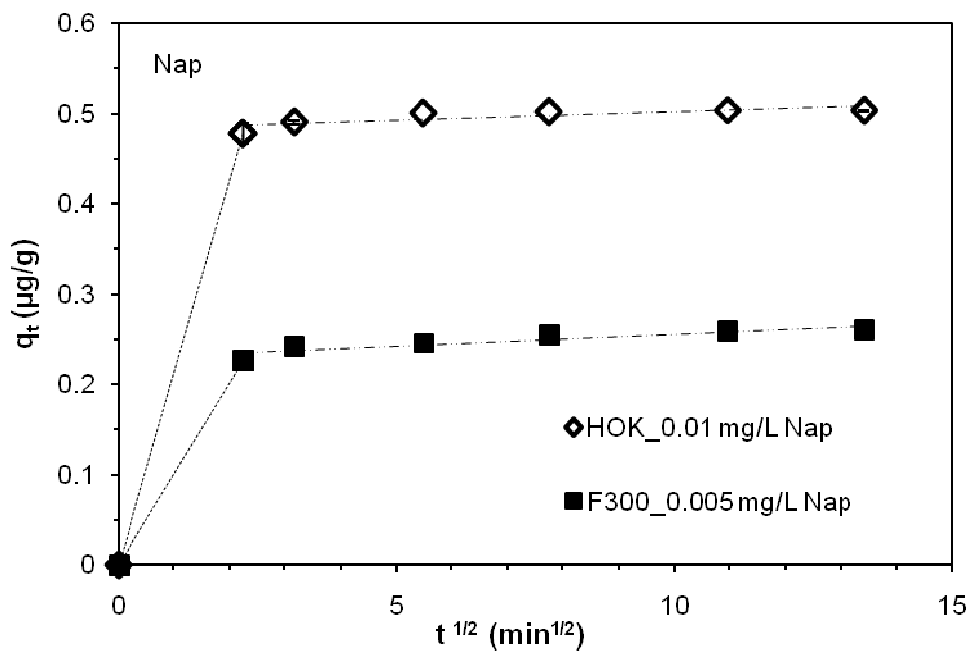
Fig. 20 Multi-linear Intra-particle diffusion plots for (a) MTBE and (b) Nap adsorption on F300 and HOK at low initial concentrations

The slopes of the plots for each stage are listed in **Table 12** and are denoted as K_{i1}, K_{i2} and K_{i3} for the rates of film, meso-pore, and micro-pore diffusion, respectively. It is evident that high initial concentrations enhanced adsorbate diffusion, while small pore sizes hindered it.

Because the plot intercept manifested the effect of the former stage (Vadivelan and Kumar, 2005), the contribution of each diffusion stage was calculated with the intercept of the sequent stage (Equation 23).

$$C\% = \frac{intercept(nextstage)}{q_e} \cdot 100\% \qquad (23)$$

As seen in **Table 12**, the contributions of meso-pore and micro-pore diffusions increased at higher initial concentrations. This is because a high initial concentration enhances the mass transfer and compensates for any hindrances due to small pore size. Compared to MTBE, this increase of micro-pore diffusion in Nap adsorption was inappreciable, revealing the stronger affinity of Nap with macro-pores (in film diffusion) and meso-pores. For both MTBE and Nap, the film diffusion played a very important role in adsorption. It was shown to contribute 41-71% for MTBE removal and 66-96% for Nap removal.

Table 12 Intra-particle model for MTBE and Nap removal on F300 and HOK

$C_{0,exp}$	$q_{e,exp}$	Intra-particle model					
		K_{i1}	$C_1\%$	k_{i2}	$C_2\%$	k_{i3}	$C_3\%$
F300_MTBE							
0.05	2.9	0.74	71%	0.1	23%	0.01	6%
12	592	192	64%	35.6	30%	2.91	6%
140	6725	1773	41%	644	46%	71.9	13%
HOK_MTBE							
0.074	3.7	0.73	43%	0.26	50%	0.02	7.2%
14	651	136	47%	29.5	29%	11.01	24%
140	5530	1484	62%	159	22%	60.2	16%
F300_Nap							
0.005	0.26	0.1	88%	0.002	12%	-	-
1	55	21.9	85%	1.41	12%	0.13	2.8%
9.3	462	156	66%	28.7	31%	1.22	3.2%
HOK_Nap							
0.01	0.5	0.21	96%	0.001	4%	-	-
1	52	17.5	67%	3.18	31%	0.07	1.8%
8.6	430	137	73%	18.9	25%	0.66	1.9%

$C_{o,exp}$ (mg/L); $q_{e,exp}$ (µg/g); K_{ij} (µg/(g·t$^{1/2}$))

5.3.1.4 Boyd model

The Boyd model and B_t-t plots (not presented) were used to identify the rate-controlling step of adsorption. B_t is a coefficient, which is related to the adsorption rate (Equation 19). **Fig. 21** presents the B_t-t plot of MTBE and Nap adsorption on HOK at low initial concentrations. The B_t-t plots at other situations also showed the

non-linear character. The non-linear character of the plots indicated that film diffusion was the rate-controlling step in both MTBE and Nap adsorption (Vadivelan and Kumar, 2005; Gasser et al., 2006). This is consistent with the result of the intra-particle kinetics model. Correspondingly, the values of D_i (Equation 20), which varied at 1.55E-07 to 7.77E-08 for MTBE adsorption and 2.59E-07 to 7.77E-08 for Nap, lying in the range of 10^{-6}-10^{-8} cm^2/s, further confirmed the controlling effect of film diffusion (Michelson et al., 1975; Gasser et al., 2006).
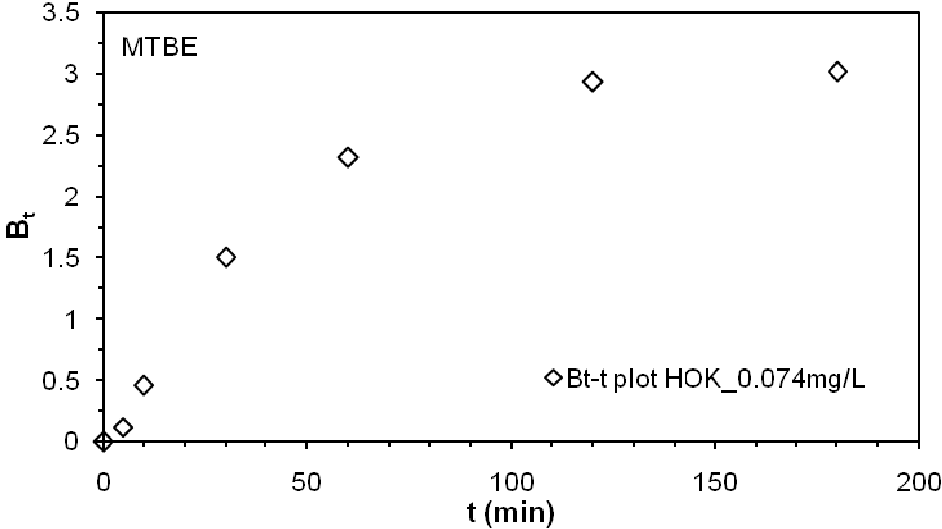
(a)
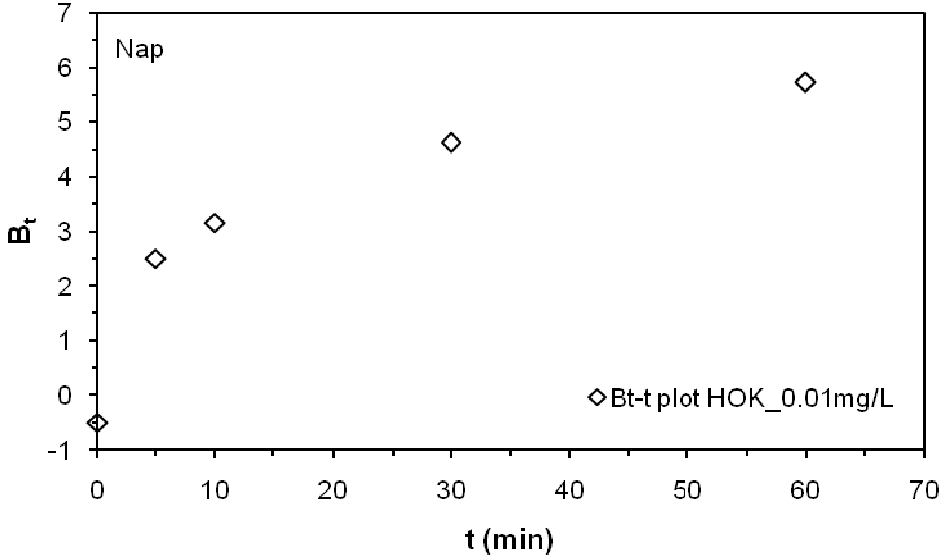
(b)

Fig. 21 B_t-t plots for (a) MTBE and (b) Nap adsorption on HOK at low initial concentration

5.3.2 Adsorption isotherms

5.3.2.1 Adsorption of MTBE

As shown in **Fig. 22(a)** and **22(b)**, the adsorption of MTBE was non-linear for both F300 and HOK. The Freundlich, Langmuir, Tóth and PDM isotherms were all in close accordance with the experimental measurements (R^2>0.985). The values for the adsorption capacity (q_m) of MTBE calculated from the different isotherms are comparable (**Table 13**), which are 194 mg/g (Langmuir), 244 mg/g (Tóth), 222 mg/g (PDM) for F300 and 24 mg/g (Langmuir), 25 mg/g (Tóth), 41 mg/g (PDM) for HOK while the experimental equilibrium values were 200 mg/L and 20 mg/L for adsorption of MTBE on F300 and HOK, respectively. Compared to the adsorption capacity of MTBE on other adsorbents, as Norit GAC 1240 (5.83 mg/g, Langmuir) (Inal et al., 2009), surfactant modified zeolite (100 mg/g, Langmuir) (Ghadiri et al., 2010), Amberlite XAD7 (8.5 mg/g, Langmuir) or Ambersorb 563 (75 mg/g, Langmuir) (Bi et al., 2005), F300 and HOK can be both regarded as effective adsorbents for MTBE removal. F300 however has a 10 times greater adsorption capacity than HOK.
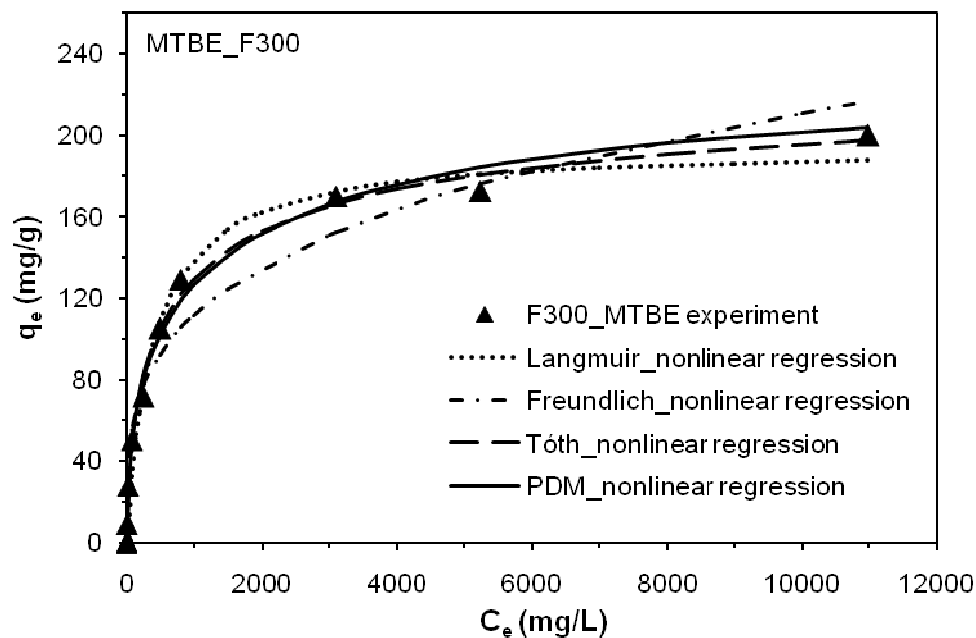
(a)
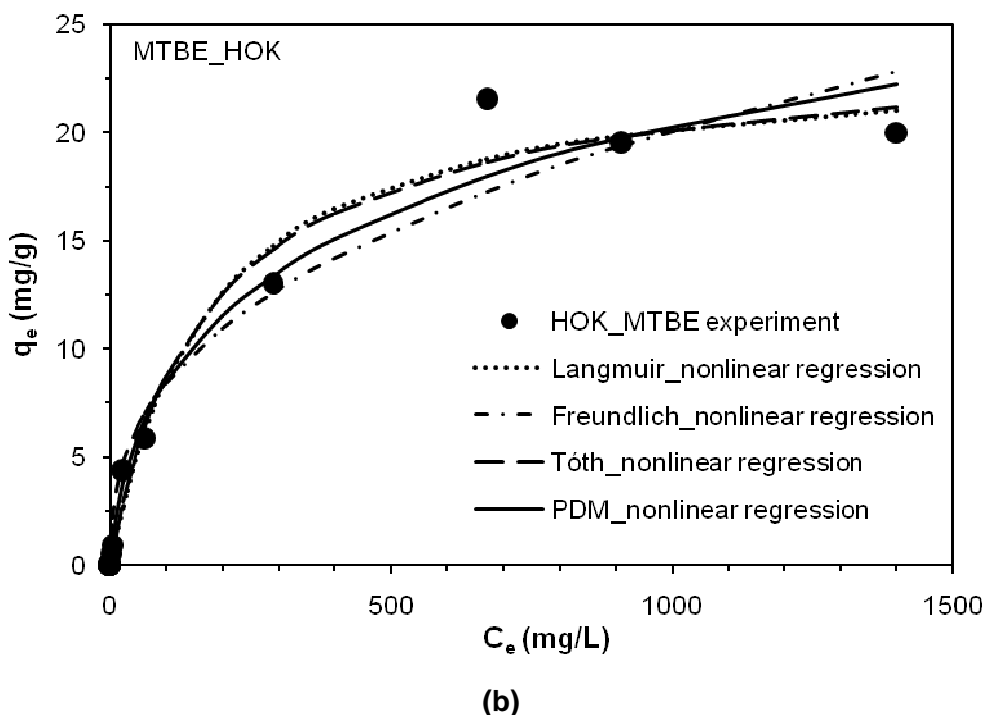
Fig. 22 Isotherm models fitting (non-linear regression) for MTBE on (a) F300 and (b) HOK

The good fitting performances of Tóth and PDM models revealed the heterogeneity of adsorbents and that pore filling was the main mechanism in MTBE adsorption. Different from surface adsorption, the adsorbed adsorbate on the pore walls can overlap each other inside the pores and the adsorption capacity therefore can be greatly enhanced (Dubinin, 1960; Sing, 1995). More micro-pores (0.47 cm^3/g) on F300 indicates its higher adsorption potential and brought higher MTBE adsorption capacity, which was about 10 times higher than that of HOK. However, the values of occupied micro-pores (V_0 in PDM isotherm) in MTBE adsorption were 0.3 cm^3/g on F300 and 0.047 cm^3/g on HOK (**Table 13**), only around 70% and 31% of their total micro-pore volume. It can be deduced that pore selection was involved in MTBE adsorption. This is consistent with the prior study that MTBE adsorption was related to the micro-pores with specific size of 7-11 Å.

Table 13 Adsorption isotherms for MTBE and Nap removal

	MTBE /F300	MTBE /HOK	Nap /F300	Nap /HOK
Freundlich_non-linear regression				
K_f (mg/g) (L/mg)$^{1/n}$	16.5	1.47	339	60.5
1/n	0.28	0.38	1	0.69
R^2	0.986	0.985	0.996	0.992
Langmuir _non-linear regression				
q_m (mg/g)	194	24	-	-
K_l (L/mg)	0.0025	0.006	-	-
R^2	0.996	0.992	-	-
Tóth model				
q_m (mg/g)	244	25	7.6	34.01
K_t (L/mg)	0.007	0.006	0.046[a]	0.0813[a]
b	0.5	0.87	1.4	0.25
R^2	0.998	0.993	0.996	0.994
PDM model[b]				
V_0 (L/g)	3.00E-04	4.70E-05	1.29E-05	4.30E-06
q_m (mg/g)[c]	222	35	13.18	4.41
E (kJ/mol)	12.9	13.07	16.5	19.8
a	2.02	2.09	2.99	3
R^2	0.998	0.99	0.981	0.996
Partitioning linear model				
($K_{oc} \cdot f_{oc}$) (L/kg)	-	-	1288[d]	1288[d]
R^2	-	-	0.996	0.977

[a] unit is (L/µg); [b] in PDM calculation, ρ_0 (g/cm^3) is 0.7404 for MTBE and 1.0253 for Nap (Mackay, 1992); S (mg/L) is 51,600 for MTBE and 30 for Nap (Mackay, 1992); [c] q_m was calculated as $q_m = V_0 \cdot \rho_0$; [d] K_{oc} (L/kg) was calculated from $log K_{oc} = 3.11$(Mackay, 1992) and $f_{oc}$was arbitrarily set as 100% to obtain the possibly maximum contribution of partitioning mechanism.

5.3.2.2 Adsorption of Nap

In **Fig. 23(a)** and **23(b)**, a nearly linear adsorption of Nap was measured with a fairly stable removal efficiency, R_e%, of 99%. Although equilibrium was not achieved because of the low solubility of Nap in water and therefore relatively low initial concentrations in the experiments, the linear adsorption and constant R_e% indicate the high adsorption potential of Nap on both F300 and HOK.

The partitioning linear model was applied to fit the linear adsorption trend. The high correlation coefficients (R^2), 0.996 for F300 and 0.977 for HOK, illustrated the linearity of Nap adsorption and the possibility of partitioning in Nap adsorption. However, the low calculated values of q_e, which were about 4% to 10% of the

experimental data on F300 and 0.1-1% on HOK, confirmed the limited effect of partitioning. Although partitioning was dominant in 1,2-dichlorobenzene adsorption on peat (Kleineidam et al., 2002), it obviously was not the main mechanism for Nap removal in these experiments.
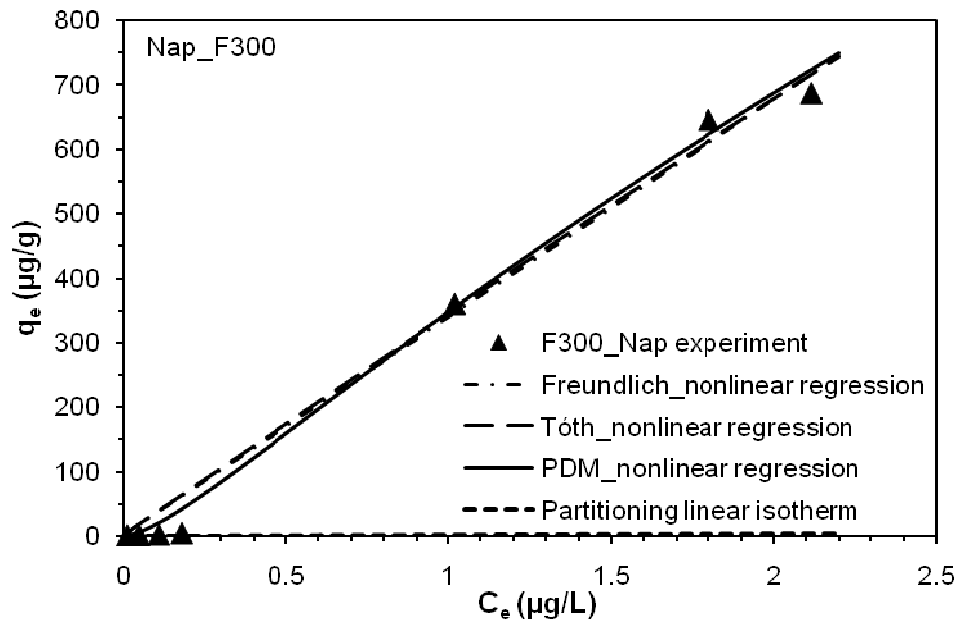
(c)
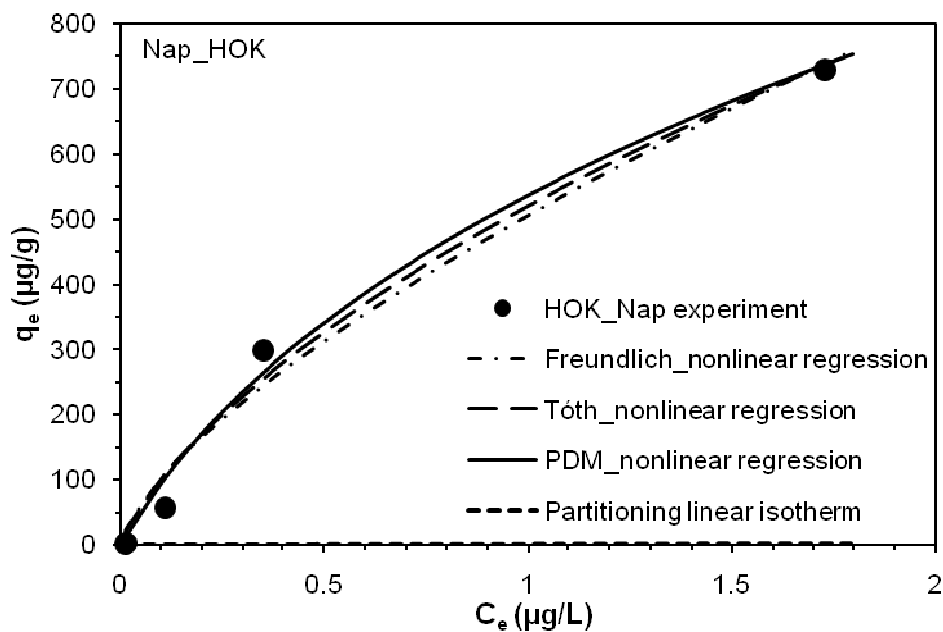
(d)

Fig. 23 Isotherm models fitting (non-linear regression) for Nap adsorption on (a) F300 and (b) HOK

Other non-linear isotherm models performed well in fitting the experimental data (**Fig. 23(a)**, **23(b)**). The values of R^2 are as high as 0.996 (**Table 13**). However, due to the ubiquity of this 'linear' adsorption portion in non-linear isotherms, the specific isotherm for Nap adsorption is difficult to determine. Therefore, pore filling cannot be simply taken as the main mechanism of Nap adsorption. Moreover, Yang et al. (2006) studied Nap adsorption on carbon nanotubes. They reported that surface adsorption was more important than pore filling in the Nap adsorption process. Considering the significant effect of film diffusion on Nap adsorption kinetics, it appears that surface adsorption is the predominant mechanism in Nap adsorption.

Due to the ubiquity of the linear adsorption portion in isotherms, Freundlich was more preferable than other isotherms to describe Nap adsorption for having less fitting parameters. A similar linear Nap adsorption on zeolite also showed good congruence with simple linear and Freundlich isotherms with a high adsorption capacity of 769 mg/g (Chang et al., 2004).

5.3.2.3 Adsorption of Zn^{2+}

In order to compare the difference between heavy metal adsorption and organic compound adsorption and to compare the adsorption capacity of Zn^{2+} between batch experiment and column experiment (section 5.5.1), the adsorption of Zn^{2+} was also tested and fitted with Freundlich model and Langmuir model (**Table 14**). It can be seen that Freundlich model describes more accurately for Zn^{2+} adsorption, indicating the heterogeneous adsorption process. HOK presented higher adsorption capacity of Zn^{2+} than F300. Based on the Langmuir model, the maximum adsorption amount of Zn^{2+} is 5.85 mg/g for F300 and 16.5 mg/g for HOK. The relative high adsorption capacity on HOK is comparable or higher than other carbon materials, like sawdust based carbon (18.53 mg/g) or F400 (10.62 mg/g) (Ramos et al., 2002).

Although F300 has more pores and larger surface area, HOK obtained higher adsorption capacity of Zn^{2+}. Compare to pore-filling mechanism, Zn^{2+} adsorption was more relevant to the mechanisms as complexation, ion-exchange or precipitation (Demirbas, 2008). That is to say, Zn^{2+} adsorption depends on the component of adsorbents (such as functional groups etc.) while MTBE and Nap adsorptions present structure dependence (such as micro-pore, surface area etc.).

Table 14 Adsorption isotherms for Zn^{2+} removal

	Freundlich non-linear regression			Langmuir non-linear regression		
	K_f (mg/g)·(L/mg)$^{1/n}$	1/n	R^2	q_m (mg/g)	K_l (L/mg)	R^2
Zn^{2+}/F300	0.93	0.32	0.981	5.85	0.028	0.961
Zn^{2+}/HOK	9.5	0.1	0.94	16.5	0.14	0.898

5.3.3 Summary

According to the discussion above, the following conclusions were drawn:

1) In the kinetics study, MTBE and Nap adsorption was shown to be rapid. Compared to pseudo first-order kinetics model, the pseudo second-order model fit the adsorption processes better. The intra-particle kinetics model revealed the co-existence of film and intra-particle diffusion in MTBE and Nap adsorption. Film diffusion played an important role in adsorption of organic pollutants, especially for Nap. The Boyd kinetics model further confirmed that adsorption was controlled by film diffusion.

2) Both the Tóth and PDM isotherms presented good congruence with MTBE adsorption, indicating the heterogeneity and pore-filling mechanism in MTBE adsorption. Based on the PDM isotherm, the adsorption capacities of MTBE were 222 mg/g and 35 mg/g on F300 and HOK, respectively. The discrepancy between the occupied micro-pore volume and the total micro-pore volume illustrated the presence of pore selection in MTBE adsorption.

3) The linear behavior of Nap adsorption was not attributed to the partitioning in adsorption, but rather showed the high adsorption potential of F300 and HOK. Surface adsorption appears to be the main mechanism in Nap adsorption. Compared to other isotherms, Freundlich model, with less fitting parameters, was more preferable to describe this linear Nap adsorption.

4) The Zn^{2+} adsorption capacities were 16.5 mg/g on HOK and 5.85 mg/g on F300. Freundlich model fitted better than Langmuir isotherm. Different from the dependence of adsorbents structure in MTBE and Nap adsorption, Zn^{2+} adsorption presented the component dependence.

5) Both F300 and HOK presented high adsorption capacities for Nap. Compared to HOK, F300 displayed a higher removal efficiency for MTBE.

6) Due to the different adsorption behaviors of F300 and HOK between organic compounds adsorption (MTBE and Nap) and heavy metal adsorption, two stages of filter system should be considered. For example, one for MTBE and Nap adsorption with F300 and the other for heavy metal adsorption with HOK.

5.4 The influence of de-icing salt, NOM and bi-adsorbate adsorption on the removal of MTBE and Nap

De-icing salt, which is used for roads at winter time in cold regions, and NOM, which is ubiquitous in environment, can be detected in road runoff and might present potential influence on main pollutants removal (Baeckstoem et al., 2003; Hung et al., 2005; Esteves da Silva and Marques, 2007; Kayhanian et al., 2008). It is known that de-icing salt displays its influence on heavy metal adsorption on zeolite (Athanasiadis, 2005), while its influence on organic compounds removal is uncertain. NOM is regarded as a complex mixture of organic compounds and varies with locations (Newcombe, 1997; Shih et al., 2003). Some studies reported the existence of NOM could greatly decrease the adsorption amount of organic compounds on activated carbon (AC) (Urano et al., 1991; Knappe et al., 1998; Shih et al., 2003). On the other hand, insignificant or no influence of NOM was also found on zeolite and AC for MTBE removal (Wilhelm et al., 2002; Hung et al., 2005). Different adsorbents, adsorbates and NOM resources would cause different extents of NOM influence on adsorption (Newcombe, 1997, 2002; Knappe et al., 1998; Hung and Lin, 2006). Moreover, the concentration of adsorbent, adsorbate and NOM might also relate with the degree of NOM influence (Wilhelm et al., 2002; Rossner 2004; Hung et al., 2005). Therefore, it is difficult to predict the NOM influence on AC adsorption process (Newcombe, 1997; Shih et al., 2003).

From the previous studies, F300 and HOK have presented good adsorption of MTBE and Nap. Considering the further application in real road runoff, the influences of de-icing salt, NOM and co-adsorption with other adsorbate (bi-adsorbate adsorption) on MTBE and Nap removal were tested in this section. While MTBE and Nap represented VOC and PAH in road runoff, humic acid and NaCl were applied as NOM and de-icing salt in experiments.

In previous studies from Hilliges (2007) on F300 and HOK, it was found that there was no influence of de-icing salt on Zn^{2+} adsorption and no desorption of readily

adsorbed Zn^{2+}. Therefore, the influence of de-icing salt was not considered on heavy metal adsorption in this section, but discussed on MTBE and Nap adsorption.

5.4.1 Influence of de-icing salt

To test the influence of de-icing salt, two concentrations (3 g/L and 5 g/L) of NaCl, were conducted in experiments. The concentrations of NaCl applied in experiments are corresponding to the real NaCl concentrations in road runoff during winter time (Helmreich et al., 2010).
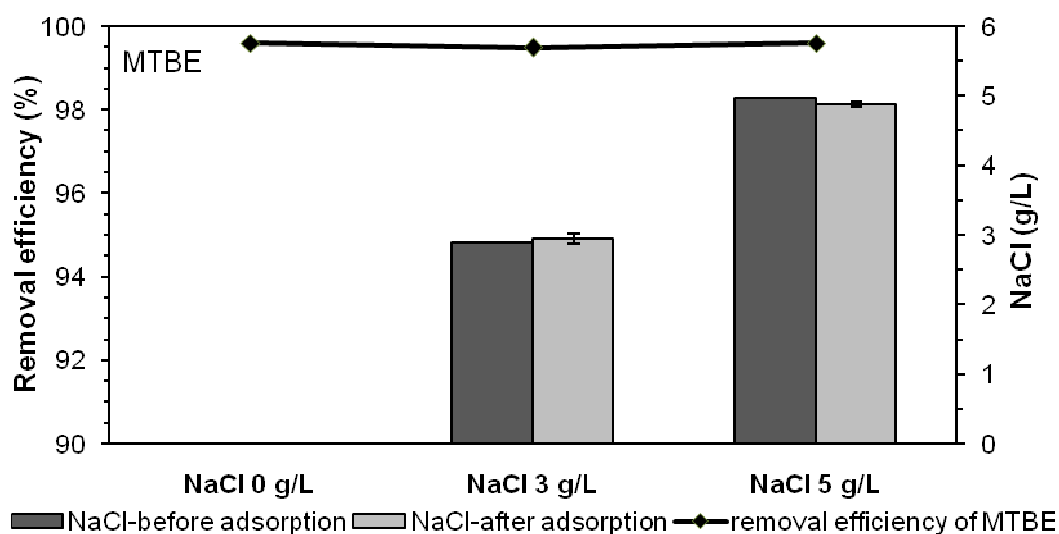
(a)
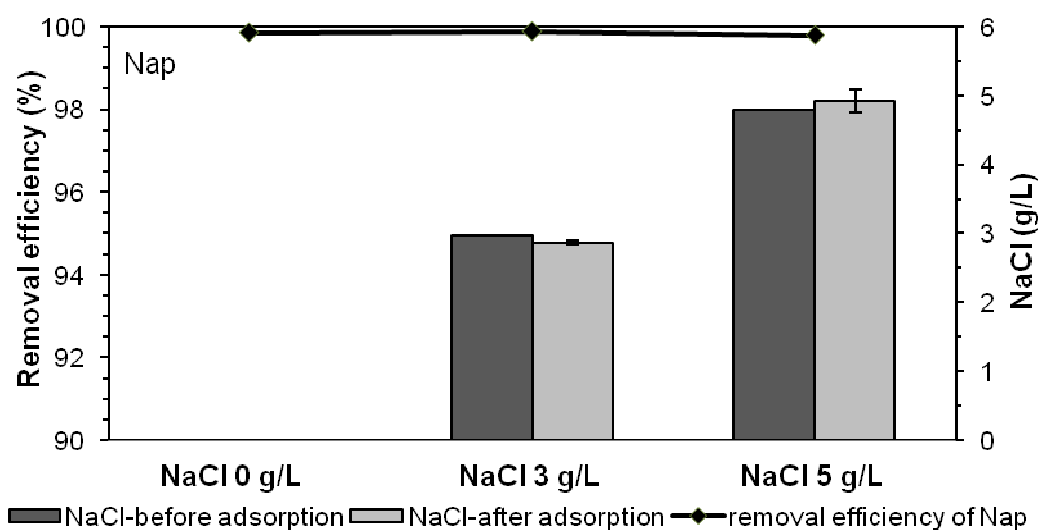
(b)

Fig. 24 Influence of NaCl on adsorption of (a) MTBE and (b) Nap on F300

Figure 24 presents the influence of de-icing salt (NaCl) on MTBE/F300 and Nap/F300 adsorption systems, where the initial concentrations of MTBE and Nap

were both 1 mg/L. The histograms in **Fig. 24** indicate the amounts of NaCl before and after 24h adsorption while the lines illustrate the removal efficiencies of MTBE or Nap at different NaCl concentrations. As shown by histograms, the amount of NaCl is not reduced after adsorption, indicating no adsorption of NaCl on adsorbent occurred. Consequently, NaCl would not have the influence on MTBE and Nap adsorptions. The lines presenting removal efficiency confirms this deduction. R_e kept the same value (99.6% for MTBE and 99.8% for Nap) with the presence of NaCl at different concentrations (0 g/L, 3 g/L and 5 g/L). It is evident that NaCl, as a representative of de-icing salt, was not adsorbed on adsorbent and had no influence on MTBE or Nap removal. The same phenomenon was also observed on HOK with a constant removal efficiency of 97.5% for MTBE and 100% for Nap removal (**Fig. 25)**.
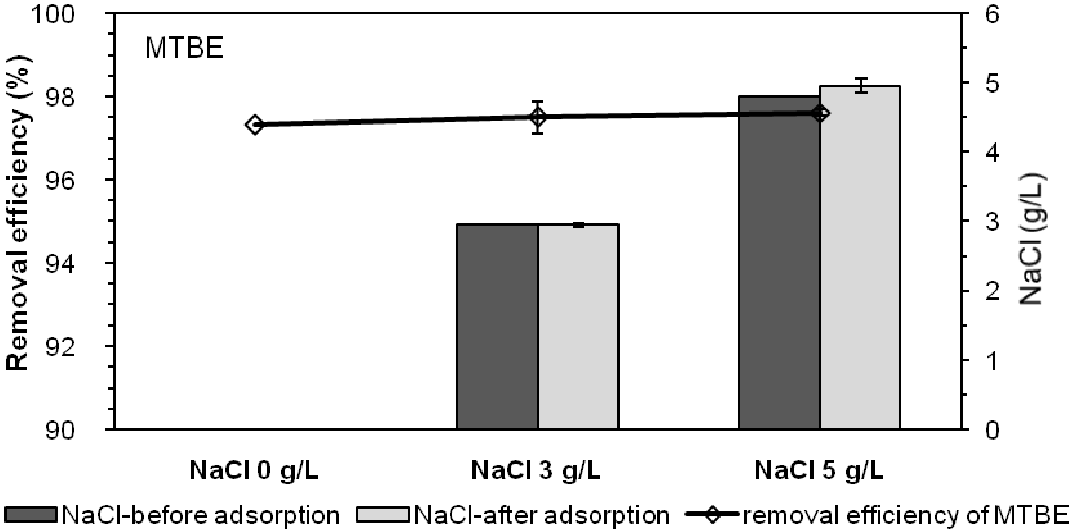
(a)
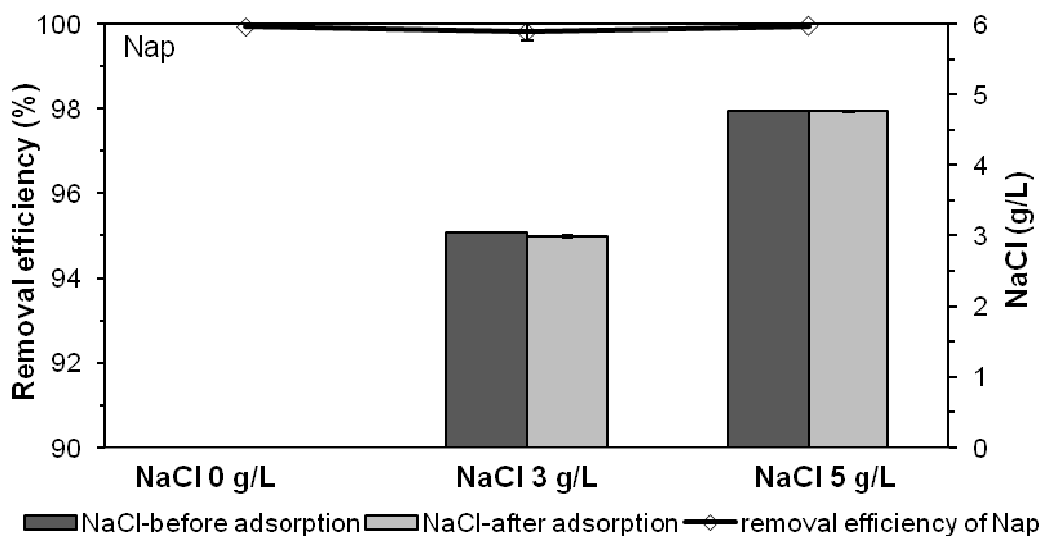
(b)

Fig. 25 Influence of NaCl on adsorption of (a) MTBE and (b) Nap on HOK

Based on these results and previous result from Hillige (2007), it is clear that both F300 and HOK can be used under real road runoff conditions. Without the influence of de-icing salt, F300 and HOK are both suitable materials for MTBE and Nap removal in road runoff treatment.

5.4.2 Influence of NOM

The influence of NOM is frequently considered on the adsorption of organic compound. As a complex mixture of organic compounds, NOM might have strong competition with the target organic adsorbate. The NOM influences on MTBE and Nap adsorption are discussed in the following parts.

5.4.2.1 NOM adsorption to F300 and HOK

Two concentrations of NOM, 4 mg/L and 10 mg/L as TOC, were carried out in experiments with MTBE and Nap on F300 and HOK.
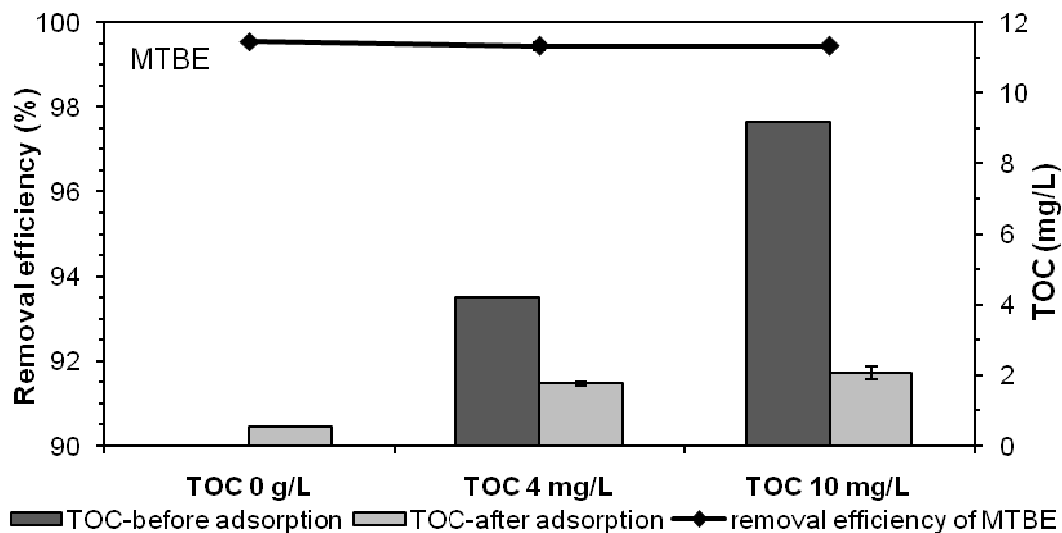
(a)
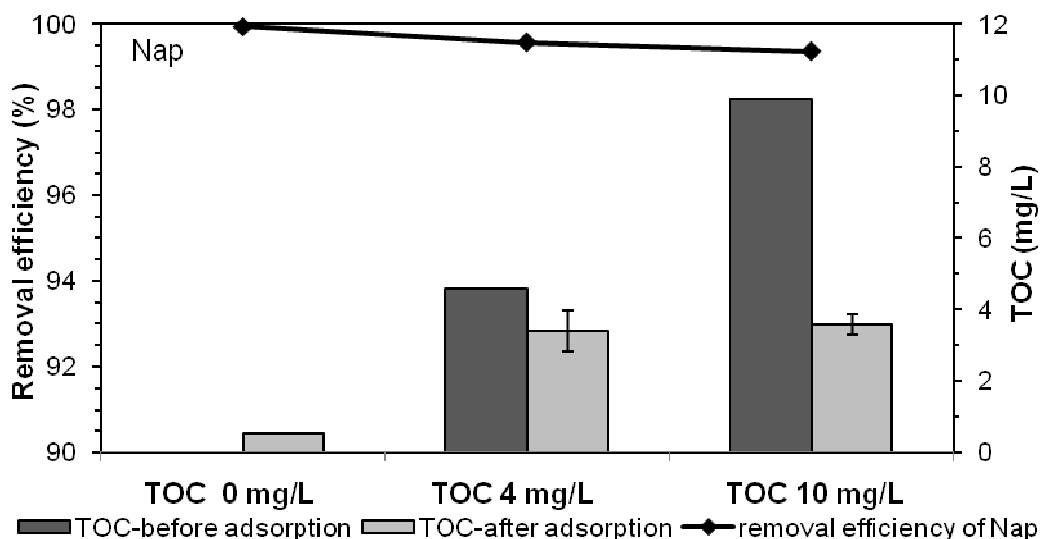
(b)

Fig. 26 NOM in adsorption of (a) MTBE and (b) Nap on F300

Figure 26 presents the influence of NOM on MTBE/F300 and Nap/F300 adsorption systems, where the initial concentrations of MTBE and Nap were both 1 mg/L. Similarly, the histograms state the NOM changes before and after adsorption processes and the lines illustrate the changes of removal efficiency of MTBE and Nap at different concentrations of NOM. It can be seen from the histograms that the amount of NOM decreased dramatically after adsorption. Despite the exuded TOC from adsorbent (F300), which was about 0.54 mg/L, the amount of adsorbed NOM was up to 77.5% (from 10 mg/L to 2 mg/L) with the presence of MTBE and 63.9% (from 10 mg/L to 4 mg/L) with the presence of Nap. It is clear that NOM is an

attractive adsorbate to adsorbent and has stronger competition with Nap for adsorption. However, no significant influence of NOM was found on MTBE adsorption, for which a constant removal efficiency of 99.5% was maintained at any test concentrations of NOM. In contrast, the removal efficiency of Nap decreased from 99.8% to 99.4% when the concentration of NOM increased from 0 mg/L to 10 mg/L, indicating distinct NOM influence on Nap adsorption. Similar results were obtained on HOK, where R_e (%) kept constant for MTBE removal (97.5%) and reduced from 99.2% to 97.9% for Nap adsorption (**Fig. 27**). It is also noticed in **Fig. 27** that HOK itself released more TOC (1.53 mg/L) than F300 (0.54 mg/L) after adsorption.
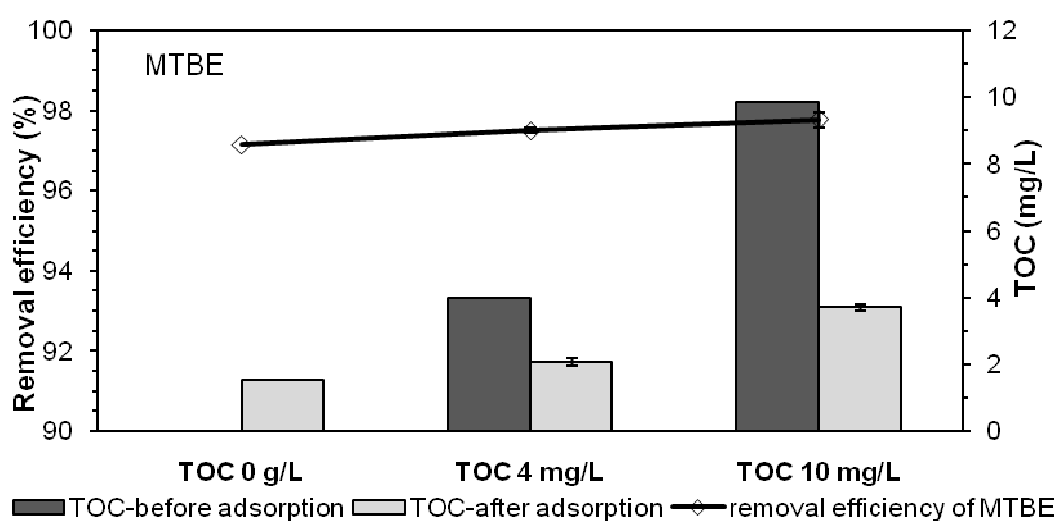
(a)
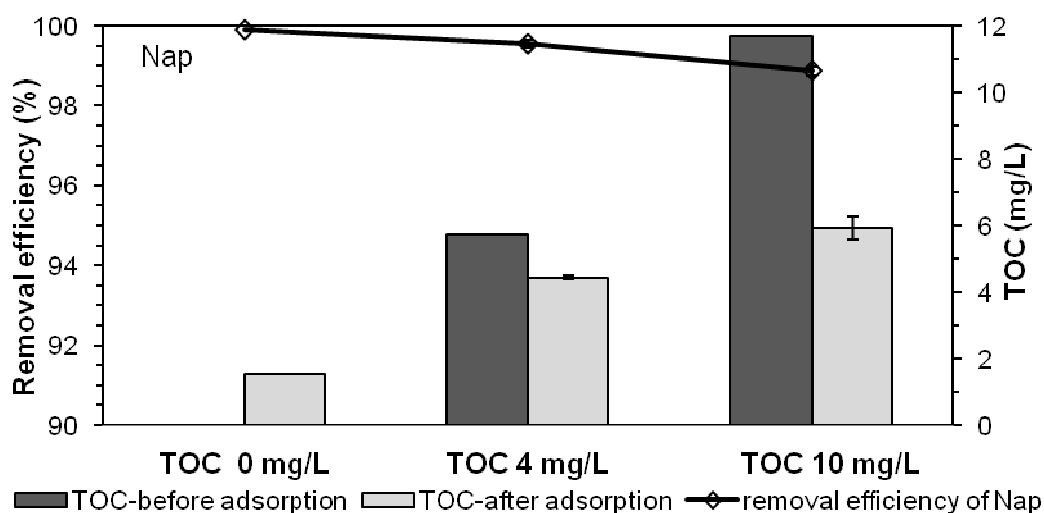
(b)

Fig. 27 NOM in adsorption of (a) MTBE and (b) Nap on HOK

NOM presented negligible competition with MTBE in adsorption and distinct competition with Nap. That might be due to the different adsorption behaviors between MTBE and Nap. It has been reported that MTBE adsorption is specifically related to the micro-pores of 8-11 Å (Li et al., 2002). Differently, Nap adsorption is not restricted to any specific pore size. As a non-polar organic compound, Nap has weak affinity with water molecule and is easy to adsorb onto adsorbent surface (Cabal et al., 2009). Therefore, only a small portion of NOM molecules, which have small molecule size, entered the micro-pores of 8-11 Å, could have the competition with MTBE for adsorption. In contrast, all the NOM molecules could have competition with Nap because of its unspecific adsorption. Similarly, Esteves da Silva and Marques (2007) reported NOM had unspecific interaction with non-polar or low polar organic compounds and this interaction increased with the decrease of compound polarity.

Moreover, with the increase of NOM concentration, the decrease of Nap removal efficiency was more significant on HOK (99.2% to 97.9%) than on F300 (99.8% to 99.4%). It suggests the NOM influence on Nap adsorption was stronger on HOK. Compare to F300, HOK has a relatively low BET surface area. The limited adsorption area might cause stronger competition between NOM and Nap for adsorption, and bring stronger influence on Nap adsorption.

However, the negligible NOM influence on MTBE adsorption seems different from some previous studies, which reported the presence of NOM reduced the adsorption amount of trace organic pollutants (herbicide atrazine, 2-methyl-isoborneol, and MTBE) at very low initial concentrations (μg/L) (Knappe et al., 1998; Hung et al., 2005). To clarify the NOM influence on organic contaminants adsorption, especially to verify the influence of NOM on MTBE adsorption behavior, MTBE and Nap adsorption experiments with variable initial concentrations and fixed NOM concentration (at 10 mg/L (TOC)) were carried out.

5.4.2.2 NOM influence on MTBE adsorption

Figure 28(a) and **28(b)** present the adsorption of MTBE on F300 and HOK, respectively, in presence of NOM (10 mg/L as TOC) in the form of Freundlich Isotherm (Equation 3 and 4) (Freundlich, 1907; Solisio, 2001). As shown in **Fig. 28(a) and 28(b)**, the adsorbed amounts of MTBE in the presence of NOM were identical to the values in single MTBE adsorption. Over the wide range of MTBE initial

concentration (55 µg/L-2,000 mg/L), the presence of NOM still did not show significant hindering effect on MTBE adsorption.

(a)

(b)
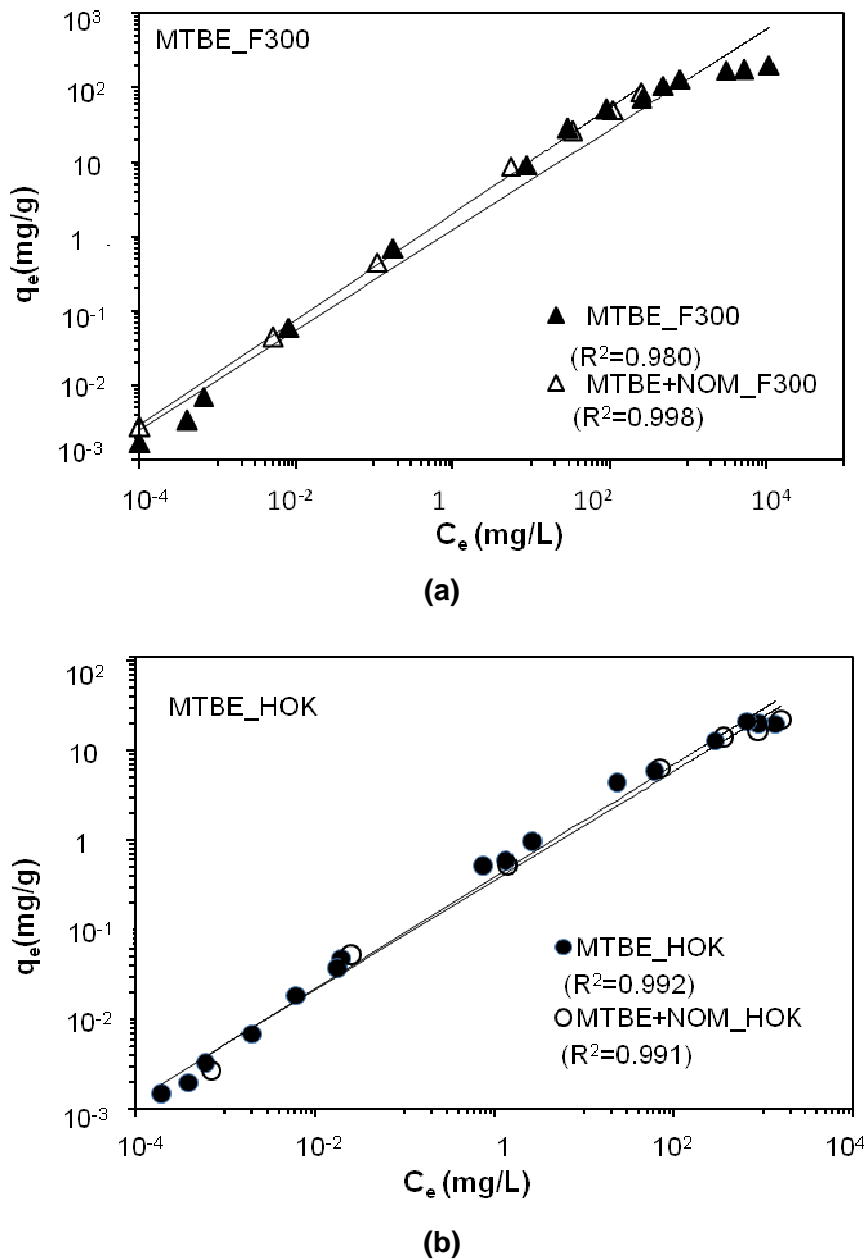
Fig. 28 NOM influence on adsorption of MTBE for (a) F300 and (b) HOK (log-log form)

The high initial concentrations of MTBE in experiment might be the main reason for the negligible influence of NOM on MTBE adsorption. Hung et al. (2005) found the extent of NOM influence was dependent on the initial concentration of MTBE. Significant NOM influence was observed at the MTBE initial concentration of 45 µg/L while the slight NOM influence was found at MTBE initial concentration of 466 µg/L. Trace concentration of target organic pollutants was the necessary condition for the

significant NOM influence on organic pollutant adsorption (Ebie et al., 2001; Matsui et al., 2003; Rossner, 2004; Abu-Lail, 2010). Wilhelm et al. (2002) investigated the NOM influence on MTBE/AC adsorption system and found no hindering effect of NOM at MTBE initial concentration of 100 mg/L. However, due to the complex and different constitution of NOM, the concentration of MTBE causing strong competition with NOM and significant influence on adsorption are different from one condition to another (Newcombe et al., 1997). In this study, MTBE adsorption at the lowest initial concentration of 55 µg/L was not impaired by NOM at 10 mg/L (as TOC).

Besides the constitution of NOM, the high amount of adsorbent dose provided in experiments might be another reason for the negligible NOM influence at low MTBE concentration (55 µg/L). Rossner (2004) compared the NOM influence on MTBE adsorption capacity of several ACs and pointed out that high adsorbent dose rendered low equilibrium liquid phase MTBE concentration (C_e) and weakened the hindering effect of NOM on adsorption. Frimmel et al. (1999) found no influence of NOM on adsorption of hydrophilic pollutants at high masses of sorbents. Compare to the variable amounts of adsorbent dose in adsorption, the adsorbent dose was fixed at 20 g/L in this study, which was quite high for MTBE removal at low initial concentration. For instance, at the initial concentration of 55 µg/L, 99.8% MTBE was removed by F300 (20 g/L) with a C_e value of 0.1 µg/L in presence of NOM. This result was comparable with single MTBE adsorption, for which the R_e value was 99.7%. Therefore, low concentration of MTBE, high concentration of NOM, and low amount of adsorbent dose would promote the hindering effect of NOM on adsorption of organic pollutant. The negligible NOM effect on MTBE adsorption in this study was attributed to the relatively high initial concentrations of MTBE and high amount of adsorbent dose.

Therefore, NOM was adsorbed to adsorbent (**Fig. 26**) without hindering the adsorption of MTBE in this study. Generally, NOM hinders organic compound adsorption by two ways: 1) direct competition for adsorption sites; 2) pore blockage, especially for the continuous adsorption system (Newcombe, 1997; Ebie et al., 2001). In this study, the negligible NOM influence revealed the weak competition between NOM and MTBE at high initial concentration of MTBE and high amount of adsorbent. Moreover, Hung et al. (2005) studied the adsorption kinetics of MTBE in the presence of NOM and found the adsorption kinetics of MTBE was not influenced by the

presence of NOM. It is quite possible that the NOM molecules did not arrive at the micro-pores before MTBE molecules adsorbed. Therefore, the MTBE adsorption could complete without being hindered. This situation could be reversed when MTBE concentration is quite low and/or the amount of adsorbent dose is deficient, for which the competition between NOM and MTBE would increase and significant NOM influence would occur on MTBE adsorption. Although NOM influence was not significant on MTBE removal in this study, the adsorbed NOM still presented its potential to cause severe influence on MTBE adsorption in the dynamic (continual) adsorption system by pore blockage.

5.4.2.3 NOM influence on Nap adsorption

Nap adsorptions in presence of NOM on F300 and HOK are presented in **Fig. 29(a)** and **29(b)**, respectively. The log-log coordinate of Freundlich isotherm illustrates the adsorption amount of Nap. Different from MTBE adsorption, NOM displayed a significant influence on Nap adsorption. At the similar equilibrium aqueous concentration (C_e) of 3 µg/L, the presence of NOM roughly lowered the adsorption amount of Nap by two orders of magnitude, from 687 µg/g to 5.45 µg/g on F300 (**Fig. 29(a)**).

(a)
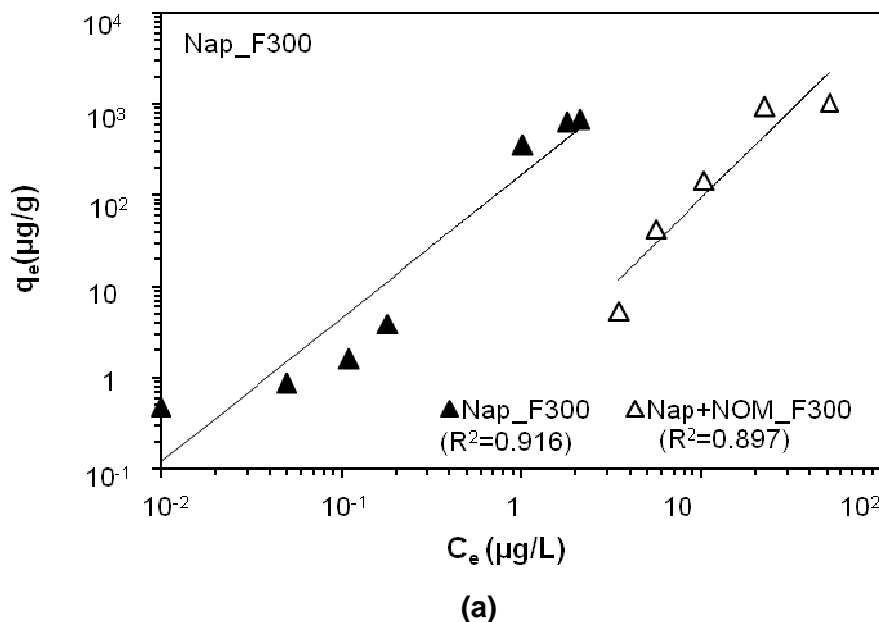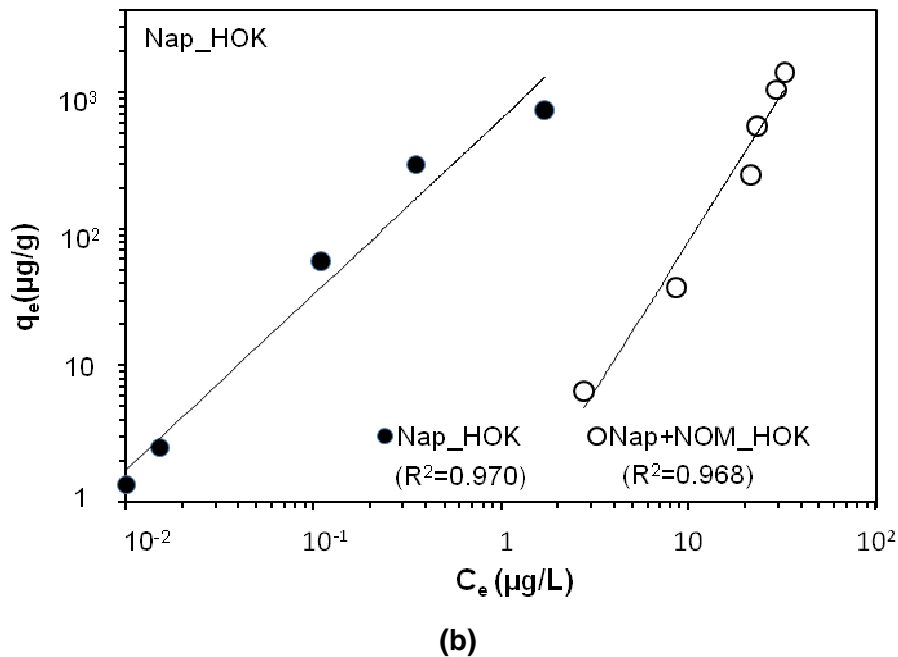
Fig. 29 NOM influence on adsorption of Nap for (a) F300 and (b) HOK (log-log form)

As discussed before, the unspecific adsorption of Nap should be the main reason for that significant NOM influence. With the influence of NOM, F300 and HOK both maintained high removal efficiency (R_e) of Nap at the test concentrations, which was 96.9-100% on F300 and 97.9-100% on HOK. Although these R_e data is slightly lower than the one without NOM presence, which were 99.6-100%, they still presented effective removal of Nap on both F300 and HOK.

5.4.3 Influence of co-adsorption

Adsorptions of MTBE and Nap in the presence of second adsorbate, Nap, MTBE or Zn^{2+}, are illustrated in **Fig. 30** in the log-log coordinate (Freundlich isotherm, Equation 4).

As shown in **Fig. 30(a)** and **30(b)**, the MTBE adsorption was not influenced by the presence of the other adsorbate (Nap or Zn^{2+}). The data from co-adsorption experiment conformed to the linear log-log isotherm obtained from the single MTBE adsorption, suggesting the negligible influence of other adsorbate on MTBE removal. Low concentration of the second adsorbate and high adsorption capacity of MTBE on F300 and HOK might be the main reasons for this slight influence. While MTBE concentrations varied at 170-2,000 mg/L, the corresponding concentration of the second adsorbate was 1 mg/L for Nap and 1.5 mg/L for Zn^{2+}, respectively. Low

concentration of the second adsorbate rendered low competition with MTBE and consequently caused slight impact on MTBE adsorption. Besides, the high adsorption capacity of MTBE on F300 (222 mg/g) and HOK (35 mg/g) suggested the strong affinity between MTBE and adsorbent, which could help MTBE to be adsorbed in the bi-adsorbate experiments.

(a)

(b)
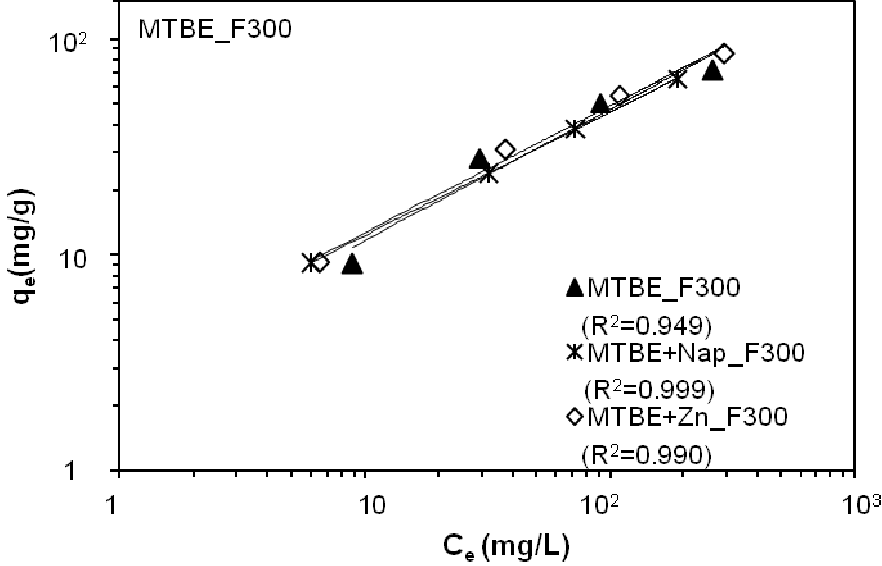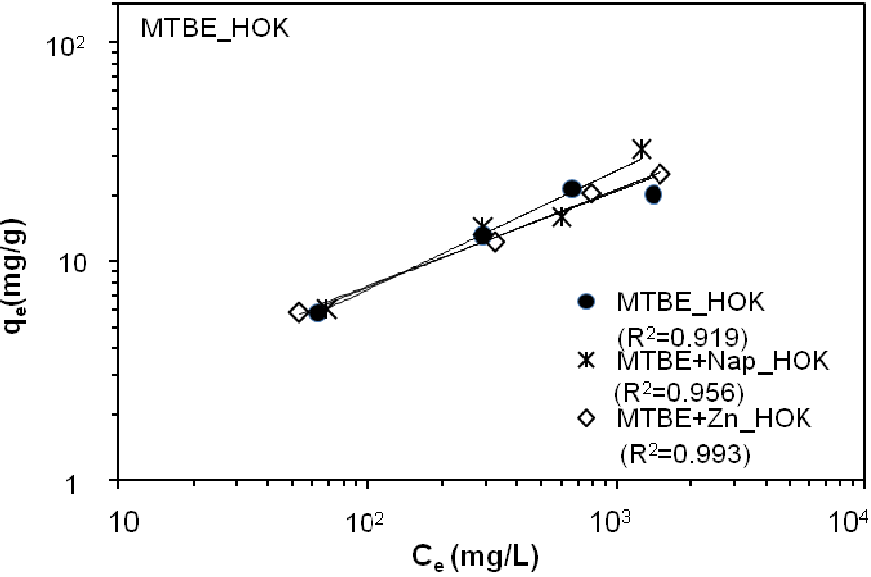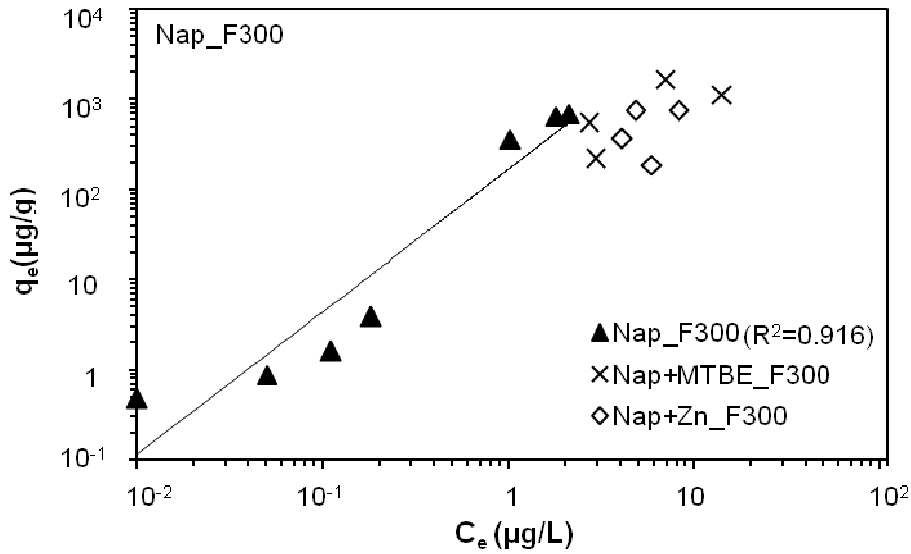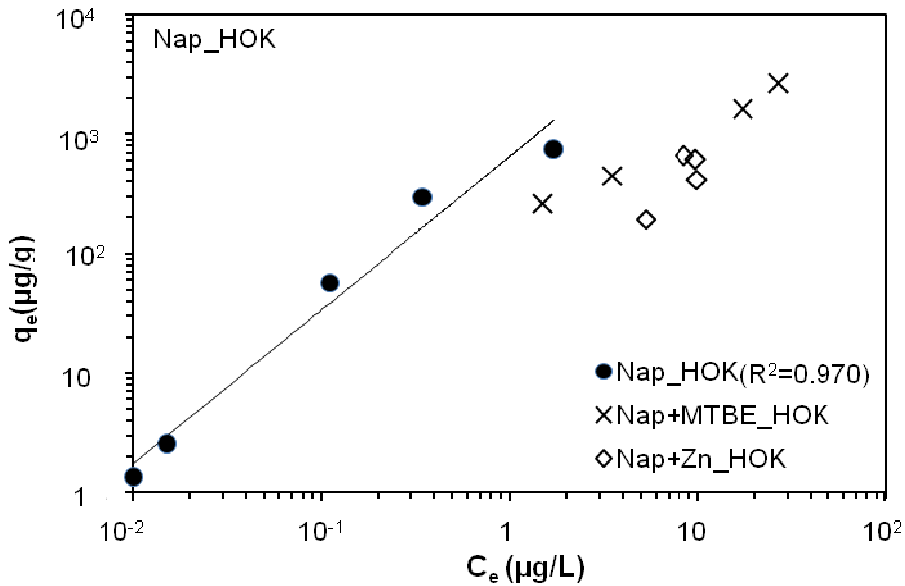
Fig. 30 Adsorption of (a,b) MTBE and (c, d) Nap in the bi-adsorbate adsorption experiments on F300 and HOK (log-log form)

Different from MTBE, Nap adsorption was influenced by the second adsorbate. As shown in **Fig. 30(c)** and **30(d)**, the data from bi-adsorbate experiments caused clear deviation from single Nap adsorption isotherm. On account of the similar conditions for bi-adsorbate experiments, the different NOM influences on MTBE and Nap removal should be attributed to their different characters. Similar as in the experiments with NOM, the unspecific adsorption of Nap might cause high competition with the second adsorbate and produce high influence on its removal. The removal efficiency (R_e) of Nap still kept high with these influences, at 99.8-100%

81

on F300 and HOK at test concentrations. The R_e values were higher than that with the presence of NOM, further indicating stronger competition existed between NOM and Nap adsorption.

Additionally, it is noted Zn^{2+} presented more influence on Nap adsorption on HOK than on F300. The more derivation of Nap adsorption with the presence of Zn^{2+} from the single Nap adsorption isotherm was observed on HOK (**Fig. 30(c)** and **30(d)**). This different Zn^{2+} influences between F300 and HOK suggests their different affinities with Zn^{2+}. HOK had stronger affinity with Zn^{2+} for its higher adsorption capacity in previous study (16.5 mg/g for HOK and 5.85 mg/g for F300). Therefore, compare to F300, stronger competition between Zn^{2+} and Nap for adsorption would happen on HOK.

From the different influences of the second adsorbate on MTBE and Nap adsorption, it can be deduced that in real road runoff, finding a versatile adsorbent to adsorb all the organic and inorganic pollutants would be a difficult task. Due to the different adsorption mechanisms of different target pollutants, the requirements for the versatile adsorbent would be various and might have conflicts. The application of multi-adsorbent in road runoff can be considered in the real road runoff treatment. A bi-adsorbent system was further tested in column experiment (section 5.5.4).

5.4.4 Summary

According to the discussion above, the following conclusions were drawn:

1) NaCl, acted as the de-icing salt, did not take part in the adsorption process and had no influence on MTBE or Nap adsorption. At the initial concentration around 1 mg/L, the removal efficiencies of MTBE and Nap kept constant when the concentration of NaCl varied at 0 g/L, 3g/L and 5g/L. The constant R_e was 99.6% for MTBE and 99.8% for Nap on F300, while the values on HOK were 97.5% and 100% for MTBE and Nap, respectively.

2) NOM, performed as an attractive adsorbate for both F300 and HOK, posing a negligible influence on MTBE and significant influence on Nap adsorption. The high concentrations of MTBE and the abundant adsorbent dose applied in experiments might be the main reasons for the negligible NOM influence on MTBE adsorption. The unspecific adsorption of Nap rendered by its non-polar character explained the distinct NOM influence on Nap adsorption. Low

concentration of adsorbate, high concentration of NOM, and low amount of adsorbent dose could promote the NOM influence on organic compounds removal.

3) In the bi-adsorbate experiments, Nap and Zn^{2+} did not impact MTBE adsorption while MTBE and Zn^{2+} decreased Nap adsorption to different extents. Considering the similar experimental conditions, the unspecific adsorption of Nap should be responsible for the different influences between MTBE and Nap adsorption. The presence of Zn^{2+} influenced the Nap adsorption more severe on HOK than on F300 because of the stronger affinity of Zn^{2+} and HOK.

4) F300 and HOK performed as effective adsorbents for MTBE and Nap removal with the co-existence of de-icing salt, NOM and other adsorbate. Although Nap adsorption was impacted by the presences of NOM, MTBE or Zn^{2+}, the high removal efficiency varying at 96.9-100% was kept on both F300 and HOK.

5) Besides the concentrations of adsorbate and adsorbent, the characters of adsorbates and their affinity with adsorbents were also related to their competitions and influences on adsorption.

5.5 Column study for MTBE, Nap and Zn^{2+} removal

Generally, before the application in the practical use, proper adsorbents and optimized operation conditions should be chosen in experimental tests. It would be expensive and time consuming to construct a full-scale treatment plant for testing. Therefore, RSSCT, which is inexpensive and rapid, becomes a useful tool to study and estimate the performances of real absorbers (Crittenden et al., 1986; Shih et al., 2003).

Although batch experiments and the related isotherm analysis can provide lots of useful information of adsorbents, adsorbates, and impact factors on adsorption, they have their own limitation in application to the practical operation for their static, equilibrium characteristics (Summers, 1992; Shih et al., 2003). RSSCTs, with continual influent, specific EBCT and influent flow rate, could precisely simulate the operation conditions of real adsorbers. The results of RSSCTs are normally presented in the form of breakthrough curves, which are the plots describing the relationship between effluent concentration and treated water volume (or treating

time or treated bed volume) (Snoeyink and Summers, 1999). It has been proved that the breakthrough curves of RSSCTs are equivalent to those curves of full-scale adsorbers (Crittenden et al., 1986; Summers, 1992; Shih et al., 2003). With this equivalence, RSSCTs could effectively present and optimize the operation parameters of full-scale adsorbers in a short period of time.

The column study for MTBE, Nap, and Zn^{2+} removal was conducted with F300 and HOK in this section. Besides the independent RSSCT runs for MTBE, Nap and Zn^{2+}, NOM influence and the co-adsorption test of MTBE and Zn^{2+} were also tested. Moreover, the combination of F300 and HOK was also applied in the co-adsorption of MTBE and Zn^{2+}. Two combination methods, mixture and two-layer, were performed and compared.

5.5.1 The removals of MTBE, Nap, and Zn^{2+} in RSSCTs

F300 and HOK were applied to remove MTBE, Nap and Zn^{2+} in six independent RSSCT runs. Their performances were compared under identical conditions of 20min EBCT, 3 mL/min influent flow rate and initial concentration of each adsorbate, which was 16 mg/L (0.18 mmol/L) for MTBE, 5 mg/L (0.04mmol/L) for Nap, and 15 mg/L (0.23 mmol/L) for Zn^{2+}, respectively (**Table 4**).

Among different design parameters, EBCT is regarded as the most important one that would affect adsorber performance. Suffet and McGuire (1980) found the EBCT from 7.5 to 22.5 min brought a proportionally increased bed life for the removal of volatile organic chloroform; Love and Eilers (1982) found a significant decrease of adsorbent usage when EBCT increased from 6 to 12 min and a stability thereafter for the removal of *cis-1,2-dichloroethylene*, *1,1,1-tri-chloroethane*, and carbon tetrachloride; Shih (2003) found no significant difference in adsorber performance as the EBCT was increased from 10 min to 20 min for MTBE removal. Considering the co-existence of NOM and Zn^{2+} in the following experiments, the EBCT was set as 20 min in this study.

Figure 31(a) and **31(b)** separately depict the performances of F300 and HOK in the removal of MTBE, Nap and Zn^{2+} in RSSCTs. It is clear that the removals ability of these three pollutants on F300 were in the order of Nap > MTBE > Zn^{2+}. By comparing the treated water volume at 50% breakthrough, it was 50 L for MTBE and 13 L for Zn^{2+}. In the whole experiment process (150 L treated water), Nap

breakthrough was lower than 10%, indicating the good adsorption ability of Nap on F300. Correspondingly, the removal ability order with treated water volume at 50% breakthrough of these pollutants on HOK is Nap (-) > Zn^{2+} (41L) > MTBE (7L). Similarly, HOK displayed its good removal ability of Nap as well. Breakthroughs of Nap on both F300 and HOK were lower than 10% in RSSCTs. The difference between F300 and HOK was exhibited in the removals of MTBE and Zn^{2+}. Different from F300, which removed MTBE better than Zn^{2+}, HOK removed Zn^{2+} better than MTBE in RSSCTs.
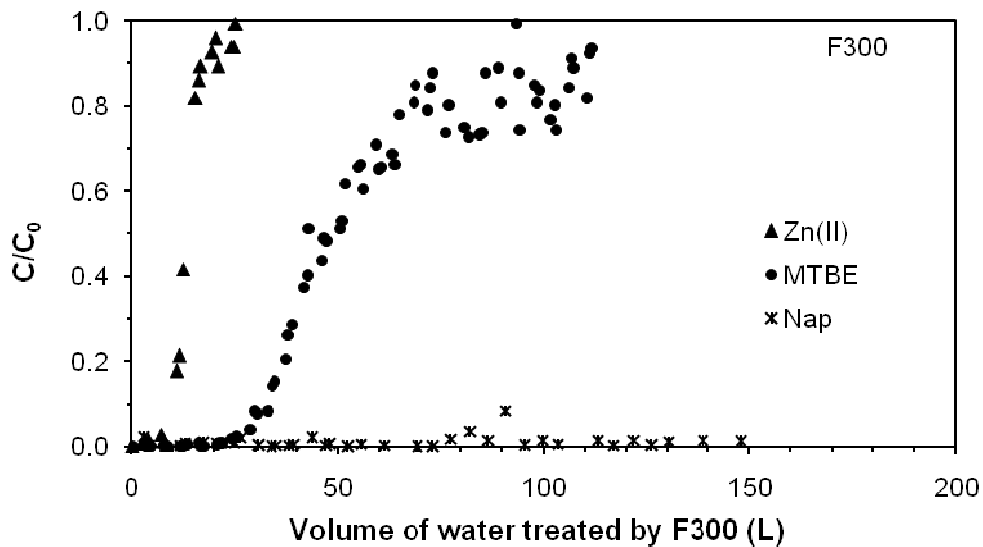
(a)
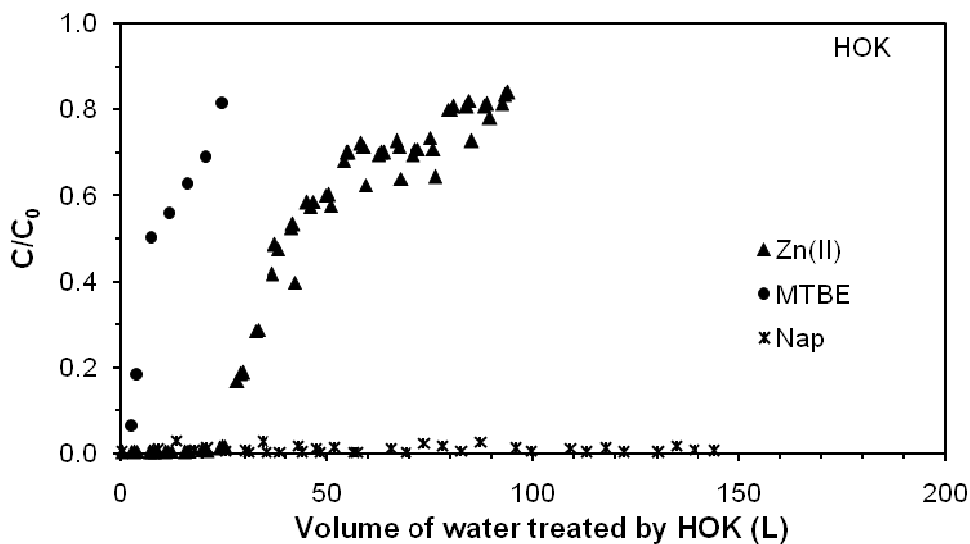
(b)

Fig. 31 Breakthrough curves of MTBE, Nap and Zn^{2+} on (a) F300 and (b) HOK

High adsorption capacity of Nap has been found on both F300 and HOK. The non-polar (hydrophobic) character enabled the strong affinity between Nap and adsorbents and brought effective removal in the column tests. Furthermore, F300 illustrated high adsorption capacity of MTBE (19.46 mg/g) and low adsorption capacity of Zn^{2+} (5.22 mg/g) in RSSCTs while HOK displayed high adsorption for Zn^{2+} (13.7 mg/g) and low adsorption for MTBE (2.32 mg/g) (**Table 15**), which were in the same order of batch experiments. However, the adsorption capacities of these pollutants were lower than those in batch experiments due to the unsaturated adsorption under dynamic column tests conditions. At 50% breakthrough, F300 can treat 50 L MTBE solution per gram of adsorbent, which was almost 7 times higher than HOK (7 L) while HOK could treat 41 L Zn^{2+} solution per gram, around 3 times higher than F300 (13 L).

Table 15 Adsorbent capacity and AUR (at 50% breakthrough) in each column

Testing number	Pollutant(s)	Adsorbent(s)	At 50% breakthrough	
			Adsorbent capacity (mg/g)	AUR (g/L)
1	MTBE	F300	19.5	0.59
2	Nap	F300	-	-
3	Zn^{2+}	F300	5.22	2.29
4	MTBE	HOK	2.32	4.7
5	Nap	HOK	-	-
6	Zn^{2+}	HOK	13.7	0.85
7	MTBE/NOM	F300	17.8	0.63
8	MTBE/Zn^{2+}	F300	19.9/1.13	0.57/5.89
9	MTBE/Zn^{2+}	F300/HOK (50 : 50 Mixture)	11.5/3.36	0.94/2.54
10	MTBE/Zn^{2+}	F300/HOK (50 : 50 Two-layer)	11.6/3.28	0.93/2.68

It is noted that F300 obtains higher adsorption capacity of MTBE than HOK while HOK has higher adsorption capacity of Zn^{2+} than F300. Therefore, it is insufficient to apply single adsorbent in real road runoff treatment, where multiply pollutants (such as heavy metals and organic compounds) need to be removed simultaneously. A system with two or more adsorbents should be considered in road runoff treatment. The combination of F300 and HOK as adsorbent in RSSCT for the co-adsorption of MTBE and Zn^{2+} were tested in section 5.5.4.

Due to the higher adsorption capacities of organic pollutants, F300 was chosen as the adsorbent for the following experiments. Meanwhile, MTBE was chosen as the representative organic pollutant for its integrated breakthrough curves in these RSSCTs.

5.5.2 NOM influence on MTBE adsorption

Compare to batch experiments, the continual influent in column experiment might aggravate the pore blockage impact on adsorbents and cause significant NOM influence on the pollutant removal.
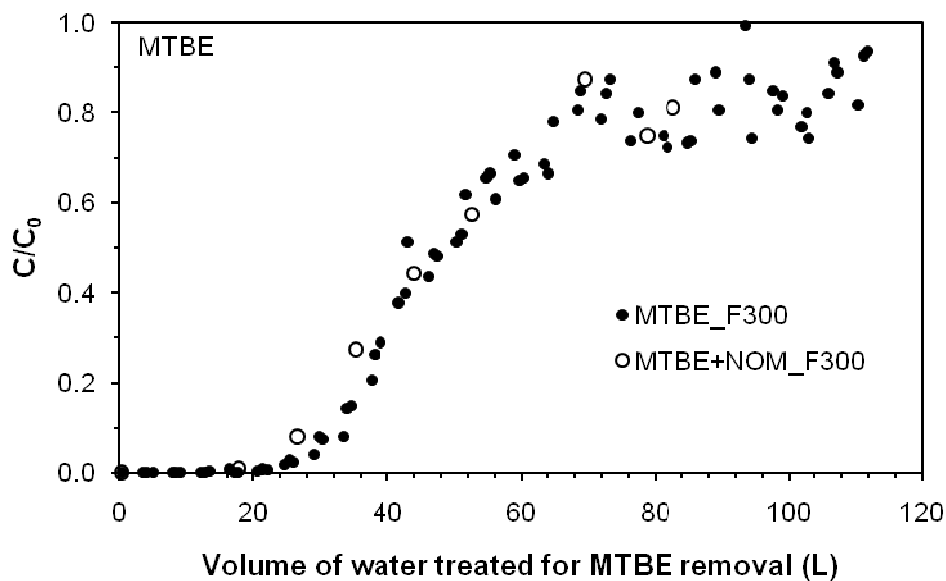
Fig. 32 Breakthrough curves of MTBE on F300 with and without the presence of NOM

Figure 32 presents the breakthrough curves of MTBE on F300 and the other one with NOM. Different from expectation, the presence of NOM did not caused a significant deviation of MTBE breakthrough curve. With the presence of NOM, the volume of treated water at 50% breakthrough of MTBE decreased slightly, from 50 L to 47 L. The negligible influence of NOM was also observed from the decrease of adsorbent capacity, which fell from 19.5 mg/g to 17.8 mg/g, and the increase of AUR, which rose from 0.59 g/L to 0.63 g/L, at 50% breakthrough (**Table 15**).

However, these decreases were not as striking as other studies. Shih et al. (2003) found with the increase of NOM (0.2 mg/L to 3.2 mg/L in TOC) the treated water volume decreased by four-time, from 28.2 L to 7.4 L at 50% breakthrough. Rossner and Knappe (2008) reported the presence of NOM decreased by 38% uptake of

MTBE. However, it is found these significant influences were found with low initial concentrations of MTBE, which were 20 μg/L and 100 μg/L, respectively. As discussed in the batch experiments, the high initial concentration (16 mg/L) contributed greatly to the stable MTBE adsorption in the competition with NOM. Although NOM displayed its adsorption on adsorbent and the adsorbed NOM might cause the hindering effect for the successive MTBE adsorption, the slight influence of NOM in this study suggested this hindering effect was limited when the initial concentration of MTBE was high.

Considering the low concentration of MTBE in real road runoff (in μg/L scale) and the relationship between MTBE initial concentration and hindering effect of NOM, another RSSCT test of adsorbent should be done with trace concentration of MTBE (μg/L) and the local NOM before the practical application.

5.5.3 Co-adsorption of MTBE and Zn^{2+} in RSSCTs

The co-adsorption of MTBE and Zn^{2+} was conducted in RSSCTs with F300 to test the interaction and competition between inorganic pollutant (Zn^{2+}) and organic pollutant (MTBE) in adsorption process. Because of the co-existence of inorganic and organic pollutants in road runoff, the performance of F300 in co-adsorption test could help to investigate its further application in practical operation. In experiments, MTBE and Zn^{2+} were at comparable initial concentrations in the influent of RSSCTs, which are 0.18 mmol/L (MTBE) and 0.17 mmol/L (Zn^{2+}), respectively.

Figure 33(a) compares MTBE breakthrough curves in co-adsorption column test (for MTBE and Zn^{2+}) and single MTBE removal, while **Fig. 33(b)** presents the comparison of Zn^{2+} breakthrough curves with and without the presence of MTBE in RSSCTs of F300. As shown in **Fig. 33(a)**, the presence of the Zn^{2+} does not caused the deviation of MTBE breakthrough curve. At 50% breakthrough, F300 column treated 52 L MTBE solution in the co-adsorption test while the data was 50 L in single MTBE removal. Moreover, the values of adsorbent capacity and AUR for MTBE removal, which were 19.9 mg/g and 0.57 g/L in co-adsorption system, were similar with the values for single MTBE removal (19.5 mg/g for capacity and 0.59 g/L for AUR) at 50% breakthrough. The removal of MTBE kept constant in both co-adsorption system and single MTBE removal. The presence of Zn^{2+} did not pose its influence on MTBE removal in the co-adsorption column tests.

However, the presence of MTBE exhibited a significant influence on Zn^{2+} removal in the co-adsorption tests. As presented in **Fig. 33(b)**, the initial Zn^{2+} breakthrough happened earlier in co-adsorption system than that in the single Zn^{2+} removal test. With the presence of MTBE, the breakthrough curve of Zn^{2+} became sharper. At 50% breakthrough, the treated water volume for Zn^{2+} reduced from 13L in single Zn^{2+} removal to 5 L in co-adsorption with MTBE. Meanwhile, the adsorbent capacity of Zn^{2+} decreased from 5.22 mg/g to 1.13 mg/g and the AUR for Zn^{2+} removal increased from 2.29 g/L to 5.89 g/L at 50% breakthrough, with the presence of MTBE (**Table 15**).

The diverse adsorption mechanisms for MTBE and Zn^{2+} removal might explain their different performances in competition. MTBE adsorption is strongly related with the amount and shape of micro-pore of adsorbents (Li et al., 2002; Seredych et al., 2005). Differently, Zn^{2+} adsorption is depended on the chemical composition of adsorbent surface, such as functional group, pH value and surface charge (Demirbas, 2008). Pore filling as the main adsorption mechanism of MTBE implies the occupations of a great deal of micro-pores on adsorbents in MTBE adsorption (Kleineidam et al., 2002). Consequently, the surface area of adsorbent is greatly reduced by these occupations, especially for F300, which has abundant micro-pores. With the decrease of surface area, the available adsorption sites for Zn^{2+} are therefore decreased. On the contrary, the Zn^{2+} adsorption mainly happens on the surface of adsorbents without being localized to micro-pores. Probably, meso-pores and macro-pores, with shorter diffusion distance, are more preferable for Zn^{2+} adsorption. Therefore, the amount of micro-pores might not be reduced greatly in Zn^{2+} adsorption, and therefore the adsorption of MTBE is not significantly impacted.
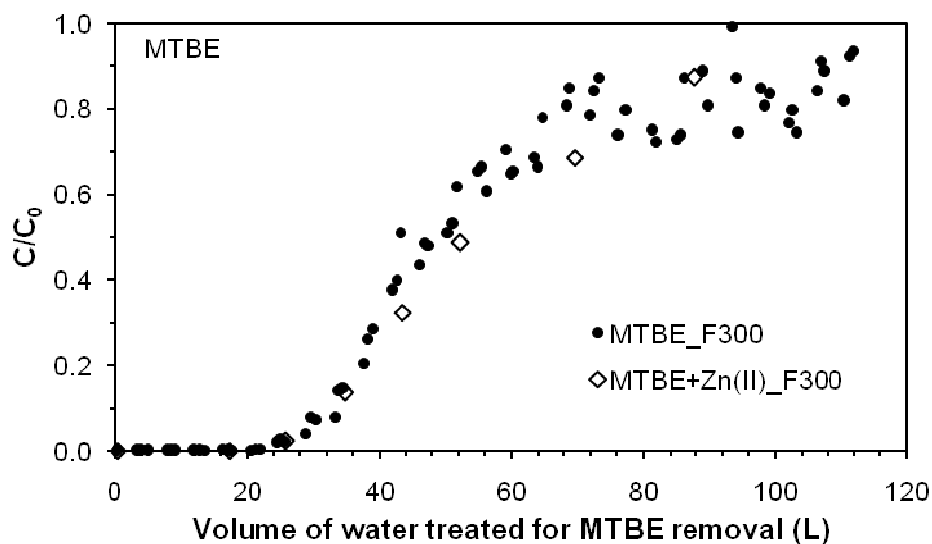
(a)
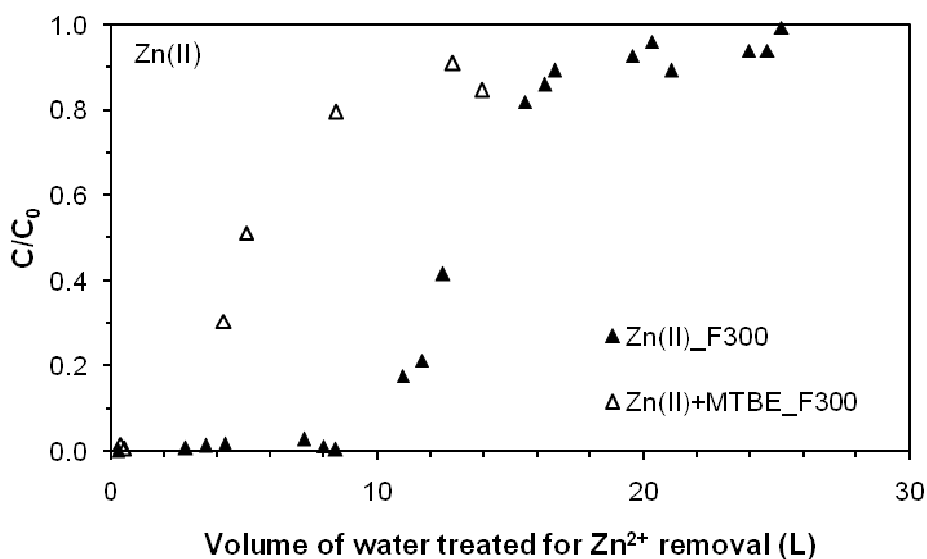
(b)

Fig. 33 Breakthrough curves of (a) MTBE and (b) Zn^{2+} in co-adsorption tests

5.5.4 Performance of bi-adsorbent for co-adsorption of MTBE and Zn^{2+}

Although F300 effectively removed MTBE in both single adsorbate and bi-adsorbate adsorptions, its removal effect of Zn^{2+} was relatively poor, especially in the co-adsorption tests. To improve Zn^{2+} removal in co-adsorption process, the bi-adsorbent system (F300 and HOK) was investigated. HOK displayed higher adsorption capacity of Zn^{2+} in single adsorbate RSSCT. The introduction of HOK as a second adsorbent into adsorbent system was expected to improve the removal effect of Zn^{2+} in co-

adsorption tests. Meanwhile, the decrease of MTBE removal capacity of bi-adsorbent was also considered.

Mixture and two-layer, as two methods to place the adsorbents were applied in bi-adsorbent system. In the two-layer placement, HOK filled in the lower half and F300 filled the rest upper half of the column with the up flow mode (from bottom to up). Other experimental conditions were as described in **Table 15**.

Figure 34(a) and **34(b)** separately present MTBE and Zn^{2+} breakthrough curves in co-adsorption tests with single adsorbent (F300) and bi-adsorbents (F300 and HOK, with two placement methods). As expected, the addition of HOK into adsorbent enhanced the removal efficiency of Zn^{2+} but reduced MTBE removal ability correspondingly. The two different placements of adsorbents did not present difference for both MTBE and Zn^{2+} removals.

As presented in **Fig. 34(a)**, the MTBE breakthrough curve of bi-adsorbent is sharper than the one of F300. At 50% breakthrough, the MTBE adsorption capacity of adsorbents was 11.5 mg/g for bi-adsorbent, which was about half of the value for single F300 (19.9 mg/g). Meanwhile, the treated water for MTBE removal was 35 L by bi-adsorbent and 52 L by single F300. Moreover, it was noted that at 60% and higher breakthrough percentage, the breakthrough curve of bi-adsorbent increased gently and gradually approached the curve of single F300. At 87% breakthrough, the treated water by bi-adsorbent was 87 L, which was almost as same as the value by single F300 (88 L). Although, with the addition of HOK, bi-adsorbent system caused earlier breakthrough in MTBE adsorption, a similar breakthrough behavior was observed around saturation point (87% breakthrough).
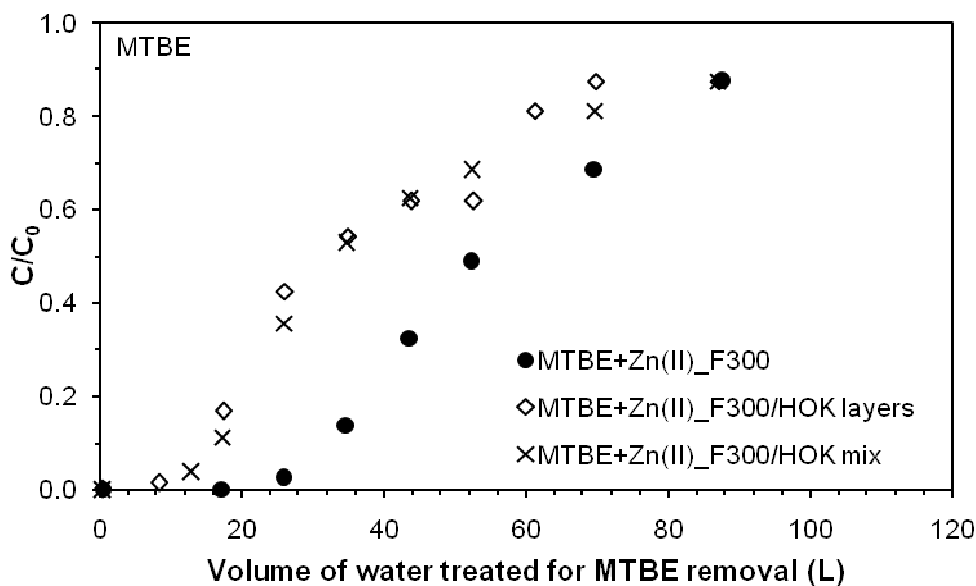
(a)
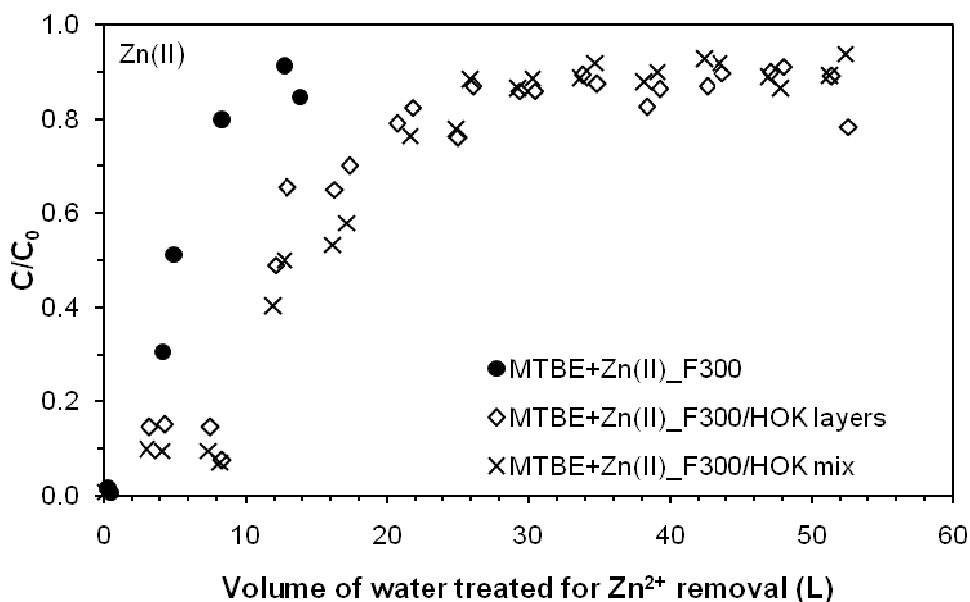
(b)

Fig. 34 Breakthrough curves of (a) MTBE and (b) Zn^{2+} in the co-adsorption tests with bi-adsorbent system

In **Fig. 34(b)**, it is clear the bi-adsorbent system greatly improved Zn^{2+} removal efficiency. With bi-adsorbent system, the treated water of Zn^{2+} increased from 5 L (single F300) to 13 L at 50% breakthrough. Meanwhile the Zn^{2+} adsorption capacity of adsorbents rose from 1.13 mg/g (single F300) to 3.36 mg/g (bi-adsorbent), which was increased by 3 times (**Table 15**). The bi-adsorbent system of F300 and HOK seemed more desirable in the co-adsorption of MTBE and Zn^{2+}. In the case with high Zn^{2+} concentration and relatively low MTBE concentration, the bi-adsorbent system

would be preferable for application. Furthermore, the hindering impact of bi-adsorbent on MTBE removal could be improved by optimizing the amount (ratio) of F300 in bi-adsorbent system.

Two placements of adsorbents (mixture and two-layer) did not present striking differences in the removals of MTBE and Zn^{2+}. Both MTBE and Zn^{2+} removals were independent on the placement of adsorbents. At 50% breakthrough of MTBE, the adsorbents capacity is 11.5 mg/g for mixture method and 11.6 mg/g for two-layer. The values for Zn^{2+} removal were 3.36 mg/g (mixture) and 3.28 mg/g (two-layer) at 50% breakthrough. Meanwhile the AUR values were 0.94 g/L for mixture and 0.93 g/L for two-layer in MTBE removal and 2.54 g/L for mixture and 2.68 g/L for two-layer in Zn^{2+} removal **(Table 15)**. All these data revealed the similarity of these two placements of adsorbents. Therefore, in the practice, the columns in-series with two or more adsorbents would be convenient and effective in multi-pollutants treatments. Moreover, the amount of each adsorbent (or the number of each adsorbent column) can be optimized to fit specific conditions.

5.5.5 Summary

In the analysis of experimental results, the following results were drawn:

1) For single pollutant removal, F300 presented best adsorption of Nap, followed by MTBE then Zn^{2+}; HOK showed best removal for Nap, followed by Zn^{2+} then MTBE. In the whole experiment process (150 L treated water with the initial concentration of 5 µg/L), Nap effluent was lower than 10% breakthrough on both F300 and HOK.

2) The influence of NOM on MTBE removal in RSSCTs was slight. At 50% breakthrough, the presence of NOM only reduced the adsorbent capacity of MTBE from 19.5 mg/g to 17.8 mg/g. The high initial concentration (16 mg/L) of MTBE should contribute to the negligible competition of NOM to MTBE. The influence of NOM could be significant with trace initial concentration of MTBE in RSSCTs.

3) In the co-adsorption of MTBE and Zn^{2+}, the removal of MTBE was as similar as that in single MTBE adsorption, indicating the slight influence of the presence of Zn^{2+}. However, the removal ability of Zn^{2+} was greatly reduced by the presence of MTBE. The adsorption capacity of Zn^{2+} decreased from 5.22

mg/g in the single Zn^{2+} removal to 1.13 mg/g in the co-adsorption tests. The diverse adsorption mechanisms for MTBE and Zn^{2+} removal might be the reason for their different performances in competition.

4) Bi-adsorbent system could improve the removal effect of Zn^{2+} in the co-adsorption tests of MTBE and Zn^{2+}. Although the introduction of HOK caused earlier MTBE breakthrough, bi-adsorbent system greatly improved the adsorption capacity of adsorbents for Zn^{2+} removal by 3 times (from 1.13 mg/g (single F300) to 3.36 mg/g (bi-adsorbent)) at 50% breakthrough. It was more desirable to apply bi-adsorbent in co-adsorption of MTBE and Zn^{2+}. The hindering impact of bi-adsorbent on MTBE removal could be improved by optimizing the amount (ratio) of F300 in bi-adsorbent system.

5) Both MTBE and Zn^{2+} removal were independent on the placements of adsorbents, mixture or two-player. Therefore, columns in-series operation would be convenient and effective in multi-pollutant treatments. Moreover, the amount of each adsorbent can be optimized to fit in the specific conditions.

6. Conclusions and outlook

From the experimental results and discussion, the following conclusions were drawn:

Bioadsorbents of red alga and beer draff in Cu^{2+} adsorption:

1) The adsorption capacity of Cu^{2+} was 12.7 mg/g for red alga and 9.01 mg/g for beer draff (Langmuir isotherm), respectively. The pH value and initial Cu^{2+} concentration can greatly influence the adsorption capacity of Cu^{2+}. The optimum pH range was 5-6 for both materials.

2) The pseudo second-order kinetics model and Langmuir isotherm model can be used to fit the adsorption process of Cu^{2+} onto bioadsorpbents. Cu^{2+} adsorption was spontaneous on both Red alga and beer draff.

3) Chemical bonding was the main mechanism in Cu^{2+} adsorption rather than ion-exchange. The functional groups, such as amino, hydroxyl, carboxyl, phenolic hydroxyl group, sulphonic group and C–O, –NH stretch, might be involved in adsorption.

4) Due to their poor mechanical strengths and COD release, the red alga and beer draff are not suitable to be used in practice for road runoff treatment.

Comparison of other four materials in MTBE and Nap removal:

1) HOK and F300 were effective adsorbents for both MTBE and Nap removal. Tixosorb presented its suitability for MTBE and Nap removal in highly contaminated areas. However, DRI displayed very poor adsorption capacity of both MTBE and Nap.

2) pH value had no effect on MTBE or Nap adsorption. Micro-pore volume of pores at 7-11 Å was crucial for MTBE adsorption. Moreover, the surface chemistry character of adsorbents (hydrophobicity, aromaticity) played an important role in Nap adsorption.

3) Tixosorb demonstrated high removal efficiency for both MTBE and Nap removal at high initial concentrations. Due to the non-polar character of Nap, Tixosorb was more effective in removing Nap than MTBE. The oxidation-reduction reaction of DRI did not help in MTBE or Nap removal.

4) Compare to MTBE, HOK and F300 showed higher adsorption capacities of Nap. Moreover, in the adsorption of MTBE, F300 displayed higher adsorption capacity than HOK.

MTBE and Nap adsorption on F300 and HOK

1) Pseudo second-order kinetics model fitted better with the adsorption processes of MTBE and Nap on both HOK and F300. The intra-particle and Boyd kinetics models revealed the co-existence of film, intra-particle diffusion and the important role of film diffusion in MTBE and Nap adsorption.

2) On HOK and F300, Tóth and PDM isotherm model presented good congruence with MTBE adsorption, indicating the heterogeneity and pore-filling mechanism in MTBE adsorption. The adsorption capacities (PDM isotherm model) of MTBE were 222 mg/g and 35 mg/g on F300 and HOK, respectively.

3) Nap adsorption on HOK and F300 presented linear adsorption behavior. Compare to the partitioning behavior, the surface adsorption was more inclined to be the mechanism in Nap adsorption.

The influence of De-icing salt, NOM, and bi-adsorbate on MTBE and Nap adsorption by HOK and F300:

1) NaCl, acted as the de-icing salt, did not take part in the adsorption process of MTBE and Nap. NOM, performed as an attractive adsorbate for both F300 and HOK, posing a negligible influence on MTBE and significant influence on Nap adsorption.

2) The high concentrations of MTBE and the abundant adsorbent dose offered in experiments might be the main reasons for the negligible NOM influence on MTBE adsorption.

3) In the bi-adsorbate experiments, the existence of Nap and Zn^{2+} did not impact MTBE adsorption. However, the existence of MTBE and Zn^{2+} decreased Nap adsorption to different extents. The presence of Zn^{2+} influenced the Nap adsorption more severe on HOK than on F300 showing the stronger affinity of Zn^{2+} and HOK.

4) Although Nap adsorption was impacted by the influences of NOM, MTBE and Zn^{2+}, the high removal efficiency varying at 96.9-100% was kept on F300 and HOK.

Column experiments of HOK and F300 in removal of MTBE, Nap, and Zn^{2+}:

1) In the removal of single pollutant, HOK and F300 followed the orders of Nap > Zn^{2+} > MTBE and Nap > MTBE >Zn^{2+}, respectively.

2) The influence of NOM on MTBE removal in RSSCTs was slight. At 50% breakthrough, the presence of NOM only reduced the adsorbent capacity of MTBE from 19.5 mg/g to 17.8 mg/g.

3) The presence of MTBE greatly influenced the removal of Zn^{2+} in RSSCT. The adsorption capacity of Zn^{2+} decreased from 5.22 mg/g in the single Zn^{2+} removal to 1.13 mg/g in the co-adsorption tests.

4) Bi-adsorbent system could improve the removal effect of Zn^{2+} in the co-adsorption test of MTBE and Zn^{2+}. Although the introduction of HOK caused earlier MTBE breakthrough, bi-adsorbent system greatly improved the adsorbents capacity of Zn^{2+} by 3 times (from 1.13 mg/g (single F300) to 3.36 mg/g (bi-adsorbent)) at 50% breakthrough.

5) Both MTBE and Zn^{2+} removal were independent on the placements of adsorbents, mixture or two-layer. Therefore, columns in-series operation would be convenient and effective in multi-pollutant treatments. Moreover, the amount of each adsorbent can be optimized to fit the specific conditions.

In the further studies, long-time run of column with the similar concentrations and component of pollutants as the real road runoff should be considered to offer more information for application because there are lots of other influences coming from road runoff. A big scale of experiments (pilot plant) might also help. Moreover, columns in-series operation can be tested with different ratios of two or more kinds of adsorbents for specific condition of road runoff. At last, a simulation model might be built based on abundant experimental data to guide the application of filter material and the operation in the practical treatment of road runoff.

7. References

Abu-Lail, L (2010). Removal of chloroform and MTBE from water by adsorption onto granular zeolites: equilibrium, kinetic and mathematical modeling study. PhD dissertation, Worcester polytechnic institute, USA.

Achten, C and Puettmann, W (2000). Determination of methyl tert-butyl ether in surface water by use of solid-phase microextraction. Environ. Sci. Technol., 34 (7), 1359-1364.

Ahmad, A, Rafatulla, M, Danish, M (2007). Sorption studies of Zn(II) and Cd(II) ions from aqueous solution on treated sawdust of sissoo wood. Eur. J. Wood Wood Prod., 65 (6), 429-436.

Ahmad R, Wong-Foy AG, Matzger AJ (2009). Microporous coordination polymers as selective sorbents for liquid chromatography. Langmuir, 25 (20), 11977-11979.

Ajmal, M, Khan, HA, Ahmad, S, Ahmad, A (1998). Role of sawdust in the removal of copper(II) from industrial wastes. Water Res., 32 (10), 3085-3091.

Akar, ST, Akar, T, Çabuk, A (2009). Decolorization of a textile dye, reactive red 198 (rr198), by Aspergillus parasiticus fungal biosorbent. Braz. J. Chem. Eng., 26 (2), 399-405.

Akçay, M and Akçay, G (2004). The removal of phenolic compounds from aqueous solutions by organophilic bentonite. J. Hazard. Mater., B113 (1-3), 189-193.

Anderson, MA (2000). Removal of MTBE and other organic contaminants from water by sorption to high silica Zeolites. Environ. Sci. Technol., 34 (4), 725-727.

Ania, CO, Cabal, B, Pevida, C, Arenillas, A, Parra, JB, Rubiera, F, Pis, JJ (2007). Removal of naphthalene from aqueous solution on chemically modified activated carbons. Water Res., 41(2), 333-340.

Ania, CO, Cabal, B, Parra, JB, Arenillas, A, Arias, B, Pis, JJ (2008). Naphthalene adsorption on activated carbons using solvents of different polarity. Adsorption, 14 (2), 343-355.

Athanasiadis, K and Helmreich, B (2005). Influence of chemical conditioning on the ion exchange capacity and on kinetic of zinc uptake by clinoptilolite. Water Res., 39 (1), 1527-1532.

Athanasiadis, K (2005). On site infiltration of roof runoff by using clinoptilplite as an artificial barrier material. PhD dissertation, Institute of Water Quality Control, Technical University of Munich, Garching.

Azizian S (2004). Kinetic models of sorption: a theoretical analysis. J. Colloid Interf. Sci., 276 (1), 47-52.

Baeckstroem, M, Nilsson, U, Håkansson, K, Allard, B, Karlsson, S (2003). Speciation of heavy metals in road runoff and roadside total deposition. Water Air Soil Poll., 147 (1), 343-366.

Ball, JE, Jenks, R, Aubourg, D (1998). An assessment of the availability of pollutant constituents on road surfaces. Sci. Total Environ., 209 (2-3), 243-254.

Ball, JE (2002). Stormwater quality at centennial park, Sydney, Austrilia. The university of new south wales school of civil and environmental engineering water research laboratory. Research report No.205.

Bang, S, Johnson, MD, Korfiatis, GP, Meng, X (2005). Chemical reactions between arsenic and zero-valent iron in water. Water Res., 39(5), 763-770.

Barraud, S, Gautier, A, Bardin, JP, Riou, V (1999). The impact of intentional stormwater infiltration on soil and groundwater. Water Sci. Technol., 39 (2), 185-192.

Barrett, EP, Joyner, LG, Halenda, PP (1951). The determination of pore volumes and area distributions in porous substances. J. Am. Chem. Soc., 73 (1), 373–380.

BBodSchV (1999). Bundes-Bodenschutz- und Altlastenverordnung. BGBl. Nr. 36, 1554.

Benhammou, A, Yaacoubi, A, Nibou, L, Tanouti, B (2005). Adsorption of metal ions onto Moroccan stevensite: kinetic and isotherm studies. J. Colloid Interf. Sci., 282 (2), 320-326.

Bi E, Haderlein SB, Schmidt TC (2005). Sorption of methyl tert-butyl ether (MTBE) and tert-butyl alcohol (TBA) to synthetic resins. Water Res., 39 (17), 4164-4176.

Borden, RC, Black, DC, McBlief, KV (2002). MTBE and aromatic hydrocarbons in North Carolina stormwater runoff. Environ. Pollut., 118(1), 141-152.

Boving, TB and Neary K (2007). Attenuation of polycyclic aromatic hydrocarbons from urban stormwater runoff by wood filters. J. Contam. Hydrol., 91 (1-2), 43-57.

100

Boyd, GE, Adamson, AW, Myers, Jr LS (1947). The exchange adsorption of ions from aqueous solutions by organic zeolites. II. Kinetics. J. Am. Chem. Soc., 69 (11), 2836-2848.

Bradford, WL (1977). Urban stormwater pollutant loadings: a statistical summary through 1972. Water pollution Control Federation, 49 (4), 613-622.

Brown, PA, Gill, SA, Allen, SJ (2000). Metal removal from wastewater using peat. Water Res., 34(16), 3907-3916.

Brown, JN and Peake, BM (2006). Sources of heavy metals and polycyclic aromatic hydrocarbons in urban sormwater runoff. Sci. Total Environ., 359 (1-3), 145-155.

Bruen, M, Johnston, P, Quinn, MK, Desta, M, Higgins, N, Bradley, C, Burns, S (2006). Impact assessment of highway drainage on surface water quality. EPA Report.2000-MS-13-M2.

Brunauer, S, Emmet, PH, Teller, F (1938). Adsorption of gases in multimolecular layers. J. Am. Chem. Soc., 60 (2), 309–319.

Cabal, B, Ania, CO, Parra, JB, Pis, JJ (2009). Kinetics of naphthalene adsorption on an activated carbon: comparison between aqueous and organic media. Chemosphere, 76(4), 433-438.

Changchaivong, S and Khaodhiar S (2009). Adsorption of naphthalene and phenanthrene on dodecylpyridinium-modified bentonite. Appl. Clay Sci., 43 (3-4), 317-321.

Chang, CF, Chang, CY, Chen, KH, Tsai, WT, Shie, JL, Chen, YH (2004). Adsorption of naphthalene on zeolite from aqueous solution. J. Colloid Interf. Sci., 277 (1), 29-34.

Chang, MY and Juang, RS (2004). Adsorption of tannic acid, humic acid, and dyes from water using the composite of chitosan and activated clay. J. Colloid Interf. Sci., 278 (1), 18-25.

Chen, X, Wright, JV, Conca, JL, Peurrung, LM (1997). Effect of pH on heavy metal sorption on mineral apatite. Environ. Sci. Technol., 31 (3), 624-631.

Chen, Y, Zhao, J, Yang, X (2012). Pollution characteristics of urban road runoff in Xi'an, China. Water Resource and Environmental Protection (ISWREP), 2011 International Symposium (4), 2904-2908.

Cheng, W, Dastgheib, SA, Karanfil, T (2005). Adsorption of dissolved natural organic matter by modified activated carbons. Water Res., 39 (11), 2281-2290.

Cruz-Guzmán, M, Celis, R, Hermosín, MC, Cornejo, J (2004). Adsorption of the Herbicide Simazine by Montmorillonite Modified with Natural Organic Cations. Environ. Sci. Technol., 38 (1), 180-186.

Cruz-Guzmán, M, Celis, R, Hermosín, MC, Koskinen, WC, Nater, EA, Cornejo, J (2006). Heavy metal adsorption by montmorillonites modified with natural organic cations. Soil Sci. Soc. Am. J., 70 (1), 215-221.

Davis, AP, Shokouhian, M, Ni, S (2001). Loading estimates of lead, copper, cadmium and zinc in urban runoff from specific sources. Chemosphere, 44, 997-1009.

Davis, B and Birch, G (2010). Comparison of heavy metal loads in stormwater runoff from major and minor urban roads using pollutant yield rating curves. Environ. Poll., 158 (8), 2541-2545.

Davis, JA and Leckie, JO (1978). Effect of adsorbed complexing ligands on trace metal uptake by hydrous oxides. Environ. Sci. Technol., 12 (12), 1309-1315.

Davis, SW and Powers, SE (2000). Alternative sorbents for removing MTBE from gasoline-contaminated ground water. J. Environ. Eng.-ASCE, 126 (4), 354-360.

Davis, TA, Volesky, B, Mucci, A (2003). A review of the biochemistry of heavy metal biosorption by brown alga. Water Res., 37 (18), 4311-4330.

Demirbas, A (2008). Heavy metal adsorption onto agro-based waste materials: a review. J. Hazard. Mater., 157 (2-3), 220-229.

Depci, T, Kui, AR, Önal, Y (2012). Competitive adsorption of lead and zinc from aqueous solution on activated carbon prepared from Van apple pulp: study in single- and multi-solute system. Chem. Eng. J., 200-202, 224-236.

Dierkes, C, Goebel, P, Lohmann, M, Coldewey, WG (2005). Development and investigation of a pollution control pit for treatment of stomwater from metal roofs and traffic areas. 10th International Conference on Urban Drainage, Copenhagen, Denmark.

Directive 2000/60/EC, (2000). EU Water Framework Directive. Off. J. L 327.

Dubey, SS and Gupta, RK (2005). Removal behavior of Babool bark (Acacia nilotica) for submicro concentrations of Hg^{2+} from aqueous solutions: a radiotracer study. Sep. Purif. Technol., 41 (1), 21-28.

Dubinin, MM (1960). The potential theory of adsorption of gases and vapors for adsorbents with energetically nouniform surfaces. Chem. Rev., 60 (2), 235-241.

Dubinin, MM and Radushkevich, LV (1947). Equation of the characteristic curve of activated charcoal, Proceedings of the Academy of Sciences. Physical Chemistry Section, U.S.S.R. 55, 331-333.

Eaton, AD, Clesceri, LS, Rice, EW, Greenberg, AE, Franson, MAH, (Eds.) (2005). Standard Methods for the Examination of Water & Wastewater, 21th Edition, American Public Health Association (APHA), American Water Works Association (AWWA) & Water Environment Federation (WEF).

Ebie, K, Li, F, Azuma, Y, Yuasa, A, Hagishita, T (2001). Pore distribution effect of activated carbon in adsorption organic micropollutants form natural water. Water Res., 35 (1), 167-179.

Eckstein, M, Sesing, M, Kragl, U, Adlercreutz, P (2002). At low water activity α-chymotrypsin is more active in an ionic liquid than in non-ionic organic solvents. Biotechnol. Lett., 24(11), 867-872.

EPA (1982). Methods for organic chemical analysis of municipal and industrial wastewater, method 610-Polynuclear aromatic hydrocarbons. United States Environmental Protection Agency.

Erdem-Şenatalar, A, Bergendahl, JA, Giaya, A, Thompson, RM (2004). Adsorption of methyl tertiary butyl ether on hydrophobic molecular sieves. Environ. Eng. Sci., 21 (6), 722-729.

Esteves, da SJ and Marques, MCPO (2007). Pentachlorophenol association with fulvic acids from recycled wastes. Environ. Poll., 146 (1), 174-179.

Eweis, J, Ergas, S, Chang, D, Schroeder, E (1998). Bioremediation principles. New York, McGraw-Hill.

Faerm, C (2002). Metal sorption to natural filter subsrates for storm water treatment-columnstudies. Sci. Total Environ., 298 (1-3), 17-24.

Faerm, C (2003). Constructed filters and detention ponds for metal reduction in storm water. Maelardalen University Dissertations, No.4. Department of Public Technology, Maelardalen University.

Faram, MG, Iwugo, KO, Andoh, RYG (2007). Characteristics of urban run-off derived sediments captured by proprietary flow-through stormwater interceptors. Water Sci. Technol., 56 (12), 21-27.

Fourest, E and Volesky, B (1996). Contribution of sulfonate groups and alginate to heavy metal biosorption by the dry biomass of *sargassum fluitans*. Environ. Sci. Technol., 30 (1), 277-282.

Fourest, E and Volesky, B (1997). Alginate properties and heavy metal biosorption by marine alga. Appl. Biochem. Biotech., 67 (3), 215-226.

Foo, KY and Hameed, BH (2010). Insights into the modeling of adsorption isotherm systems. Chem. Eng. J., 156 (1), 2-10.

Foo, KY and Hameed, BH (2012). Adsorption characteristics of industrial solid waste derived activated carbon prepared by microwave heating for methylene blue. Fuel Process. Technol., 99, 103-109.

Freundlich, H (1907). Ueber die Adsorption in Loesungen. Zeitschrift fuer Physikalische Chemie, 57 A, 385-470.

Frimmel, FH, Assenmacher, M, Soerensen, M, Abbt-Braun, G, Graebe, G (1999). Removal of hydrophilic pollutants from water with organic adsorption polymers Part I. Adsorption behavior of selected model compounds. Chem. Eng. Process., 38 (4-6), 601-610.

Gan, H, Zhuo, M, Li, D (2008). Quality characterization and impact assessment of highway runoff in urban and rural area of Guangzhou, China. Environ. Monit. Assess., 140 (1), 147-159.

Gasperi, J, Gromairea, MC, Kafi, M, Moilleron, R, Chebbo, G (2010). Contributions of wastewater, runoff and sewer deposit erosion to wet weather pollutant loads in combined sewer systems. Water Res., 44 (20), 5875-5886.

Gasser, MS, Morad, GA, Aly, HF (2006). Equilibrium and kinetics study of Gd(III) and U(VI) adsorption from aqueous solutions by modified Sorrel's cement. Adsorption, 12 (1), 65-76.

Ghadiri, SK, Nabizadeh, R, Mahvi, AH, Nasseri, S, Kazemian, H, Mesdaghinia, AR, Nazmara, Sh (2010). Methyl tert-butyl ether adsorption on surfactant modified natural zeolites. Iran J. Environ. Healt., 7 (3), 241-252.

Gupta, VK and Ali, I (2004). Removal of lead and chromium from wastewater using bagasse fly ash-a sugar industry waste. J. Colloid Interf. Sci., 271 (2), 321-328.

Hatt, BE, Fletcher, TD, Deletic A (2007). Treatment performance of gravel filter media: implications for desigen and application of stormwater infiltration systems. Water Res., 41(12), 2513-2524.

Harrison, RM, Johnston, WR, Ralph, JC, Wilson, SJ (1985). The budget of lead, copper and cadmium for a major highway. Sci. Total Environ., 46 (1-4), 137-145.

Helmreich, B, Hilliges, R, Schriewer, A, Horn, H (2010). Runoff pollutants of a highly trafficked urban road – correlation analysis and seasonal influences. Chemosphere 80(9), 991-997.

Hilliges, R (2007). Entwicklung eines dezentralen Behandlungssystems fuer hochbelastete Verkehrsflaechenablaeufe im urbanen Raum. PhD dissertation, Institute of Water Quality Control, Technical University of Munich, Garching.

Ho, YS and McKay, G (1998). Sorption of dye from aqueous solution by peat. Chem Eng. J., 70 (2), 115-124.

Ho, YS and McKay, G (1999). Pseudo-second order model for sorption process. Process Biochem., 34 (5), 451-465.

Hoffmann, EJ, Latimer, JS, Mills, GL, Quinn, JG (1982). Petroleum hydrocarbons in urban runoff from a commercial land use area. Journal WPCF, 54 (11), 1517-1525.

Hoffman, EJ, Latimer, JS, Hunt, CD, Mills, GL, Quinn, JG (1985). Stormwater runoff from highways. Water Air Soil Poll., 25(4), 349-364.

Holan, ZR, Volesky, B, Prasetyo, I (1993). Biosorption of cadmium by biomass of marine algae. Biotechnol. Bioeng., 41 (8), 819-825.

Horvath, G and Kawazoe, K (1983). Method for the calculation of effective pore size distribution in molecular sieve carbon. J. Chem. Eng. Jpn.,16 (5), 470–475.

Huang, J, Du, P, Ao, C, Ho, M, Lei, M, Zhao, D, Wang, Z (2007). Multivariate analysis for stormwater quality characteristics identification from different urban surface types in Macau. B. Environ. Contam. Tox., 79 (6), 650-654.

Hung, HW, Lin, TF, Baus, C, Sacher, F, Brauch, HJ (2005). Competitive and hindering effects of natural organic matter on the adsorption of MTBE onto activated carbons and zeolites. Environ. Technol., 26 (12), 1371-1382.

Hung, HW and Lin, TF (2006). Adsorption of MTBE from contaminated water by carbonaceous resins and mordenite zeolite. J. Hazard. Mater., 135 (1-3), 210-217.

Hvitved-Jacobsen, T, Vollertsen, J, Nielsen, AH (2010). Urban and highway stormwater pollution. Taylor & Francis Inc, 347.

Inal, F, Yetgin, S, Aksu, GT (2009). Activated carbon adsorption of fuel oxygenates MTBE and ETBE from water. Water Air Soil Pollut, 204 (1), 155-163.

Inglezakis, VJ, Loizidou, MD, Grigoropoulou, HP (2002). Equilibrium and kinetic ion exchange studies of Pb^{2+}, Cr^{3+}, Fe^{3+} and Cu^{2+} on natural clinoptilolite. Water Res., 36 (11), 2784-2792.

Jiries, AG, Hussein, HH, Lintelmann, J (2003). Polycyclic aromatic hydrocarbon in rain and street runoff in Amman, Jordan. J. Environ. Sci., 15 (6), 848-853.

Kadirvelu, K, Thamaraiselvi, K, Namasivayam, C (2001). Removal of heavy metals from industrial wastewaters by adsorption onto activated carbon prepared from an agricultural solid waste. Bioresource Technol., 76(1), 63-65.

Kayhanian, M, Stransky, C, Bay, S, Lau, SL, Stenstrom, MK (2006). Toxicity of urban highway runoff with respect to storm duration. Sci. Total Environ., 389 (2-3), 386-406.

Keum, Y and Li, QX (2004). Reduction of nitro aromatic pesticides with zero-valent iron. Chemosphere, 54(3), 255-263.

Kleineidam, S, Schueth, C, Grathwohl, P (2002). Solubility-normalized combined adsorption-partitioning sorption isotherms for organic pollutants. Environ sci. Technol., 36 (21), 4689-4697.

Knappe, DRU, Matsui, Y, Snoeyink, VL (1998). Predicting the capacity of powdered activated carbon for trace organic compounds in nature water. Environ. Sci. Technol., 32 (11), 1694-1698.

Kumar, YP, King, P, Prasad, VSRK (2006). Removal of copper from aqueous solution using *Ulva fasciata sp.*-A marine green algae. J. Hazard. Mater., 137 (1), 367-373.

Lacher, C and Smith, RW (2002). Sorption of Hg(II) by Potamogeton natans dead biomass. Miner. Eng., 15 (3), 187–191.

Lagergren S (1898). Zur Theorie der Sogenannten Adsorption geloester Stoffe. Kungliga Svenska Vetenskapsakademiens. Handlingar, 24 (4), 1-39.

Langmuir, I (1918). The adsorption of gases on plane surfaces of glass, mica and platinum. J. Am. Chem. Soc., 40 (9), 1361-1403.

Lawrence, AI, Marsalek, J, Ellis, JB, Urbonas, B (1996). Stormwater detention and BMPs. J. Hydraul. Res., 34 (6), 799-813.

Lee, H, Lau, S, Kayhanian, M, Stenstrom, MK (2004). Seasonal first flush phenomenon of urban stormwater discharges. Water Res., 38(19), 4153-4163.

Lee, SY and Kim, SJ (2002). Adsorption of naphthalene by HDTMA modified kaolinite and halloysite. Appl. Clay Sci., 22(1-2), 55-63.

Legret, M and Pagotto, C (1999). Evaluation of pollutant loadings in the runoff waters from a major rural highway. Sci. Total Environ., 235 (1-3), 143-150.

Li, L, Quinlivan, PA, Knappe, DRU (2002). Effects of activated carbon surface chemistry and pore structure on the adsorption of organic contaminants from aqueous solution. Carbon, 40(12), 2085-2100.

Li, Y, Helmreich, B, Horn, H (2011). Biosorption of Cu (II) ions from aqueous solution by red alga (Palmariapalmata) and Beer draff. Mat. Sci. Appl., 2(2), 70-80.

Lithoxoos, GP, Peristeras, LD, Boulougouris, GC, Economou, IG (2012). Monte Carlo simulation of carbon monoxide, carbon dioxide and methane adsorption on activated carbon. Molecular Physics: An International Journal at the Interface, 110 (11-12), 1153-1160.

Liu, S, Gao, J, Qu, B, Yang, Y, Xin, X (2009). Study on the adsorption characteristics of heavy metal ions on steel slag adsorbent. Proceedings of the 11th

International Conference on Environmental Science and Technology. Chania, Crete, Greece.

Long C, Li A, Wu H, Zhang Q (2009). Adsorption of naphthalene onto macroporous and hypercrosslinked polymeric adsorbent: effect of pore structure of adsorbents on thermodynamic and kinetic properties. Colloid Surface A, 333 (1-3), 150-155.

Love OT and Eilers RG (1982). Treatment of drinking water containing trichloroethylene and related industrial solvents. J. Am. Water Works Assoc., 74 (8), 413-425.

Mackay, D, Shiu, WY, Ma, CK (1992). Illustrated handbook of physical-chemical properties and environmental fate for organic chemicals -3, Boca Raton, Lewis Publishers.

Malca, J and Freire, F (2006). Renewability and life-cycle energy efficiency of bioethanol and bio-ethyl tertiary butyl ether (bioETBE): assessing the implications of allocation. Energy, 31 (15), 3362-3380.

Maltby, L, Boxall, ABA, Forrow, DM, Calow, P, Betton, CI (1995). The effect of motorway runoff on fresh water ecosystems: 2.identifying major toxicants. Environ. Toxico. Chem., 14 (6), 1093-1101.

Matsui, Y, Fukuda, Y, Inoue, T, Matsushita, T (2003). Effect of natural organic matter on powdered activated carbon adsorption of trace contaminants: characteristics and mechanism of competitive adsorption.   Water Res., 37 (18), 4413-4424.

Manes, M (1998). In Encyclopedia of environmental analysis and remediation, Meyers, RA, Ed., John Wiley, New York.

Marsalek, J, Brownlee, B, Mayer, T, Lawal, S, Larkin, GA (1997). Heavy metals and PAHs in stormwater runoff from the Skyway Bridge, Burlington, Ontario. Water Qual. Res. J. Can., 32(4), 815–827.

Marsalek, J, Rochfort, B, Brownlee, B, Mayer, T, Servos, M (1999). An exploratory study of urban runoff toxicity. Water Sci. Technol., 39 (12), 33-39.

McCready, S, Spyrakis, G, Greely, CR, Birch, GF, Long, ER (2004). Toxicity of surficial sediments from Sydney harbour and vicinity, Australis. Environ. Monit. Assess., 96 (1-3), 53-83.

Michelson LD, Gideon PG, Pace EG, Kutal LH (1975). Removal of soluble mercury from waste water by complexing techniques. US Dept. Industry, Office of Water Research and Technology, Bulletin No. 74.

Murphy, V, Hughes, H, McLoughlin, P (2007). Cu(II) bonding by dried biomass of red, green and brown macroalgae. Water Res., 41 (4), 731-740.

Newcombe, G, Drikas, M, Hayes, R (1997). Influence of characterized natural organic material on activated carbon adsorption: II. Effect on pore volume distribution and adsorption of 2-methylisoborneol. Water Res., 31 (5), 1065-1073.

Newcombe, G, Morrison, J, Hepplewhite, C (2002). Simultaneous adsorption of MIB and NOM onto activated carbon. I. Characterisation of the system and NOM adsorption. Carbon, 40 (12), 2135-2146.

Ngabe, B, Bidleman, TF, Scott, GI (2000). Polycyclic aromatic hydrocarbons in storm runoff from urban and coastal South Carolina. Sci. Total Environ., 255(1-3), 1-9.

Ngah, WSW and Hanafiah, MAKM (2008). Surface modification of rubber (Hevea rasiliensis) leaves for the adsorption of copper ions: kinetic, thermodynamic and bonding mechanisms. J. Chem. Technol. Biot., 84 (2), 192-201.

Nichols, E and Drogos, D (2000). Strategies for characterizing subsurface releases of Gasoline containing MTBE. American Petroleum Institute, publication no. 4699, Washington.

Nuhoglu, Y, Malkoc, E, Gürese, A, Canpolat, N (2002). The removal of Cu(II) from aqueous solutions by *Ulothrix zonata*. Bioresource Technol., 85 (3), 331-333.

NSTC (National Science and Technology Council) (1997). Interagency Assessment of Oxygenated Fuels. Office of Science and Technology Policy, Washington.

Onyango, MS, Kojima, Y, Aoyi, O, Bernardo, EC, Matsuda, H (2004). Adsorption equilibrium modeling and solution chemistry dependence of fluoride removal from water by trivalent-cation-exchanged zeolite F-9. J. Colloid Interf. Sci., 279 (2), 341-350.

Opher, T, Ostfeld, A, Friedler, E (2009). Modeling highway runoff pollutant levels using a data driven model. Water Sci. Technol., 60(1), 19-27.

Oyanedel-Craver, VA, Fuller, M, Smith, JA (2007). Simultaneous sorption of benzene and heavy metals onto two organoclays. J. Colloid. Interf. Sci., 309 (2), 485-492.

Park, JW and Jaffe, PR (1993). Partitioning of the three nonionic organic compounds between adsorbed surfactants, micelles, and water. Environ. Sci. Technol., 27 (12), 2559-2565.

Park, Y, Ayoko, GA, Frost, RL (2011). Application of organoclays for the adsorption of recalcitrant organic molecules from aqueous media. J. Colloid. Interf. Sci., 354(1), 292-305.

Pitt, R, Clark, S, Field, R (1999). Groundwater contamination potential from stormwater infiltration practices. Urban Water, 1(3), 217-236.

Prestes, EC, Anjos, Vanessa Ed, Sodré, FF, Grassi, MT (2006). Copper, lead and cadmium loads and behavior in urban stormwater runoff in Curitiba. Brazil. J.Braz. Chem. Sic., 17 (1), 53-60.

Ramos, RL, Jacome, LAB, Barron, JM, Rubio, LF, Coronado, RMG (2002). Adsorption of zinc (II) from an aqueous solution onto activated carbon. J. Hazard. Mater., 90(1), 27-38.

Ran, Y, Xing, B, Rao, PSC, Fu, J (2004). Importance of adsorption (hole-filling) mechanism for hydrophobic organic contaminants on an aquifer kerogen isolate. Environ. Sci. Technol., 38 (16), 4340-4348.

Ridder, DJD, Verliefde, ARD, Heijman, BGJ, Gelin, S, Pereira, MFR, Rocha, RP, Figueiredo, JL, Amy, GL, Dijk, HCV (2012). A thermodynamic approach to assess organic solute adsorption onto activated carbon in water. Carbon, 50 (10), 3774-3781.

Rossner, A and Knappe, DRU (2008). MTBE adsorption on alternative adsorbents and packed bed adsorber performance. Water Res., 42 (8-9), 2287-2299.

Rossner, A, Snyder, SA, Knappe, DRU (2009). Removal of emerging contaminants of concern by alternative adsorbents. Water Res., 43(15), 3787-3796.

Rossner, A (2004). Adsorption of Methyl tertiary-butyl Ether on highsilica zeolites: effects of adsorbent characteristics and natural organic matter on adsorption isotherms. Master Dissertation, North Carolina State University, USA.

Sansalone, JJ and Buchberger, SG (1997). Partitioning and first flush of metals in urban storm water. J. Environ. Eng.-ASCE, 123 (2), 134-143.

Schmidt, TC (2003). Analysis of methyl tert-butyl ether (MTBE) and tert-butyl alcohol (TBA) in ground and surface water. Trends Anal. Chem., 22 (10), 776-784.

Semadeni-Davies, A, Hernebring, C, Svensson, G, Gustafsson, LG (2008). The impact of climate change and urbanization on drainage in Helsingborg, Sweden: Combined sewer system. J. Hydrol., 350 (1-2), 100-113.

Seredych MM, Gun'ko VM, Gierak A (2005). Structural and energetic heterogeneities and adsorptive properties of synthetic carbon adsorbents. Appl. Surf. Sci., 242 (1-2), 154-161.

Shih, TC, Wangpaichitr, M, Suffet, M (2003). Evaluation of granular activated carbon technology for the removal of methyl tertiary butyl ether (MTBE) from drinking water. Water Res., 37 (2), 375-385.

Shutes, RBE and Sriyaraj, K (2001). An assessment of the impact of motorway runoff on a pond, wetland and steam. Environ. Int., 26 (5-6): 433-439.

Sing, KSW, Everett, DH, Haul, RAW, Moscou, L, Pierotto, RA, Rouquerol, J, Siemieniewska, T (1985). Reporting physisorption data for gas/solid systems with special reference to the determination of surface area and porosity. Pure & Appl. Chem., 57 (4), 603-619.

Sing, KSW (1995). Physisorption of nitrogen by porous materials. J. Porous. Mat., 2 (1), 5-8.

Smith, EH (1996). Uptake of heavy metals in batch systems by a recycled iron-bearing material. Water Res., 30(10), 2424-2434.

Solisio, C, Lodi, A, Borghi, MD (2001). Treatment of effluent containing micropollutants by means of activated carbon. Waste Manage, 21(1), 33-40.

Song, XL, Zhang, Y, Yan, CY, Jiang, WJ, Xie, HJ (2012). Adsorption of mercury ion on anctivated carbons from rice husk. Appl. Mechan. Mater., 161, 162-166.

Soto, ML, Moure, A, Domínguez, H, Parajó, JC (2011). Recovery, concentration and purification of phenolic compounds by adsorption: a review. J. Food Eng., 105 (1), 1-27.

Stanley, DW (1996). Pollutant removal by a stormeater dry detention pond. Water Environ. Res., 68 (6), 1076-1083.

Stefan, C (2006), Improvement of characterization of single and multisolute adsorption of methyl tert-butyl ether (MTBE) on zeolites. PhD Dissertation, Technical University of Dresden.

Stockmeyer, MR, Madsen, FT, Kahr, G (1995). Contaminant transport in organophilic waste deposit liners. Hazard. Waste Hazard. Mater., 12(2), 149-166.

Stotz, G (1987). Investigations of the properties of the surface water run-off from federal highways in the FRG. Sci. Total Environ., 59, 329-337.

Suffet IH and McGuire MJ (1980). Activated carbon adsorption of organics from the aqueous phase, Vol.1. Ann Arbor Science Publishers, Collingwood. Michigan, USA.

Tchobanoglous, G, Burton, F, Stensel, HD (2003). Wastewater Engineering: Treatment and Reuse. Metcalf & Eddy, Inc., fourth edition. McGraw-Hill, New York.

Terzyk, AP, Chatłas, J, Gauden, PA, Rychlicki, G, Kowalczyk, P (2003). Developing the solution analogue of the Tóth adsorption isotherm equation. J. Colloid Interf. Sci., 266 (2), 473-476.

Urano, K, Yamamoto, E, Tonegawa, M, Fujie, K (1991). Adsorption of chlorinated organic compounds on activated carbon from water. Water Res., 25 (12), 1959-1964.

US EPA (U.S. Enviromental Protection Agency) (1997). Drinking Water Advisory: Consumer Acceptability Advice and Health Effects Analysis on Methyl Tertiary-butyl ether (MtBE) (EPA-822-F-97-009).Office of water 4304.

USGS (U.S. Geological Suevey) (1996). Occurrence of the gasoline oxygenate MTBE and BTEX compounds in urban storm water in the US: 1991-1995. Technical Report, Water Research Investigations Report 96-4146.

Vadivelan V and Kumar KV (2005). Equilibrium, kinetics, mechanism, and process design for the sorption of methylene blue onto rice husk. J. Colloid Interf. Sci., 286 (1), 90-100.

Villaescusa, I, Fiol, N, Martinez, M, Miralles, N, Poch, J, Serarols, J (2004). Removal of copper and nickel ions from aqueous solutions by grape stalks wastes. Water Res., 38 (4), 992–1002.

Villaescusa, I, Martinez, M, Miralles, N (2000). Heavy metal uptake from aqueous solution by cork and yohimbe bark wastes. J. Chem. Technol. Biot., 75 (9), 812-816.

Vijayaraghavan, K, Jegan, RJ, Palanivelu, K, Velan, M (2004). Copper removal from aqueous solution by marine green alga *Ulva reticulate*. Electron. J. Biotechn., 7 (1), 61-71.

Volesky, B (2007). Review: Biosorption and me, Water Res., 41(18), 4017-4029.

Vreysen, S, Maes, A, Wullaert, H (2008). Removal of organotin compounds, Cu and Zn from shipyard wastewaters by adsorption-flocculation: a technical and economical analysis. Mar. Pollut. Bull., 56 (1), 106-115.

Weber, WJ and Morris, JC (1963). Kinetics of adsorption on carbon from solution. J. Sanit Engng. Div. Am. Soc. Civ. Engrs., 89 (SA2), 31-39.

Westerlund, C and Viklander, M (2006). Particles and associated metals in road runoff during snowmelt and rainfall. Sci. Total Environ., 362 (1-3), 143-156.

Wilhelm, MJ, Adams, VD, Curtis, JG, Middlebrooks, EJ (2002). Carbon adsorption and air-stripping removal of MTBE from River Water. J. Environ. Eng.-ASCE, 128 (9), 813-823.

Wik, A, Lycken, J, Dave, G (2008). Sediment quality assessment of road runoff detention systems in Sweden and the Potential Contribution of tire wear. Water Air Soil Poll., 194 (1), 301-314.

Wong, THF, Breen, PF, Somes, NLG (1999). Ponds vs wetlands-performance considerations in stormwater quality management, proceedings of the 1st South Pacific Conference on Comprehensive Stormwater and Aquatic Ecosystem Management, Auckland, New Zealand, 22-26,2, 223-231.

Xu, Z, Zhang, Q, Wu, C, Wang, L (1997). Adsorption of naphthalene derivatives on different macroporous polymeric adsorbents. Chemosphere, 35(10), 2269-2276.

Yan, G. and Viraraghavan, T (2003). Heavy-metal removal from aqueous solution by fungus *Mucor rouxii*. Water Res., 37 (18), 4486-4496.

Yang, K, Zhu, L, Xing, B (2006). Adsorption of polycyclic aromatic hydrocarbons by carbon nanomaterials. Environ. Sci. Technol., 40 (6), 1855-1861.

Yang, K, Wang, X, Zhu, L, Xing, B (2006). Competitive sorption of pyrenephenanthrene and naphthalneneon multiwalled carbon nanotubes. Environ. Sci. Technol., 40 (18), 5804-5810.

Yu, B, Zhang, Y, Shukla, A, Shukla, SS, Dorris, LK (2001). The removal of heavy metals from aqueous solutions by sawdust adsorption-removal of lead and comparison of its adsorption with copper. J. Hazard. Mater., 84 (1). 83-94.

Yun, YS, Park, D, Park, JM, Volesky, B (2001). Biosorption of trivalent chromium on the brown seaweed biomass. Environ. Sci. Technol., 35 (21), 4353-4358.

Zeng, L, Tang, R, Luo, J, He, J (2012). Research development of treatment measures on road runoff pollution. Second international conference on intelligent systems design and engineering application (ISDEA), 1095-1098.

Zhang, W, Zhang, S, Yue, D, Wan, C, Ye, Y, Wang, X (2008). Charaterization and loading estimation of polycyclic aromatic hydrocarbons in road runoff from urban regions of Beijing, China. Environ. Toxicol. Chem., 27 (1), 31-37.

Zhao, G, Wu, X, Tan, X, Wang, X (2011). Sorption of heavy metal ions from aqueous solution: a review. Open Colloid Sci. J., 4, 19-31.

8. List of symbols and abbreviations:

a	Empirical exponent in PDM isotherm; indicate the heterogeity of adsorbent surface	(-)
AADT	Annual average daily traffic	
AC	Activated carbon	
AUR	Adsorbent usage rate	(g/L)
b	Tóth adsorption coefficient; represent the heterogeneity of adsorbent surface	(-)
B	Coefficient of Boyd kinetics model, the slope of Bt-t plot	(-)
BBodSchV	Bundes-Bodenschutz- und Altlastenverordnung	
BJH	Barrett-Joyner-Halenda theory	
BMPs	Best management practices	
C	Carbon	
Cd	Cadmium	
C_e	Adsorbate concentration at equilibrium	(mg/L or µg/L)
C_0	Initial concentration of adsorbate in the aqueous phase	(mg/L or µg/L)
COD	Chemical oxygen demand	
Cu	Copper	
$CuNO_3$	Copper nitrate	
DA	Dubinin-Astakhov equation	
D_i	Coefficient of Boyd kinetics model; the self-diffusion coefficient	(cm^2/s)
DIPE	Di-isopropyl ether	
DMDO	Dimethyl-diocta-decyl ammonium	
D-R	Dubinin-Radushkevich models	
DRI	Sponge iron	

E	Coefficient of PDM isotherm; indicates the free energy of adsorption	(kJ/mol)
EBCT	Empty bed contact time	
EDX	Energy dispersive X-ray emission	
EPA	Environment Protection Agency	
ETBE	Ethanol ethyl tert-butyl ether	
F300	Activated carbon	
f_{oc}	Fraction of organic carbon of adsorbents	(%)
FTIR	Fourier transform infra-red spectroscopy	
ΔG^o	Gibbs free energy	
GC	Gas chromatography	
h	Kinetic constant in the pseudo kinetics models	(mg/(g. min) or µg/(g·min))
H	Hydrogen	
HK	Horvath-Kawazoe theory	
HNO_3	Nitric acid	
HOK	Activated lignite	
K_1	Kinetic constant in the pseudo kinetics models	(1/min)
K_2	Kinetic constant in the pseudo kinetics models	(g/(mg . min) or g/(µg·min))
K_f	Coefficient of Freundlich model; denotes the maximum adsorption capacity	$(mg/g) (L/mg)^{1/n}$
KH_2PO_4	Potassium phosphate monobasic	
k_i	Intra-particle diffusion rate in Intra-particle model	$(µg/(g·min^{1/2}))$
K_l	Coefficient of Langmuir model; indicate consumed energy in the adsorption process	(L/mg or L/µg)
$(K_{oc} \cdot f_{oc})$	Partitioning coefficient	
K_{oc}	Organic carbon normalized partitioning coefficient	(L/kg)

116

K_t	Tóth adsorption coefficient	(L/g)
log K_{OC}	Organic carbon partition coefficient	
log K_{OW}	Partitioning coefficient between octanol and water	
$m_{adsorbent}$	Weight of adsorbent used in the experiments; 2 g/100 mL in this study	(g)
Milli-Q	Deionized water	
MOTH	Mineral oil type hydrocarbons	
MS	Mass spectrometry	
MTBE	Methyl tert-butyl ether	
n	Freundlich model Coefficient; indicates adsorption intensity or adsorbents heterogeneity (n>1)	
N	Nitrogen	
NaCl	Sodium chloride	
$Na_2HPO_4{\cdot}2H_2O$	Di-sodium hydrogen phosphate dehydrate	
NaOH	Sodium hydroxide	
Nap	Naphthalene	
NOM	Natural organic matter	
PAHs	Polycyclic aromatic hydrocarbons	
Pb	Lead	
PDM	Polanyi-Dubinin-Manes isotherm	
q_e	Adsorbed amount of adsorbate on adsorbent	(mg/g or µg/g)
q_m	Coefficient of Langmuir model; the saturated amount of adsorbate on adsorbents	(mg/g or µg/g)
q_t	Adsorbed amount of adsorbate at time t (min)	(mg/g or µg/g)
$q_{e,cal}$	Calculated adsorption amount at equilibrium	(mg/g or µg/g)
$q_{e,exp}$	Experimental adsorption amount at equilibrium	(mg/g or µg/g)
r	Coefficient of Boyd kinetics model; radius of the adsorbent granule (1.75 mm in this study)	(cm)

R	Ideal gas constant, 8.3145 J/(mol·K)	
Re	Removal efficiency	(%)
RSSCTs	Rapid small-scale column tests	
S	Solubility of adsorbate	(mg/L)
T	Absolute temperature, 297 K in this study	(K)
TAME	Tert-amyl ether	
TBA	Tert-butyl alcohol	
Tixosorb	Semi-organophilic bentonite	
TOC	Total organic carbon	
ρ_0	Coefficient of PDM isotherm; denotes the density of adsorbate	(mg/L)
V_0	Coefficient of PDM isotherm; occupied micro-pore volume on adsorbent	(L/g)
V	Volume of solution	(L)
VOCs	Volatile organic compounds	
Zn	Zinc	
$ZnNO_3$	Zinc nitrate	